

Katharina Dokulil, Bsc.

Cloning, expression and characterisation of 7-cyano-7-deazaguanine synthases

Masterarbeit

zur Erlangung des akademischen Grades
eines Diplomingenieurs
der Studienrichtung Biotechnologie
an der Technischen Universität Graz

Begutachter

Univ.-Prof.i.R. Dipl.-Ing. Dr.techn. Helmut Schwab

Dipl.-Ing. Dr.techn. Margit Winkler

Institut für Molekulare Biotechnologie, Technische Universität Graz

ACIB GmbH, Graz

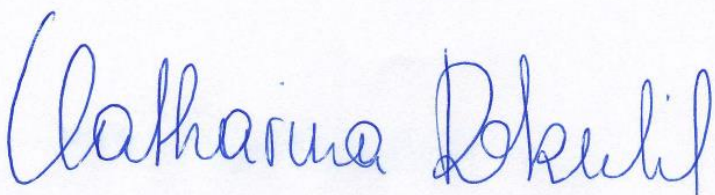
2016

Ehrenwörtliche Erklärung

Ich erkläre ehrenwörtlich, dass ich die vorliegende Arbeit selbstständig und ohne fremde Hilfe verfasst, andere als die angegebenen Quellen nicht benutzt und die den Quellen wörtlich oder inhaltlich entnommenen Stellen als solche kenntlich gemacht habe. Die Arbeit wurde bisher in gleicher oder ähnlicher Form keiner anderen inländischen oder ausländischen Prüfungsbehörde vorgelegt und auch noch nicht veröffentlicht. Die vorliegende Fassung entspricht der eingereichten elektronischen Version.

25.3. 2016

Unterschrift



Katharina Bockel

Acknowledgements / Danksagung

An erster Stelle möchte ich meiner Betreuerin Margit Winkler, Herrn Prof. Helmut Schwab, der ACIB GmbH und der Technischen Universität Graz danken, dass ich im Zuge des reverse Nitrilase Projektes meine Diplomarbeit absolvieren durfte. Außerdem gilt ein großer Dank dem Bundesministeriums für Verkehr, Innovation und Technologie (BMVIT) und der Initiative FEMtech für die finanzielle Unterstützung. Margit Winkler möchte ich besonders für die tolle wissenschaftliche Unterstützung danken, da ich dadurch viel Erfahrung im wissenschaftlichen Bereich, sowie im Laboralltag sammeln konnte. Danke auch an Thorsten Bachler, der mich in HPLC-Dingen sehr gut eingeschult hat und bei Problemen immer helfend zur Seite stand. Außerdem möchte ich mich beim ganzen ACIB Team, meinen Studienkollegen und insbesondere Eva-Maria Köhler für das kollegiale Miteinander und die schönen Stunden gemeinsam im Labor bedanken.

Meinen Freund und Lebenspartner Lukas Müller möchte ich auch danke sagen, dass er immer ein offenes Ohr für meine Probleme hat und besonders in diesem so schwierigen Jahr immer für mich da war. Ein herzliches Danke möchte ich auch an meine restliche Familie und Freunde richten, die für mich große Stützen sind und ohne die ich mein letztes Studienjahr nicht gemeistert hätte!

Mein allergrößter Dank gilt meiner Mutter, die mir ermöglicht hat, mein Studium zu absolvieren und mich in Allem immer unterstützt hat. Ohne sie hätte ich mein Leben nie so positiv gestalten und meine Ausbildung mit Erfolg absolvieren können. Ich konnte von ihr so viel fürs Leben lernen und Sie war für mich immer die größte Stütze. Da meine Mutter leider 2015 unerwartet verstorben ist, widme ich ihr diese Diplomarbeit.

Zusammenfassung

Das Enzym 7-Cyano-7-deazaguanine Synthase (QueC) katalysiert die Umwandlung eines Carboxylates zu einem Nitril. In dieser enzymatischen Reaktion wird ATP als Co-Faktor gebraucht und als Stickstoffquelle wird Ammonium benötigt. Die Sequenzen des Enzyms 7-Cyano-7-deazaguanine Synthase wurden aus verschiedenen Organismen (*G. kaustophilus*, *E. coli*, *P. atrosepticum*, *A. sulficallidus* und *B. subtilis*) in den pEHISTEV-Vektor kloniert und in *E. coli* heterolog exprimiert. Mittels neu entwickelten HPLC-basierten, Aktivitätsassays wurden die Enzyme charakterisiert. Unter Verwendung von ^{31}P NMR-Spektrometrie und eines fluoreszenzbasierten Thermo-shift Assay wurden weitere Experimente zur Aufklärung der Reaktionsprodukte und der Substratspezifität vorgenommen. AMP und Pyrophosphat wurden als Nebenprodukte der preQ₀-Bildung ermittelt. Mit Ausnahme von QueC aus *B. subtilis* waren alle Enzyme aktiv und zeigten eine hohe Spezifität zum natürlichen Substrat 7-Carboxy-7-Deazaguanin (CDG).

Abstract

7-Cyano-7-deazaguanine synthase is an enzyme which catalyses the formation of a nitrile from a carboxylic acid. This reaction is ATP dependent and ammonia serves as the nitrogen source. 7-Cyano-7-deazaguanine synthases from *G. kaustophilus*, *E. coli*, *P. atrosepticum*, *A. sulficallidus* and *B. subtilis* were expressed and characterised, based on a newly developed HPLC based activity assay. Further analyses were performed using ^{31}P NMR-spectrometry and a fluorescence-based thermal-shift assay. Furthermore, the net reaction could be explained and AMP and pyrophosphate could be determined as by-products to preQ₀. With the exception of the *B. subtilis* derived enzyme, all heterologously expressed enzymes were active. and showed a high specificity to the natural substrate 7-carboxy-7-deazaguanine (CDG).

Content

Acknowledgements / Danksagung	3
Zusammenfassung.....	4
Abstract.....	5
Content.....	I
Figures	VII
Schemes.....	XI
Tables.....	XII
Abbreviations	XIII
1 Introduction	1
1.1 The deazapurine biosynthetic pathway	1
1.2 The 7-cyano-7-deazaguanine synthase	1
1.2.1 General information.....	1
1.2.2 Reaction.....	2
1.3 The 7-cyano-7-deazaguanine reductase from <i>Geobacillus kaustophilus</i> , the successor of QueC in queuosine pathway	3
1.4 Gibson cloning.....	4
1.5 <i>Escherichia coli</i> as expression strain and corresponding vector system .	4
1.6 High pressure liquid chromatography as analysis tool.....	5
1.7 NMR spectrometry.....	7
1.8 Fluorescence-based thermal shift assay	7
1.9 The synthesis of nitriles and their role for the industry.....	8
2 Objectives.....	10
3 Experimental Procedures.....	11
3.1 Plasmid, strains and primers	11
3.1.1 Plasmid	11
3.1.2 Strains.....	11
3.1.2.1 Strain for transformation:	11
3.1.2.2 Strain for expression:.....	12
3.1.3 Enzymes	12

3.1.4	Primers, sequencing primers and G-blocks	13
3.2	Equipment and devices	14
3.2.1	Electroporator and associated materials	14
3.2.2	Centrifuges and associated materials	14
3.2.3	Fast protein liquid chromatography (FPLC) and associated materials	14
3.2.4	Gel electrophoresis and associated materials	14
3.2.4.1	Agarose gel electrophoresis	14
3.2.4.2	SDS-Page	15
3.2.5	High performance liquid chromatography-UV (HPLC) and associated materials	15
3.2.5.1	HPLC-UV Agilent 1100 series	15
3.2.5.2	HPLC-MS Agilent 1200 series	15
3.2.5.3	Columns	16
3.2.6	NMR spectrometer	16
3.2.7	Pipettes and micropipettes and devices	16
3.2.8	PCR-cyclers and associated materials	16
3.2.9	Photometer and associated materials	16
3.2.10	Reaction vessels	17
3.2.11	Shakers and incubators	17
3.2.12	Additional instruments and materials	17
3.3	Reagents, buffers, stocks and media	17
3.3.1	Reagents	17
3.3.2	Stocks	19
3.3.2.1	Antibiotics	19
3.3.2.2	Additional stocks	20
3.3.3	Media and buffers	20
3.3.3.1	LB-medium (Low Salt Luria Bertani)	21
3.3.3.2	LB-agar	21
3.4	Software and web tools	21
3.4.1	Software	21
3.4.2	Web tools	21
	BLAST (Basic Local Alignment Search Tool), http://blast.ncbi.nlm.nih.gov/Blast.cgi	22

3.5	Kits and methods.....	22
3.5.1	GeneJET™ Plasmid Miniprep Kit.....	22
3.5.2	Wizard® SV Gel and PCR Clean-Up System	22
3.5.3	General methods	22
3.5.3.1	<i>E. coli</i> transformation	22
3.5.3.2	Agarose gel electrophoresis	23
3.5.3.3	Preparation of glycerol stocks.....	23
3.5.4	Construction of protein expression strains	23
3.5.4.1	Amplification of the pEHsTEV vector	23
3.5.4.2	Gibson cloning	24
3.5.4.3	Vector opening, QueC fragments preparation and ligation 26	
3.5.4.4	Cloning of 7-cyano-7-deazaguanine synthase from <i>G. kaustophilus</i> and <i>Escherichia coli</i>	27
3.5.4.5	Sequencing.....	28
3.5.5	Cultivation and protein expression	28
3.5.5.1	Small scale cultivation	28
3.5.5.2	Large scale cultivation	28
3.5.5.3	Protein purification	29
3.5.5.4	SDS-Page to control expression levels of the different 7- cyano-7-deazaguanine synthases	29
3.5.5.5	BugBuster lysis	29
3.6	Activity assays.....	30
3.6.1	<i>In vitro</i> activity assay for characterisation of 7-cyano-7- deazaguanine synthases	30
3.6.2	Activity assay and calculation of the specific activity of 7-cyano-7- deazaguanine synthases	30
3.6.2.1	Calculation of enzyme activity.....	30
3.6.3	Activity assay for exploration of the reaction mechanism of 7- cyano-7-deazaguanine synthase.....	31
3.6.3.1	Method for detection of ATP, ADP and AMP with capHPLC.....	31
3.6.4	HPLC based substrate and product detection.....	31
3.6.4.1	Method „KDO_CDG“ for HPLC-UV and HPLC-MS.....	32

3.6.4.2	Method „Phenomenex PreQ ₀ “ for HPLC-MS	32
3.6.4.3	Method „Indole-method“ for HPLC-MS used for Indole-3-carboxylic acid, 2-methyl-4-oxo-4,5,6,7-tetrahydro-1H-indole-3-carboxylic acid and the corresponding nitriles.....	32
3.6.4.4	Method “Cinnamonnitrile” for HPLC-MS used for cinnamic acid and the corresponding nitrile	33
3.6.4.5	Method „Cinnamonnitrile“ for HPLC-UV and HPLC-MS	33
3.6.4.6	Method „PCA“ for HPLC-UV and HPLC-MS used for Pyrrole-2-carboxylic acid.....	33
3.6.5	Fluorescence-based Thermal Shift (FTS) assay.....	33
3.6.6	<i>In vitro</i> reconstruction of Queosine biosynthesis in <i>G. kaustophilus</i> : two step cascade from 7-carboxy-7deazaguanine to PreQ ₁	35
3.6.6.1	Cultivation, protein expression and purification of nitrile reductase from <i>G. kaustophilus</i>	35
3.6.6.2	Activity assay for the two step cascade from 7-carboxy-7deazaguanine to preQ ₁	35
3.6.7	³¹ P NMR experiments for co-product identification in 7-cyano-7-deazaguanine synthase catalysed nitrile formation	36
3.6.8	Active site analysis.....	37
4	Results and discussion	38
4.1	Selection of 7-Cyano-7-deazaguanine synthases	38
4.2	Construction of <i>E. coli</i> BL21 strains expressing 7-cyano-7-deazaguanine synthases from different organisms	39
4.3	Optimization of culture conditions to obtain possibly high expression levels.....	44
4.4	Assay development	46
4.5	Exploration of the reaction mechanism of 7-cyano-7-deazaguanine synthases.....	47
4.5.1	Exploration experiments by capHPLC analysis.....	47
4.5.2	Exploration of the net reaction products by NMR spectrometry ..	52
4.5.3	Exploration of the active site residues from 7-cyano-7-deazaguanine synthases.....	55
4.6	Characterisation of different QueCs	57

4.6.1	Functionality and specific activity of 7-cyano-7-deazaguanine synthases	57
4.6.2	Determination of temperature and pH optimum of 7-cyano-7-deazaguanine synthases of <i>G. kaustophilus</i> and <i>E. coli</i>	59
4.6.3	Stability of 7-cyano-7-deazaguanine synthases from <i>G. kaustophilus</i> and <i>E. coli</i> on ice.....	66
4.6.4	Exploration of the substrate scope of the different QueCs	66
4.6.4.1	Measurements with HTP Fluorescence-based Thermal Shift (FTS) assay	66
4.6.4.2	Measurements with HPLC-UV and HPLC-MS	70
4.7	In Vitro reconstruction of Queosine biosynthesis in <i>G. kaustophilus</i> : two step cascade from 7-carboxy-7-deazaguanine to preQ ₁	73
5	Conclusion	75
6	References.....	77
6.1	Literature	77
6.2	Lab-book.....	80
Appendix	81
	Strain information.....	81
	DNA sequences	81
	QueC <i>G. kaustophilus</i>	81
	QueC <i>E. coli</i>	81
	QueC <i>A. flavithermus</i>	82
	QueC <i>A. sulfaticallidus</i>	82
	QueC <i>C. sativus</i>	83
	QueC <i>P. atrosepticum</i>	83
	ToyM <i>S. rimosus</i>	84
	QueC <i>B. subtilis</i>	84
	Protein sequences	85
	QueC <i>G. kaustophilus</i> (NC_006510.1 (1000474..1001148)).....	85
	QueC <i>E. coli</i> (NC_000913.3 (464852..465547)).....	85
	QueC <i>A. flavithermus</i> (NC_011567.1(1947599..1948264)).....	85
	QueC <i>A. sulfaticallidus</i> (CP005290.1, (1578638..1579342))	85

QueC <i>C. sativus</i> (NC_026655.1)	86
QueC <i>P. atrosepticum</i> (NZ_CP009125.1, (1291182..1291877))	86
ToyM <i>S. rimosus</i> (NZ_JMGX01000038.1 (5525..6199))	86
QueC <i>B. subtilis</i> (NC_000964.3, (1439448..1440107))	86
Alignment of protein sequences	87

Figures

- Figure 1:** Monomer structure of *B. subtilis* QueC. **(A)** Structure of QueC in detail. Helices are coloured red, β - strands are coloured yellow, and loops are coloured green. **(B)** Picture of the surface of QueC, where the conserved residues are coloured magenta and unconserved regions are grey. Zinc interacting residues are plotted in yellow and the phosphate and magnesium ions are coloured cyan and blue.⁵ 2
- Figure 2:** The pEHisTEV cloning vector. 11
- Figure 3:** Preparative agarose gel of amplified pEHisTEV vector. Slot 1 to 6 show the application of amplified pEHisTEV vectors, without gel slices of pEHisTEV vectors with the size of interest (5343bp). GeneRuler™ DNA Ladder Mix was used as standard..... 39
- Figure 4:** Control agarose gel of QueC fragments cloned into pEHisTEV vector by Gibson cloning. Digest was done with restriction enzymes XbaI and XhoI. Slot 1: Digest of QueC fragment of *S. rimosus* in pEHisTEV vector. Slot 2: Digest of QueC fragment of *A. flavithermus* in pEHisTEV vector. Slot 3: Digest of QueC fragment of *C. sativus* in pEHisTEV vector. Slot 4: Digest of QueC fragment of *P. atrosepticum* in pEHisTEV vector. Slot 5: Digest of QueC fragment of *A. sulficallidus* in pEHisTEV vector. Slot 6: Digest of QueC fragment of *B. subtilis* in pEHisTEV vector. GeneRuler™ DNA Ladder Mix was used as standard..... 40
- Figure 5:** Control agarose gel of QueC fragments in nonfunctional pEHisTEV vector. Digest was done with restriction enzymes HindIII and NdeI. Slot 1: Digest of QueC fragment of *C. sativus*. Slot 2: Digest of QueC fragment of *B. subtilis*. Slot 3: Digest of QueC fragment of *P. atrosepticum*. Slot 4: Digest of QueC fragment of *S. rimosus*. Slot 5: Digest of QueC fragment of *A. sulficallidus*. Slot 6: Digest of QueC fragment of *A. flavithermus*. GeneRuler™ DNA Ladder Mix was used as standard. 41
- Figure 6:** SDS-control gel of the different fractions of the BugBuster lysis. Page Ruler Prestained Protein Ladder (10-170kDa) was used as standard. The samples with different QueCs were arranged as follows: First *A. flavithermus*, second *A. sulficallidus*, third *B. subtilis*, fourth *P. atrosepticum*, fifth *C. sativus* and sixth *S. rimosus*. Slot 8,9,10, 11, 12, and 14 give pellet 1 (cell components). Slot 15 to 21 show pellet 2 (inclusion body fraction). Slot 1 to 7 show the supernatant to show

the expression levels of soluble 7-cyano-7-deazaguanine synthases from different organisms. The results of the negative control are shown in slot 7, 14 and 21. QueC of *A. sulficallidus* (26.4kDa), *B. subtilis* (24.5kDa), and *P. atrosepticum* (25.4kDa) show a slight overexpression marked with a red ellipse. 42

Figure 7: SDS-control gel of the different fractions of the BugBuster lysis. Page Ruler Prestained Protein Ladder (10-170kDa) from Fermentas has been used as standard. P1 pictures cell components which were separated in the first centrifugation step of the BugBuster lysis. P2 visualizes inclusion bodies. SN pictures the expression levels of the 7-cyano-7-deazaguanine synthases from different organisms by induction with 1mM IPTG and 0.1 mM ZnSO₄ at 25°C..... 43

Figure 8: SDS-control gel of the different fractions of the protein purification with Ni-affinity chromatography. In slot 1 the purified enzyme and in slot 2 the purified enzyme-concentrate from *A. sulficallidus* is given. In slot 3 the purified enzyme and in slot 4 the purified enzyme-concentrate from *P. atrosepticum* is given. In slot 5 the purified enzyme-concentrate from *B. subtilis* is given. Page Ruler Prestained Protein Ladder (10-170kDa) is used as standard. 44

Figure 9: SDS-control gel of the different fractions of the BugBuster lysis. Slot 1 to slot 6 shows the monitoring of the inclusion bodies formed during the cultivation. Slot 7 and 10 shows the expression of soluble QueCs using 1mM IPTG. Slot 8 and 11 shows the expression of soluble QueC using 1mM IPTG and 0.1 mM ZnSO₄. Slot 9 and 12 shows the monitoring of the expression level of QueC using 0.1mM IPTG and 0.1 mM ZnSO₄. 45

Figure 10: SDS-control gel of the different fractions of the protein purification with Ni-affinity chromatography. Slot 1 and 2 show the crude lysate from QueC of *E. coli* and *G. kaustophilus*. Slot 3 to 5 show selected fractions, which were taken during purification of QueC of *E. coli*. Slot 6 to 8 show selected fractions, which were taken during purification of QueC of *G. kaustophilus*. Slot 9 and 10 show purified enzyme stock of QueC from *E. coli* and *G. kaustophilus*, respectively. Page Ruler Prestained Protein Ladder (10-170kDa) was used as standard. 46

Figure 11: HPLC analysis, showing ATP and the formation of AMP and ADP over time from the blank, where no 7-cyano-7-deazaguanine synthase from *G. kaustophilus* was present. After 5, 10 and 20 minutes samples were taken, the reaction terminated and analysed with HPLC..... 48

Figure 12: HPLC analysis, showing ATP and the formation of AMP and ADP over time from the bioconversion, where 7-cyano-7-deazaguanine synthase from <i>G. kaustophilus</i> converted CDG to preQ ₀ under consumption of ATP. After 5, 10 and 20 minutes samples were taken, the reaction terminated and analysed with HPLC.....	49
Figure 13: Application of the calibration curves for the determination of ATP, ADP and AMP concentrations (ng/μL) which are related to the detection areas from the HPLC measurements.	50
Figure 14: Monitoring of the ADP and AMP formation during the activity assay with QueC from <i>G. kaustophilus</i> at 5, 10 and 20 minutes.	51
Figure 15: Monitoring of the ATP consumption during the activity assay with QueC from <i>G. kaustophilus</i> at 5, 10 and 20 minutes.	52
Figure 16: Monitoring of phosphorous containing species during preQ ₀ formation compared with the reference measurements with ATP, ADP, AMP, phosphate and pyrophosphate. The bottom spectrum shows the biotransformation mixture without addition of CDG. In the top four spectra, the reference measurements are displayed. 30 spectra were recorded during 1.28h. Every third spectrum is shown here over time course. ³⁵	53
Figure 17: View of the crystal structure of QueC from <i>G. kaustophilus</i> designed under use of the crystal structure of QueC from <i>B. subtilis</i> , where AMP is modelled to the active site cavity. All proposed residues are conserved in GkQueC and BsQueC. The hydrophilic regions are plotted in blue and hydrophobic residues are plotted in red. ³⁵	55
Figure 18: Active site view of structure of QueC from <i>G. kaustophilus</i> designed under use of the crystal structure of QueC from <i>B. subtilis</i> where residues are shown, which might be involved in the AMP and CDG binding. The zinc ion is shown as a grey sphere. ³⁵	56
Figure 19: Calibration curve for the determination of the preQ ₀ concentration (mM) by read-out of the Area in mAU (milli Absorbance units) of preQ ₀ from the HPLC measurements (UV trace, 254nm).	57
Figure 20: Relative activities of five QueCs from different organism referring to the activity of QueC from <i>G. kaustophilus</i>	58

Figure 21: Effect of temperature on the activity of QueC from *G. kaustophilus*: The optimum temperature for the enzyme was determined by plotting different temperatures against the amount of generated product preQ₀ in mM. 59

Figure 22: Fluorescence-based thermal shift assay for determination of the melting temperature of QueC from *G. kaustophilus* in HEPES buffer with pH 7.5. Temperature was plotted against relative fluorescence units (10³) of the TAMRA reporter signal after detection. 60

Figure 23: Fluorescence-based thermal shift assay for determination of the melting temperature of QueC from *G. kaustophilus* in buffers with different pH values. Temperature was plotted against relative fluorescence units (10³) of the TAMRA reporter signal. 61

Figure 24: Effect of buffer system and pH on the activity of QueC from *G. kaustophilus*: The optimum buffer system and pH for the enzyme was determined by plotting different buffer systems and pH values against the amount of generated product preQ₀. 62

Figure 25: Effect of temperature on the activity of QueC from *E. coli*: The optimum temperature for the enzyme was determined by plotting different temperatures against the amount of generated product preQ₀. 63

Figure 26: Fluorescence-based thermal shift assay for determination of the melting temperature of QueC from *E. coli* in buffers with different pH values. Temperature was plotted against relative fluorescence units (10³) of the TAMRA reporter signal. 64

Figure 27: Effect of buffer system and pH on the activity of QueC from *E. coli*: To find the best buffer system and pH optimum for the enzyme, different buffer systems and pH values were plotted against the amount of generated product preQ₀. 65

Figure 28: Melting temperatures detected by fluorescence-based thermal shift assay for exploration of the substrate scope of **QueC from *G. kaustophilus*** in HEPES buffer at pH 7.5. Different assay conditions are plotted against the melting temperature (°C). The used shortcuts are described in “Experimental procedure”. 67

Figure 29: Melting temperatures detected by fluorescence-based thermal shift assay for exploration of the substrate scope of **QueC from *P. atrosepticum*** in HEPES buffer at pH 7.5. Different assay conditions are plotted against the melting

temperature (°C). The used shortcuts are described in “Experimental procedure”.	67
Figure 30: Melting temperatures detected by fluorescence-based thermal shift assay for exploration of the substrate scope of QueC from <i>G. kaustophilus</i> in HEPES buffer at pH 7.5, without ATP . Different assay conditions are plotted against the melting temperature (°C). The used shortcuts are described in “Experimental procedure”.	68
Figure 31: Melting temperatures detected by fluorescence-based thermal shift assay for exploration of the substrate scope of QueC from <i>E. coli</i> in HEPES buffer at pH 7.5, without ATP . Different assay conditions are plotted against the melting temperature (°C). The used shortcuts are described in “Experimental procedure”.	69
Figure 32: Melting temperatures detected by fluorescence-based thermal shift assay for exploration of the substrate scope of QueC from <i>P. atrosepticum</i> in HEPES buffer at pH 7.5, without ATP . Different assay conditions are plotted against the melting temperature (°C). The used shortcuts are described in “Experimental procedure”.	70
Figure 33: Summary of all HPLC measurements for exploration of the substrate scope of QueC from <i>G. kaustophilus</i> , <i>E. coli</i> and <i>P. atrosepticum</i> in HEPES buffer at pH 7.5. In the blank, 1mM of each carboxylic acid and nitrile was used.	72
Figure 34: HPLC chromatograms, showing conversion of the natural substrate CDG to preQ ₀ and further to preQ ₁ with 7-cyano-7-deazaguanine synthase and 7-cyano-7-deazaguanine reductase from <i>Geobacillus kaustophilus</i> . The simulation was performed in a reaction buffer containing 100mM Tris, 50 mM KCl and 1mM TCEP (pH7.5). The conversion was stopped with a stopping-solution, containing 80% MeOH and 20% DMSO. (*) Impurities from the QueF preparation (low-molecular weight components).	73

Schemes

Scheme 1: Net reaction of CDG to preQ ₀ .	3
Scheme 2: Reaction scheme of the enzymatic reduction of preQ ₀ to preQ ₁ . ⁸	4
Scheme 3: Reaction scheme the Hydroxynitrile lyase reaction ³⁴	9
Scheme 4: Net-reaction scheme of ATP dependent nitrile formation	54
Scheme 5: Proposed mechanism of ToyM from <i>Streptomyces rimosus</i> . ³⁹	54

Tables

Table 1: Sample preparation scheme for the double digest with NdeI and HindIII of vector pEHisTEV with different QueCs.....	26
Table 2: T4 Ligation preparation scheme of the vector and the QueCs fragments from different organisms.....	27
Table 3: Listing of all carboxylic acids, which were used for the exploration of the substrate scope of QueCs from different organism with FTS assay.....	34
Table 4: Summary of ingredients for the <i>in vitro</i> reconstruction of queosine biosynthesis in <i>G. kaustophilus</i> : two step cascade from 7-carboxy-7-deazaguanine to preQ ₁	36
Table 5: Parameters for ³¹ P NMR-spectrometry measurement. ³⁵	37
Table 6: 7-Cyano-7-deazaguanine synthases, which have been selected based on a BLAST search.	38
Table 7: Summary of all buffer systems with corresponding pH values, used for the determination of the pH optimum of QueC from <i>G. kaustophilus</i>	62
Table 8 Summary of all buffer systems with corresponding pH values, used for the determination of the pH optimum of QueC from <i>E. coli</i>	65
Table 9: Carboxylic acids, which have been used for exploration of the substrate scope with HPLC.....	71
Table 10: Strain designation and culture collection number of collected strains with QueC from different organisms.	81

Abbreviations

ADG	7-amido-7-deazaguanine
ADP	adenosine-5'-diphosphate
AMP	adenosine-5'-monophosphate
<i>A. flavithermus</i>	<i>Anoxybacillus flavithermus</i>
<i>A. sulficallidus</i>	<i>Archaeoglobus sulficallidus</i>
ATP	adenosine-5'-triphosphate
<i>B. subtilis</i>	<i>Bacillus subtilis</i>
CDG	7-carboxy-7-deazaguanine
CDS	coding DNA sequence
<i>C. sativus</i>	<i>Cumumis sativus</i>
DNA	Deoxyribonucleic acid
ddH ₂ O	distilled, deionised water
DMSO	dimethyl sulfoxide
dNTP	desoxy nucleoside triphosphate
DTT	dithiothreitol
<i>E. coli</i>	<i>Escherichia coli</i>
FPLC	Fast protein liquid chromatography
<i>G. kaustophilus</i>	<i>Geobacillus kaustophilus</i>
GkNRedWT	nitrile reductase from <i>Geobacillus kaustophilus</i> wild type
GTP	guanosine-5'-triphosphate
HCl	hydrochloric acid
HEPES	4-(2-hydroxyethyl)-1-piperazineethanesulfonic acid
His-tag	polyhistidine tag
HPLC	high performance liquid chromatography
HPLC-UV	high performance liquid chromatography with UV-detector
HPLC-MS	high performance liquid chromatography with mass spectrometric detector
IPTG	Isopropyl β -D-1-thiogalactopyranoside
kDa	kilodalton

LB	lysogeny broth
MCS	multiple cloning site
NADPH	Nicotinamide adenine dinucleotide phosphate
NaOH	Sodium hydroxide
NMR spectrometry	nuclear magnetic resonance spectroscopy
<i>P. atrosepticum</i>	<i>Pectobacterium atrosepticum</i>
PCR	polymerase chain reaction
PreQ ₀	2-amino-5-cyanopyrrolo[2,3-d]pyrimidin-4-one
PreQ ₁	2-amino-5-aminomethyl-pyrrolo[2,3-d]pyrimidin-4-one
SDS-Page	sodium dodecyl sulfate polyacrylamide gel electrophoresis
<i>S. rimosus</i>	<i>Streptomyces rimosus</i>
TEV	tobacco etch virus
Zn	zinc

1 Introduction

1.1 The deazapurine biosynthetic pathway

In this biosynthetic pathway, the deazapurine nucleoside preQ₀ is produced from guanosine-5'-triphosphate (GTP) in a four enzyme cascade. First, GTP gets converted to 7,8-dihydroneopterin triphosphate by the enzyme GTP cyclohydrolase. Further, the pathway includes the conversion to the 6-carboxy-5,6,7,8-tetrahydropterin by QueD from *E. coli*. The enzyme QueE from *B. subtilis*, which is a member of the radical SAM enzyme family, converts 6-carboxy-5,6,7,8-tetrahydropterin to CDG. In the last step, the carboxylate moiety on CDG is converted to a nitrile by QueC from for example *B. subtilis* and preQ₀ is formed.¹

7-Deazapurines are compounds, containing the pyrrolopyrimidine core, which form a structurally diverse class of nucleoside analogs. Further, they show often antibiotic, antineoplastic and antiviral activities.¹

1.2 The 7-cyano-7-deazaguanine synthase

1.2.1 General information

7-Cyano-7-deazaguanine synthase (E.C. 6.3.4.20) is an enzyme which is part of the biosynthetic pathway to the deazapurine nucleoside preQ₀.¹

In addition, 7-cyano-7-deazaguanine synthases are part of the biosynthetic pathway of several other deazapurine containing compounds like queosine, archaeosine and toyocamycin, because they catalyse the conversion of 7-carboxy-7-deazaguanine (CDG) to 2-amino-5-cyanopyrrolo[2,3-d]pyrimidin-4-one (preQ₀).^{1,2,3}

An important 7-deazapurine compound is the hypermodified 7-deazaguanosine nucleoside queosine, which is located in the anticodon wobble position of four amino acid specific tRNAs.⁴ In literature 7-cyano-7-deazaguanine synthase (QueC) was described from *S. rimosus*¹, *B. subtilis*⁵ and *E. coli*⁶, but not elaborately. With ToyM from *S. rimosus* and QueC from *E. coli* the reaction from the sub-

strate 7-carboxy-7-deazaguanine (CDG) to preQ₀ was reconstructed *in vitro* for a qualitative proof of principle.¹

In literature some structural information of QueC can be found⁵

Nenad Cimil and his group from the department of Biochemistry of the University of Illinois already performed structural studies on QueC from *B. subtilis*. In figure 1, the monomer structure of QueC (of *B. subtilis*) is shown.

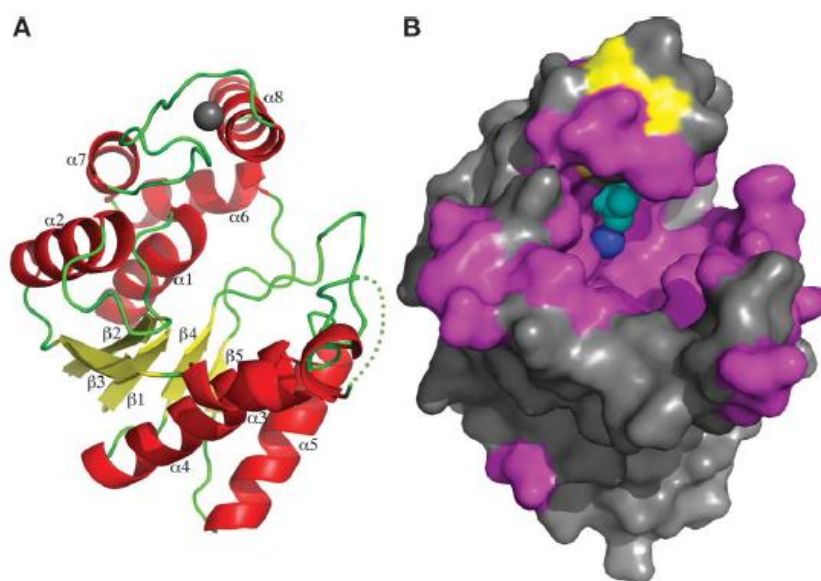
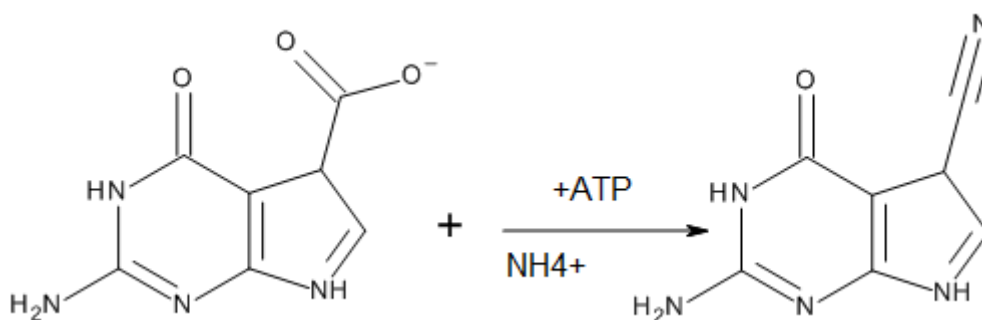


Figure 1: Monomer structure of *B. subtilis* QueC. **(A)** Structure of QueC in detail. Helices are coloured red, β -strands are coloured yellow, and loops are coloured green. **(B)** Picture of the surface of QueC, where the conserved residues are coloured magenta and unconserved regions are grey. Zinc interacting residues are plotted in yellow and the phosphate and magnesium ions are coloured cyan and blue.⁵

The monomer-structure consists of a five parallel-stranded β -sheet, surrounded by six helices (α 1 to α 6) and three additional helices (α 7 to α 9). In solution, the protein exists as a dimer, where interactions take place between two helices of each monomer. The conserved regions, which are probably part of the active site of the protein, are forming a cavity. With its size of about 25 kDa the protein is not very large. The substrate specificity may be limited due to the position of the active site, which is located in a narrow cave.⁵

1.2.2 Reaction

QueC converts 7-carboxy-7-deazaguanine (CDG) to 2-amino-5-cyanopyrrolo[2,3-d]pyrimidin-4-one (preQ₀) (see scheme 1).



Scheme 1: Net reaction of CDG to preQ₀.

With ATP the carboxylate gets activated.¹

In the structure of QueC from *B.subtilis* a Zn (Zinc) ion was found by X-ray crystal structure analysis. So, the reaction seems to be Zn dependent.⁵ In this work, Zn depending experiments will be performed to investigate the Zn dependence.

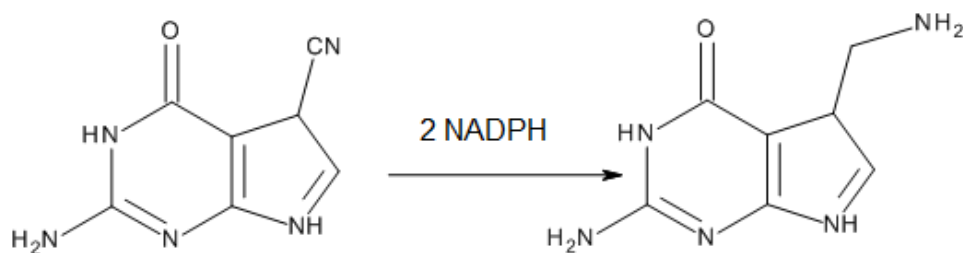
Furthermore, ammonium is needed as amine donor. In labelling studies the source of the nitrile nitrogen could be explored to be ammonia on basis of ¹⁵N incorporation from [¹⁵N] ammonium sulfate.¹

Comparing the reaction mechanism of QueC with nitrilases, which catalyze the conversion of a nitrile into the corresponding acid plus ammonia⁷, QueC behave like a reverse nitrilase.⁶ Up to now the enzymatic reaction of QueC has not been described detailed in literature. The net reaction of QueC is not completely explored and the by products of preQ₀ are not resolved yet.

1.3 The 7-cyano-7-deazaguanine reductase from *Geobacillus kaustophilus*, the successor of QueC in queuosine pathway

7-Cyano-7-deazaguanine reductase (QueF) converts preQ₀ to the primary amine 2-amino-5-aminomethyl-pyrrolo[2,3-*d*]pyrimidin-4-one (preQ₁) in an NADPH-dependent reaction (Figure 2).⁸

PreQ₁ is then transferred to a t-RNA molecule and modified in two enzymatic steps to Q-tRNA.⁹



Scheme 2: Reaction scheme of the enzymatic reduction of preQ₀ to preQ₁.⁸

At that point, QueF type enzymes are the only known enzymes, which can reduce a nitrile to the primary amine in a one-step reaction.⁸ In this work, one aim was the *in vitro* simulation of two steps of the preQ₁ biosynthesis with QueC and QueF from *G. kaustophilus*.

1.4 Gibson cloning

With the Gibson assembly method, DNA can be generated and amplified in one isothermal reaction. Overlapping DNA molecules can be assembled and multiplied using a reaction mix, which includes a 5' exonuclease, a DNA polymerase, a DNA ligase and other buffer components.¹⁰ This reaction mix is incubated for one hour at 50°C. During this time, the exonuclease digests the ends of a DNA double-strand fragment at the 5'-end partially. Then, generated single-stranded ends (sticky ends) can anneal with homologous single-stranded regions. In a second step, DNA-polymerase can close the existing gaps with nucleotides on the DNA-double strand. The DNA ligase connects the generated DNA strands *in vitro* with each other and removes any nicks in the DNA.¹¹ In this work, Gibson cloning was used for the construction of protein expression strains.

1.5 *Escherichia coli* as expression strain and corresponding vector system

E. coli gathered great importance in science as standard expression host for the production of recombinant proteins. *Escherichia coli* is a gram-negative bacterium with a circular genome of 4.6 mega base pairs.¹² Usually it is the system of choice for protein expression, because it can grow on defined media. During exponential

growth it doubles every 20 to 30 minutes and can be used for high yield production of recombinant proteins. Nearly every strain used for recombinant DNA expression is descended from *E. coli* K-12 strain, isolated from the excrements of an diphtheria patient in 1922.^{13,14,15} In this work the *Escherichia coli* BL21 (DE3) gold strain was used as the expression host. This expression host carries a few mutations in order to facilitate special recombination work. It carries the λ lysogen carrying gene for T7 RNA polymerase. Furthermore, it contains mutations in the *ompT* and *lon* genes for enhancing recombinant protein production and does not carry the F-plasmid. Furthermore, it has a mutation in the *dcm* gene for blocking the cytosine methylation at CC(A/T)GG sequences to make the DNA cleavage possible by some restriction enzymes and *hsdS* gene mutation which yield to inactivation of *Eco* site-recognition activity. A mutation in the *gal* gene blocks the galactose utilization of the galactose metabolism in *Escherichia coli* BL21 (DE3) gold strain.¹⁶

Since this strain carries the T7 RNA polymerase, the pET-vector system can be used for expression based on the T7 phage RNA polymerase promoter and the pBR322 origin of DNA replication. Special pET-vector systems exist, which lead to expression of an affinity tag consisting of 6 histidine residues to make purification of the expressed recombinant protein possible by affinity chromatography.^{17,18} One of these pET-vectors which offers this advantage is the pEHisTEV vector.¹⁹ Besides the 6 histidine residues, it has the ability to cut the recombinant protein with the TEV protease from the His-tag after purification.^{20,19}

1.6 High pressure liquid chromatography as analysis tool

The high pressure liquid chromatography (HPLC) is the analytical separation technique which is most commonly used for the separation of small molecules.²¹ This instrumental chromatography technique is fast and delivers qualitative and quantitative analytical results. HPLC is suitable for the separation of soluble, non-volatile or thermally unstable compounds such as amino acids, hydrocarbons, carbohydrates, antibiotics, and numerous other organic substances.²²

The stationary phase for the separation process is packed in columns, either as particles or as monolithic material. As mobile phase, water and organic solvents can be applied. The column material is very often derivatised silica material and may be either film-coated or porous particles. In this work, partition chromatography is used in reversed phase mode, which is characterised by using a nonpolar stationary phase and a polar, water based mobile phase. Two different columns have been applied:

- Chromolith® performance RP 18E 4.6x100 mm HPLC column
- Phenomenex Gemini® NX 3 C18 110 Å, LC column (150 x 2.0 mm, Ea) with a SecurityGuard™ Cartridge 4 x 2.0 mm column

Because of the high porosity of the Chromolith column, very high flow rates with low back pressures can be used. The Chromolith column can lead about four times faster runs than a standard separation with a particle based column. It consists of highly porous monolithic silica rods with a bimodular porestructure.²³

The Phenomenex Gemini column combines silica and polymer particles. The NX process uses crosslinked ethylene groups to reinforce the silica gel mechanically and chemically. These columns are commonly used for the analytical and preparative separation of basic and acidic compounds. With this two-in-one technology, the pH stability increases (pH 1 to 12 is possible) and mechanical strength is optimised. The wide pH range leads to great flexibility in the choice of mobile phase, and thus even greater control over the retention and selectivity of compounds.²⁴

For detection, two different systems have been used. UV/Vis- absorption and mass spectrometry.

The mass spectrometry gives information about the molecular mass from ions in a high vacuum system. The mass spectrometer consists of an ion-source (electron-impact), mass analysis tool (quadrupol) and a detector. The sample molecules get ionised by an electrical field, accelerated and separated in a magnetic field depending on the mass of the ion-particles.²¹

The fields ionize the particles and control them in a vertical flow. Only specified particles in a defined mass area are then able to pass the mass filter.²¹

UV/Vis spectroscopy is generally used in analytics for the quantitative and qualitative determination of compounds. With the UV/Vis-absorption technique the molecules in the sample, which pass the detector, contain π -electrons or non-bonding electrons (n-electrons). These electrons absorb the energy of the ultraviolet or visible light to excite these electrons to higher anti-bonding molecular orbitals.^{21,22}

1.7 NMR spectrometry

The nuclear magnetic resonance spectroscopy (NMR) is based on the measurement from electromagnetic radiation between 4MHz to 1200MHz. Molecules, which can be activated by the electromagnetic waves lead to absorption. In contrast to the ultraviolet, visible and infrared absorption, atomic nuclei are involved in the absorption process at these wave lengths. In order to stimulate cores to an appropriate energy status for absorption, it is necessary to expose the analysts to a strong magnetic field. The nuclear magnetic moment is caused by an intrinsic rotation (= magnetic resonance) of the atomic nucleus. The nuclear spin is quantised. This quantum number 1 can have entire or half values from 0 to 6. The four cores that are most commonly used are ^1H , ^{13}C , ^{19}F and ^{31}P . These four cores have the spin quantum number 1/2.²¹

NMR is one of the most important methods for chemists and biochemists to elucidate structures of organic and inorganic species. In this work the one-dimensional NMR spectroscopy (in particular ^{31}P spectroscopy) is used to explore the reaction products of 7-cyano-7-deazaguanine synthase. The chemical shift of an atom from a reference substance is measured.²⁵

1.8 Fluorescence-based thermal shift assay

With the fluorescence-based thermal shift assay (FTS) the stability of proteins can be determined and inhibitors of proteins can be identified in high throughput manner. This technique is based on the online-detection of a fluorescence signal during a time period. When the temperature is increased, proteins start to unfold. Furthermore, the affinity to bind to the hydrophobic surface of proteins increases. This

allows the sensitive fluorescent dye (SYPRO Orange protein gel stain dye) to bind to the protein and emit light. The changes of melting temperature of a protein under different conditions and by addition of different ligands, inhibitors and substrates, can lead to new findings concerning substrates and ligand affinity to a target protein. Therefore, the thermal shift assay is an inexpensive method for temperature controlled measurement under fluorescence detection.²⁶

In this work, the assay is used for the exploration of the substrate scope of several 7-cyano-7-deazaguanine synthases and exploration of the enzyme stabilities at different assay-conditions.

1.9 The synthesis of nitriles and their role for the industry

Nitriles are a group of chemical compounds with the general formula $R-C\equiv N$. The functional group of a carbon and triple bonded nitrogen is called nitrile or cyano group. Nitriles are formally derived from the hydrocyanic acid (HCN) by replacing the hydrogen atom on an organic residue.²⁷

In industry, nitriles are e.g. prepared by addition of HCN to alkenes and by catalytic oxidation of alkenes and ammonia with air.²⁸ On laboratory scale, nitriles can be prepared by reaction of alkali metal cyanides (alkali metal salts of hydrogen cyanide) with alkyl halides (Kolbe nitrile synthesis).²⁹ Other possibilities are the dehydration of aldoximes with for example phosphorus pentachloride (PCl_5).³⁰

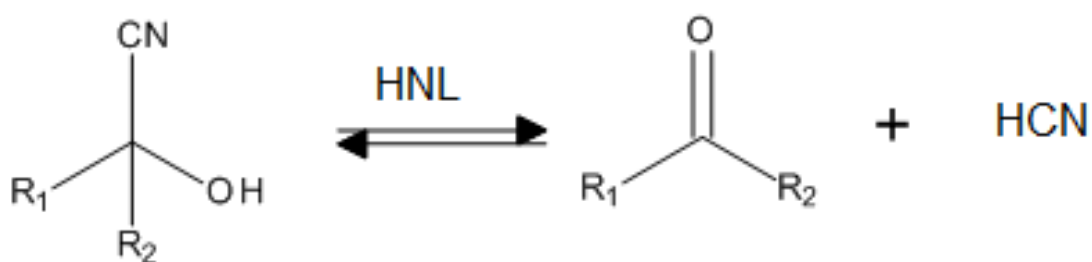
Since these synthetic reactions take place mostly under harsh conditions, a one step enzymatic reaction, where a nitrile is generated may be of interest for the industry.

Enzymatically, 7-cyano-7-deazaguanine synthases, aldoxime dehydratases and hydroxynitrile lyases can be used for nitrile production from different substrates.^{31,32}

Aldoxime dehydratases catalyse the dehydration of aldoximes to nitriles. For example, arylalkylaldoximes or alkylaldoximes can be converted to the corresponding nitriles in one enzymatic step. During this reaction, no elongation of one carbon

atom during nitrile formation takes place, similar to 7-cyano-7-deazaguanine synthase.³²

Hydroxynitrile lyases (HNLs) catalyse the reversible stereoselective addition of hydrogen cyanide (HCN) to aldehydes and ketones (see scheme 3). HNLs are already known as industrial biocatalysts for the synthesis of chiral cyanohydrins, which are important building blocks for pharmaceuticals and agrochemicals.^{33,31}



Scheme 3: Reaction scheme the Hydroxynitrile lyase reaction³⁴

2 Objectives

Very little is known about 7-cyano-7-deazaguanine synthases, its mechanism and requirements. The aim of this work was the cloning, expression and characterisation of 7-cyano-7-deazaguanine synthases from different organisms. In a second part of this work, a suitable assay was developed and the substrate scope of these enzymes (7-cyano-7-deazaguanine synthases) that can convert a carboxylic acid to a nitrile explored. In addition, particular steps of the biosynthetic pathway were reconstructed.

3 Experimental Procedures

3.1 Plasmid, strains and primers

3.1.1 Plasmid

The pEHisTEV cloning vector was used for protein expression in *Escherichia coli* BL21 (DE3) gold (see figure 2). It has a polyhistidine (6xHis) tag near the multiple cloning site (MCS), to get N-terminally linked to the inserted gene. The expression of the gene of interest is regulated by the T7 promoter. The pEHisTEV cloning vector contains a kanamycin resistance gene. Further, the His tag is cleavable using TEV-protease.

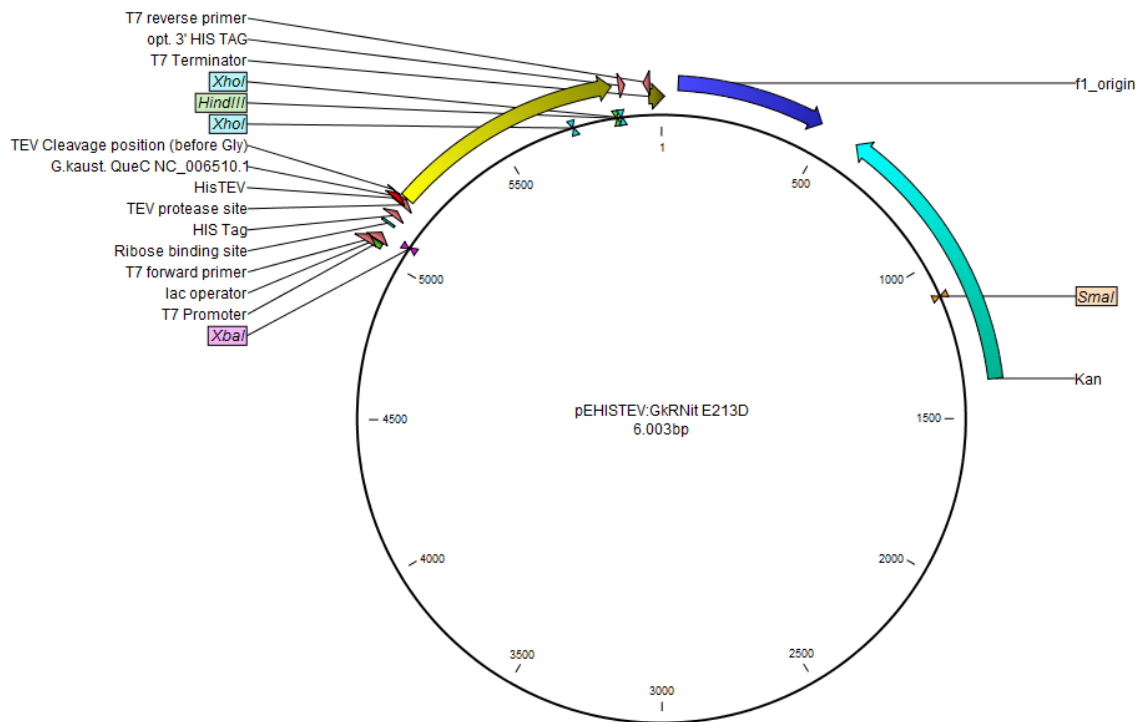


Figure 2: The pEHisTEV cloning vector.

3.1.2 Strains

3.1.2.1 Strain for transformation:

Escherichia coli Top10F', genotype: F' $\{lacIq, Tn10(TetR)\}$ *mcrA* $\Delta(mrr-hsdRMS-mcrBC)$ $\Phi80lacZ\Delta M15 \Delta lacX74$ *recA1* *araD139* $\Delta(ara leu)$ 7697 *galU galK rpsL* (Str^R) *endA1 nupG*, Invitrogen, Carlsbad, USA¹⁰

3.1.2.2 Strain for expression:

Escherichia coli BL 21 (DE3) Gold, genotype: F⁻ *ompT hsdSB*(rB⁻, mB⁻) *gal dcm* (DE3), Invitrogen, Carlsbad, USA¹⁰

3.1.3 Enzymes

Restriction enzymes	Restriction sequence	Specification	Source
XbaI	5'...TCTAGA...3' ' 3'...AGATCT...5' '	1FDU/μL	FastDigest XbaI, Thermo Scientific – Austria GmbH, Vienna, Austria
XhoI	5'...CTCGAG... 3' 3'...GAGCTC... 5'	1FDU/μL	FastDigest XhoI, Thermo Scientific – Austria GmbH, Vienna, Austria
NdeI	5'...CATATG...3' ' 3'...GTATAC...5' '	1FDU/μL	FastDigest NdeI, Thermo Scientific – Austria GmbH, Vienna, Austria
HindIII	5'...AAGCTT...3' ' 3'...TTCGAA...5' '	1FDU/μL	FastDigest HindIII, Thermo Scientific – Austria GmbH, Vienna, Austria
Enzymes		Concentration	Source
T4 DNA-Ligase		5U/μL	Thermo Scientific – Austria GmbH, Vienna, Austria
PhusionR high fidelity DNA polymerase		2U/μL	New England Biolabs, Ipswich, USA
GkNRedWT (nitrile reductase from <i>G. kaustophilus</i> wild type)			Margit Winkler ACIB GmbH, Graz, Austria

3.1.4 Primers, sequencing primers and G-blocks

Primer	Sequence [5'-3']	T _m [°C]	Source
Fw-Vector pHisTev	AAGCTTGCGGCCG- CACTCGAGCACCAC- CAC	74	IDT, integrated DNA technologies, Inc., USA
Re-Vector pHisTev	CATGGCGCCCTGAAAAT ACAGGTTTTCGGTCGTT GGG	71.9	IDT, integrated DNA technologies, Inc., USA
P42002 pEHisTEV Fw	AAGCTTGCGGCCG- CACTCGAG	65.3	IDT, integrated DNA technologies, Inc., USA
P42001 pEHis TEV Re	GGC GCC CTG AAA ATA CAG GTT TTC GGT CG	64.7	IDT, integrated DNA technologies, Inc., USA
T7 prom	TAATACGACTCAC- TATAG	44.5	IDT, integrated DNA technologies, Inc., USA
T7 term	GTCAG- TTATTGCTCAGCG	53.4	IDT, integrated DNA technologies, Inc., USA
G-block		source	
G-block of QueC <i>B. subtilis</i>		IDT, integrated DNA technologies, Inc., USA	
G-block of QueC <i>S. rimosus</i>		IDT, integrated DNA technologies, Inc., USA	
G-block of QueC <i>P. atrosepticum</i>		IDT, integrated DNA technologies, Inc., USA	
G-block of QueC <i>A. flavithermus</i>		IDT, integrated DNA technologies, Inc., USA	
G-block of QueC <i>A. sulficallidus</i>		IDT, integrated DNA technologies, Inc., USA	
G-block of QueC <i>C. sativus</i>		IDT, integrated DNA technologies, Inc., USA	

3.2 Equipment and devices

3.2.1 Electroporator and associated materials

MicroPulser™ Electroporator, BIO-RAD, USA

Electroporation Cuvettes, cell projects, Kent, United Kingdom

3.2.2 Centrifuges and associated materials

Centrifuge 5810 R, Eppendorf AG, Hamburg, Germany

Centrifuge 5415 R, Eppendorf AG, Hamburg, Germany

Avanti™ centrifuge J-20 XP/ Beckman Coulter™, Inc, Vienna, Austria

Nalgene® Labware 500mL PPCO Centrifuge Bottlers, Thermo Scientific, Rochester, NY, USA

Ultracentrifuge Optima LE80K/ Beckman Coulter™, Inc, Vienna, Austria

3.2.3 Fast protein liquid chromatography (FPLC) and associated materials

ÄKTA Purifier 100 with Frac-950, GE Healthcare Europe GmbH, Vienna, Austria

ÄKTA Prime, GE Healthcare Europe GmbH, Vienna, Austria

HiLoad™ 16/60 Superdex™ 200 prep grade 120 mL, GE Healthcare Europe GmbH, Vienna, Austria

HiPrep™ 26/10 Desalting 53 mL, GE Healthcare Europe GmbH, Vienna, Austria

His trap™ FF, 5 mL, GE Healthcare Europe GmbH, Vienna, Austria

Cellulose acetate filter, 0.2 µm pore size, Sartorius Mechatronics Austria GmbH, Vienna, Austria

Sample Pump P-950, GE Healthcare Europe GmbH, Vienna, Austria

Diaphragm pump, VACUUBRAND GMBH + CO KG, Wertheim, Germany

Polysulfone reusable bottle top filter holder, Nalge Nunc International Corporation, Rochester, NY, USA

3.2.4 Gel electrophoresis and associated materials

3.2.4.1 Agarose gel electrophoresis

PowerPac™ Basic Power supply: Bio-Rad Laboratories, Vienna, Austria

Sub-cell GT, Bio-Rad Laboratories: Vienna, Austria

Chroma 43 medium-wave 302 nm: Laborgeräte Vetter GmbH, Wiesloch, Germany

Biozym LE Agarose: Biozym Biotech Trading GmbH, Vienna, Austria

6x DNA Gel loading dye: Thermo Fisher Scientific Inc., Waltham, MA, USA

GeneRuler™ 1kb DNA Ladder: Thermo Fisher Scientific Inc., Waltham, MA, USA

3.2.4.2 SDS-Page

PowerEase 500 power supply: Invitrogen™ life technologies, Lofer, Austria

XCell SureLock™ Mini-cell: Invitrogen™ life technologies, Lofer, Austria

Bolt® 4-12% Bis-Tris Plus Gels, 10-well, Life Technologies, Vienna, Austria

Bolt® 4-12% Bis-Tris Plus Gels, 15-well, Life Technologies, Vienna, Austria

3.2.5 High performance liquid chromatography-UV (HPLC) and associated materials

3.2.5.1 HPLC-UV Agilent 1100 series

G1316A thermostated column compartment (TCC)

G1321B fluorescence detector (1260 FLD)

G1379A degasser

G311A quaternary pump

G1367A high performance autosampler WPLAS

G1330B ASL thermostat

G1316A thermostated column compartment

G1315B diode array detector

G1364C fraction collector

3.2.5.2 HPLC-MS Agilent 1200 series

G1379B degasser

G1312B binary pump SL

G1367C high performance autosampler SL

G1310A isocratic pump

G1314 variable wavelength detector SL

6120 Agilent Technologies, quadrupole LC/MS detector with a G1918B electrospray ionization source

G1316B thermostated column compartment

3.2.5.3 Columns

Chromolith performance RP 18E 4.6x100 mm HPLC Column

Phenomenex Gemini® NX 3 C18 110 Å, LC column (150 x 2.0 mm, Ea) with a SecurityGuard™ Cartridge 4 x 2.0 mm column

3.2.6 **NMR spectrometer**

Varian/Agilent INOVA NMR spectrometer, Agilent Technologies, Inc., USA

3.2.7 **Pipettes and micropipettes and devices**

peqPETTE one-canal pipettes (1000µL, 200µL, 20µL, 10µL, 2µL): PEQLAB Biotechnologie GmbH, Erlangen, Germany

Pipette tips 200, Greiner Bio-One GmbH, Frickenhausen, Germany

Pipette tips 1000, Greiner Bio-One GmbH, Frickenhausen, Germany

Pipette tips, micro P10, Greiner Bio-One GmbH, Frickenhausen, Germany

Biohit® Tips 300µL, Biohit Plc., Helsinki, Finland

Biohit® Tips 1200µL, Biohit Plc., Helsinki, Finland

Biohit Proline® multichannel electronic pipettor, 5-100µL: Biohit Plc., Helsinki, Finland

3.2.8 **PCR-cyclers and associated materials**

2720 Thermal cycler, Applied Biosystems, Singapore

7500 Real Time PCR system, Applied Biosystems, Singapore

MicroAMP® optical 96-well reaction plate, Applied Biosystems, Foster City, USA

MicroAMP® optical adhesive covers, Applied Biosystems, Foster City, USA

3.2.9 **Photometer and associated materials**

Nanodrop 2000c Spectrophotometer, PEQLAB Biotechnologie, Germany

BioPhotometer Plus, Eppendorf AG, Hamburg, Germany

Cuvettes (10 x 4 x 45mm), Sarstedt, Germany

3.2.10 Reaction vessels

Micro-centrifuge tubes, 1.5mL with lid, Greiner Bio GmbH, Frickenhausen, Germany

50mL Greiner tube, Greiner Bio GmbH, Frickenhausen, Germany

15mL Greiner tube, Greiner Bio GmbH, Frickenhausen, Germany

300mL shaking flasks with baffles, Greiner Bio GmbH, Frickenhausen, Germany

2L shaking flasks with baffles, Greiner Bio GmbH, Frickenhausen, Germany

3.2.11 Shakers and incubators

Titramax 1000, Heidolph Instruments, Schwabach, Germany

RS 306 rotary shaker (50 mm), Infors AG, Bottmingen-Basel, Switzerland

Thermomixer comfort (1.5mL), Eppendorf AG, Hamburg, Germany

Multitron II incubator shaker, Infors AG, Bottmingen-Basel, Switzerland

Binder drying oven, Binder GmbH, Tuttlingen, Germany

3.2.12 Additional instruments and materials

Vortex-Genie 2, Scientific Industries Inc., Bohemia, NY, USA

Vivaspin 20 centrifugal concentrators, Sartorius AG, Göttingen, Germany

ABS 220-4 analytical balance, Kern & Sohn GmbH, Balingen, Germany

GP3202 Precision Balance, Sartorius AG, Göttingen, Germany

3.3 Reagents, buffers, stocks and media

3.3.1 Reagents

Reagent	Source
Acetonitrile (HPLC grade)	Avantor Performance Materials B. V., Deventer, Netherlands
Ammonium acetate	Sigma-Aldrich Handels GmbH, Vienna, Austria
ATP	Roche Diagnostics GmbH, Mannheim, Germany
Aqua bidest.	Fresenius Kabi GmbH, Graz, Austria
Chloroform	Carl Roth GmbH, Karlsruhe, Germany

DTT	Carl Roth GmbH, Karlsruhe, Germany
DMSO	Carl Roth GmbH, Karlsruhe, Germany
Ethanol	Merck KGaA, Darmstadt, Germany
Ethidium bromide (>98%)	Carl Roth GmbH, Karlsruhe, Germany
Formaldehyde	Carl Roth GmbH, Karlsruhe, Germany
Formic acid	Carl Roth GmbH, Karlsruhe, Germany
HCl (37%)	Merck KGaA, Darmstadt, Germany
HEPES	Sigma-Aldrich Handels GmbH, Vienna, Austria
NaOH	Carl Roth GmbH, Karlsruhe, Germany
GeneJET Plasmid Miniprep Kit	Fermentas-Thermo Fisher Scientific, Germany
GeneRuler™ 1kb Plus DNA Ladder	Fermentas-Thermo Fisher Scientific, Germany
GeneRuler™ DNA Ladder Mix	Fermentas-Thermo Fisher Scientific, Germany
Glycerol	Carl Roth GmbH, Karlsruhe, Germany
Imidazole	Carl Roth GmbH, Karlsruhe, Germany
Magnesiumchloride heptahydrate	Carl Roth GmbH, Karlsruhe, Germany
Methanol (>99.8%)	Carl Roth GmbH, Karlsruhe, Germany
NADPH	Carl Roth GmbH, Karlsruhe, Germany
Sodium chloride (NaCl)	Sigma-Aldrich Handels GmbH, Vienna, Austria
Sodium hydroxide (NaOH)	Carl Roth GmbH, Karlsruhe, Germany
PageRuler™ Prestained Protein Ladder (10 to 170kDa)	Fermentas GmbH, St.Leon-Rot, Germany
Phusion Buffer HF	Fermentas-Thermo Fisher Scientific, Germany
Phusion DNA Polymerase	Fermentas-Thermo Fisher Scientific, Germany
Potassium dihydrogen phosphate (KH ₂ PO ₄)	Carl Roth GmbH, Karlsruhe, Germany
Potassium hydrogen phosphate (K ₂ HPO ₄)	Carl Roth GmbH, Karlsruhe, Germany
Simply Blue™ Safe Stain	Life Technologies, Vienna, Austria
NuPAGE® LDS Sample Buffer (4X)	Life Technologies, Vienna, Austria
NuPAGE® MOPS SDS Running Buffer (20X)	Life Technologies, Vienna, Austria

T4 DNA Ligase and T4 DNA Ligase Buffer	Fermentas-Thermo Fisher Scientific, Germany
Wizard® SV Gel and PCR Clean-Up System	Promega
2-amino-4-oxopyrrolo(2,3- <i>d</i>)pyrimidin-5-carboxylic acid (CDG)	Birgit Wilding, Institute of Organic Chemistry, Graz University of Technology and ACIB GmbH, Austria
2-amino-4-oxo-4,7-dihydro-3 <i>H</i> -pyrrolo(2,3- <i>d</i>)pyrimidine-5-carbonitrile (preQ ₀)	Birgit Wilding, Institute of Organic Chemistry, Graz University of Technology and ACIB GmbH, Austria
2-amino-5-aminomethylpyrrolo[2,3- <i>d</i>] pyrimidin-4(3 <i>H</i>)-one (preQ ₁)	Birgit Wilding, Institute of Organic Chemistry, Graz University of Technology and ACIB GmbH, Austria
Benzoic acid	Sigma-Aldrich Handels GmbH, Vienna, Austria
Phenylacetic acid, Cinnamic acid, Indole-3-carboxylic acid, Pyrrole-2-carboxylic acid, Propionic acid, Mandelic acid, Nicotinic acid	Birgit Wilding, Institute of Organic Chemistry, Graz University of Technology and ACIB GmbH, Austria
2-methyl-4-oxo-4,5,6,7-tetrahydro-1 <i>H</i> -indole-3-carboxylic acid	Matrix Scientific GmbH, Columbia, USA
Pyridinecarboxylic acid	Sigma-Aldrich Handels GmbH, Vienna, Austria
Pyrazinecarboxylic acid	Sigma-Aldrich Handels GmbH, Vienna, Austria
Sypro Orange fluorescence dye	Molecular Probes, Life Technologies

3.3.2 Stocks

3.3.2.1 Antibiotics

Antibiotics	Concentration	Storage	Source
Ampicillin sodium salt	100mg/mL	-20°C	Ampicillin sodium salt, Sigma Aldrich GmbH, Schnelldorf, Germany
Kanamycin sulphate	100mg/mL	-20°C	Carl Roth GmbH, Karlsruhe, Germany

3.3.2.2 Additional stocks

Stock	Stock-concentration	Storage	solvent
IPTG	1M	-20°C	ddH ₂ O
ATP	25mM	-20°C	ddH ₂ O
NADPH	10mM	-20°C	ddH ₂ O
CDG	50mM	-20°C	ddH ₂ O
PreQ ₀	50mM	-20°C	ddH ₂ O
PreQ ₁	50mM	-20°C	ddH ₂ O

3.3.3 Media and buffers

E. coli media	LB ^{Kan} agar plates	10g/L tryptone, 5g/L yeast extract, 10g/L NaCl, 15g/L agar, 50mg/L kanamycin
	LB medium	10g/L tryptone, 5g/L yeast extract, 5g/L NaCl, 15g/L agar, 50mg/L kanamycin
	SOC medium	20g/L bacto tryptone, 0.58g/L NaCl, 5g/L bacto yeast extract, 2g/L MgCl ₂ , 0.16g/L KCl, 2.46g/L MgSO ₄ , 3.46g/L dextrose
SDS-Page	NuPAGE® MOPS SDS Running Buffer (20X), Life Technologies	50mM MOPS, 50mM Tris Base, 0.1% SDS, 1mM EDTA, pH 7.7
	NuPAGE® LDS Sample Buffer (4X)	780µL dissociation buffer, 200µL Tris-HCl buffer, pH8.8, 20µL β-mercaptoethanol
Activity Assay	QueC Buffer 1	20mM HEPES/NaOH, pH 7.5, 100mM NaCl, 10mM MgCl ₂ , 10 mM DTT and 5 mM ammonium sulfate
	QueC Buffer 2	40mM HEPES/NaOH, pH 7.5, 200mM NaCl, 20mM MgCl ₂ and 10 mM DTT
	QueC Buffer 3	100mM Hepes, (NaOH to pH 7.5), 200mM NaCl and 20mM MgCl ₂ and 10mM DTT
Protein purification	Buffer A	20mM potassium phosphate, 500mM KCl, 40mM Imidazole, pH7.2
	Buffer B	20mM potassium phosphate, 500mM KCl,

		500mM Imidazole, pH7.2
	Desalting Buffer	20mM HEPES, 20mM NaOH
<i>in vitro</i> reconstruction	NRed buffer	100mM Tris/HCl, 50mM KCl, 1mMTris(2 - carboxyethyl) phosphine hydrochloride (TCEP), pH 7.5 ⁸

3.3.3.1 LB-medium (Low Salt Luria Bertani)

20g/L LB-medium was dissolved in ddH₂O and autoclaved. After heat dissipation to at least 55°C, antibiotics were added, if necessary.

3.3.3.2 LB-agar

35g/L LB- agar were dissolved in ddH₂O and autoclaved. After heat dissipation to at least 55°C, antibiotics were added as described before.

3.4 Software and web tools

3.4.1 Software

PyMOL, DeLano Scientific LLC, Palo Alto, USA

ChemSketch, Advanced Chemistry Development, Inc., Toronto, Canada

Gene Designer 2.0, DNA 2.0, Inc., USA

CLC-Main Workbench 7, CLC Bio EMEA (Qiagen), Aarhus C, Denmark

APE-Plasmid Editor, Biology Labs Online (California State University System and Pearson Inc.), USA

Software Unicorn™ 6.3, GE Healthcare Europe GmbH, Vienna, Austria

Software PrimeView 5.0, Life Sciences, GE Healthcare Europe GmbH, Vienna, Austria

3.4.2 Web tools

Calculation of MW and pI, http://web.expasy.org/compute_pi/

Multiple sequence alignment, <http://www.ebi.ac.uk/Tools/msa/clustalw2/>

Translation, <http://web.expasy.org/translate/>

Calculation of molar Ratio, <http://bioinfo.clontech.com/infusion/molarRatio.do>

Literature search, <http://www.ncbi.nlm.nih.gov/>; www.scopus.com/home.url,

BLAST (Basic Local Alignment Search Tool), <http://blast.ncbi.nlm.nih.gov/Blast.cgi>

3.5 Kits and methods

3.5.1 GeneJET™ Plasmid Miniprep Kit

In order to produce sufficient cell material, *E. coli* colonies were streaked out on LB^{Kan} media plates and incubated overnight at 37°C. The cell material was taken with a sterile toothpick. Isolation of the pEHsTEV- vector from *E. coli* TOP10F' cells and *E. coli* BL21 cells was performed as described in the manual of GeneJET™ Plasmid Miniprep Kit. The plasmid-DNA was eluted with 40µL nuclease-free water, tempered on 60°C. The concentration of isolated plasmid-DNA was determined with the Nanodrop 2000c Spectrophotometer.

3.5.2 Wizard® SV Gel and PCR Clean-Up System

DNA purification was performed with the Wizard® SV Gel and PCR Clean-Up System, according to the protocol for use of this promega-kit. The DNA was eluted with 50µL nuclease-free water. The concentration of the purified DNA was measured with Nanodrop 2000c Spectrophotometer.

3.5.3 General methods

3.5.3.1 *E. coli* transformation

For the transformation with electroporation, the frozen electrocompetent *E. coli* TOP10F' cells were defrosted on ice and mixed with 2 - 4µL of desalted DNA. The mixture was transferred to electroporation cuvettes and incubated on ice for 5 minutes. The cell-mixture got pulsed with the MicroPulser™ using program EC2, for 5 to 6ms at 2.5kV. Afterwards, 600µL of SOC medium were added to the cuvette and the solution was transferred to a sterile reaction vessel. After transformation, the cells were incubated for 35 minutes at 37°C and 300 rpm. Depending

on the transformation rate, aliquots or the whole cell suspension was plated on LB^{Kan} agar-plates and incubated overnight at 37°C.

3.5.3.2 Agarose gel electrophoresis

To determine the size of a DNA fragment either a preparative agarose gel or an analytical 1% agarose gel was used to visualize the DNA. GeneRuler™ DNA ladder mix was used as DNA standard. 2.5g of agarose and 250mL of 1x TAE buffer were mixed and heated to dissolve the agarose by using a microwave. Ethidium bromide was added for visualizing the DNA. To cure the mixture, it was poured into a gel chamber. Analytical control gels were run for 45 minutes at 120V (volts). Preparative agarose gels were run for 1.5 hours at 90V. For loading the DNA on the gel, 6x mass ruler DNA loading dye, or 10x FastDigest Green buffer for direct loading were used. Gels were analysed under UV light. If necessary, bands of interest were cut out with a scalpel from the preparative agarose gel and gel pieces were collected in reaction vessels. DNA was purified using Wizard® SV Gel and PCR Clean-Up System.

3.5.3.3 Preparation of glycerol stocks

For preparation of an overnight culture (ONC) cell material from the desired *E. coli* strain was picked with a sterile toothpick and 20mL LB medium with the respective antibiotic inoculated. The cell suspension was incubated at 37°C overnight. For 1mL glycerol stock, 500µL ONC, 250 µL 50% glycerol and 250 µL LB^{Kan} medium were mixed carefully and filled into sterile cryogenic tubes. The glycerol stocks with an end concentration of 12.5% glycerol were stored at -80°C.

3.5.4 **Construction of protein expression strains**

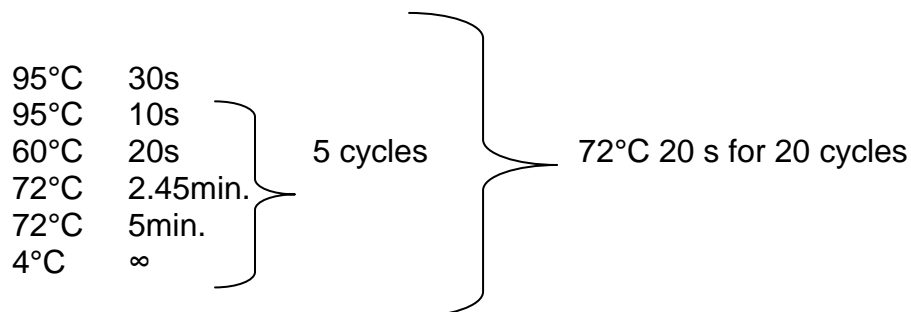
3.5.4.1 Amplification of the pEHisTEV vector

The vector pEHisTEV was amplified via PCR. Therefore, the primers “FW p42001” and “RE p42002” (see primers and sequencing primers) were used. First of all, the primers for the amplification were diluted with ddH₂O to a stock concentration of 100pmol. Subsequently, the stocks got diluted to a working concentration of 10pmol/µL. The PCR reaction was set up as follows:

1 μ L template DNA (5ng/ μ L pEHisTEV plasmid)
1 μ L forward primer (10pmol/ μ L)
1 μ L reverse primer (10pmol/ μ L)
1 μ L dNTPs (100mM)
10 μ L phusion buffer HF (5x)
1 μ L Phusion polymerase (1kb/30sec.)
35 μ L ddH₂O

50 μ L total reaction volume

The pEHisTEV vector with a size of 5343bp was amplified with the primer pair from above, using the following PCR cycling conditions:



Afterwards, the PCR sample was loaded on a preparative agarose gel and an agarose gel electrophoresis was performed. The specific bands were isolated and the DNA of the pEHisTEV plasmid was purified with the Wizard® SV Gel and PCR Clean-Up System. The DNA concentration was measured via Nanodrop.

3.5.4.2 Gibson cloning

G-blocks of several 7-cyano-7-deazaguanine synthase genes and primers for amplification of the pEHisTEV-vector were ordered from Integrated DNA Technolo-

gies, Inc.. Amplified vector DNA was controlled by sequencing. G-blocks were diluted in ddH₂O to a concentration of 20ng/μL. With the webtool “molarRatio” the concentrations of vector and gene with a total volume of 5μL for the ligation mixture were calculated. Further, ligation mixture and Gibson master mix were combined and the ligation procedure was performed for 1 hour at 50°C in a PCR-machine. Afterwards the samples were desalted for 45 minutes on a filter membrane (Millipore MFTM membrane filter 0.025μm VSWP), which floated on ddH₂O in a petri-dish.¹¹

With the intention to control the ligation, a digest with the restriction enzymes XbaI and XhoI was performed using 10μL of each sample. The digest took place under the conditions as follows:

1μL XbaI (FastDigest)
1μL XhoI (FastDigest)
10μL Plasmid sample
2.2μL 10x FastDigest green buffer
8μL H₂O RNase free

22.2μL reaction volume

The double digest was performed for 30 minutes at 37°C and restriction enzymes were inactivated at 80°C for 10 minutes.

1μL of each sample, mixed with 6x DNA loading dye, was loaded onto a preparative agarose gel for analysis. Finally, the plasmids generated by Gibson cloning were transformed into electro competent *E. coli* Top10F' cells. Subsequently, the samples were sent for sequencing and those with positive sequences were selected and transformed into *E. coli* BL21 cells.

After a small scale cultivation, none of the cultivates showed an overexpression of the protein 7-cyano-7-deazaguanine synthase. We assumed that the pEHisTEV vector was nonfunctional. The already cloned constructs were double digested with HindIII and NdeI, and the resulting inserts were used for a classical cloning, described below.

3.5.4.3 Vector opening, QueC fragments preparation and ligation

To linearise the vectors and to remove the current insert HNL-1, the vector pEHis-TEV containing QueC-inserts (created by Gibson cloning) and the vector pEHis-TEV containing HNL-1 insert were cleaved with NdeI and HindIII. Samples for the double digest of vector pEHisTEV with different QueCs were prepared as shown in table 1.

Table 1: Sample preparation scheme for the double digest with NdeI and HindIII of vector pEHisTEV with different QueCs.

Protein and host organism	Amount DNA [ng]	Vol. DNA [μ L]	NdeI [μ L]	HindIII [μ L]	R buffer [μ L]	H ₂ O [μ L]	Total volume [μ L]
ToyM <i>S. rimosus</i>	3000	42	6	3	6	3	60
QueC <i>C. sativus</i>	4000	42	8	4	6	0	60
QueC <i>A. flavithermus</i>	3100	42	6,2	3.1	6	3	60.3
QueC <i>B. subtilis</i>	2500	42	5	2.5	6	5	60.5
QueC <i>P. atrosepticum</i>	4000	42	8	4	6	0	60
QueC <i>A. sulficallidus</i>	5000	42	10	5	7	6	70

The digestion was performed for 2.5 hours at 37°C. Afterwards, restriction enzymes were inactivated at 75° for 5 minutes.

For the double digest of vector pEHisTEV with the HNL-1 insert, FastDigest enzymes NdeI and HindIII were used to create complementary single stranded ends. The digest was performed using conditions as follows and was performed for 30 minutes at 37°C:

17 μ L vector-DNA (5000ng)
5 μ L HindIII (FastDigest)
5 μ L NdeI (FastDigest)
5 μ L 10x FastDigest green buffer
18 μ L H₂O RNase free

50 μ L reaction volume

The enzymatical digest was inactivated thermally in an Eppendorf Thermomixer at 80°C for 10 minutes.

Samples from both double digests were purified using a preparative agarose gel and subsequent extraction with the Wizard® SV Gel and PCR Clean-Up System. The DNA-concentration was measured with a Nanodrop 2000c spectrophotometer.

Vector and insert fragments were ligated by T4-ligase.

The summary of ligation reactions is shown in table 2.

Table 2: T4 Ligation preparation scheme of the vector and the QueCs fragments from different organisms

Vector ID	Insert ID	Vector [μL]	Insert [μL]	Ligase [μL]	Bf 10x [μL]	H ₂ O [μL]	Sum [μL]
pEHisTEV	ToyM <i>S. rimosus</i>	2	5.6	1	2	9.4	20
pEHisTEV	QueC <i>A. flavithermus</i>	2	4.6	1	2	10.4	20
pEHisTEV	QueC <i>C. sativus</i>	2	4.3	1	2	10.7	20
pEHisTEV	QueC <i>A. sulficallidus</i>	2	0	1	2	15	20
pEHisTEV	QueC <i>P. atrosepticum</i>	2	4.4	1	2	10.6	20
pEHisTEV	QueC <i>B. subtilis</i>	2	6	1	2	9	20
pEHisTEV	Negative control	2	0	1	2	15	20

The ligation was performed for 1 hour at room temperature. Finally, the ligation-samples were desalted for 50 minutes on a filter membrane (Millipore MF™ membrane filter 0.025μm VSWP), which floated on ddH₂O in a petri-dish and 5μL were transformed into electro competent *E. coli* Top10F' cells. A further transformation into *E. coli* BL21 (DE3) strain was done in parallel for protein expression.

3.5.4.4 Cloning of 7-cyano-7-deazaguanine synthase from *G. kaustophilus* and *Escherichia coli*

The gene encoding QueC was amplified from *G. kaustophilus* HTA426, with primers GkQueC f 5'-cat cac gat tac gac atc cca acg acc gaa aac ctg tat ttt cag ggc gcc atg atg aag atg aat gaa gaa aag gcg g-3' and GkQueC r 5'-gcc gga tct cag tgg tgg tgg tgg tgc tgc agt gcg gcc gca agc ttt tat cgc gac tcc acc tcc gct ttt tc-3' and Phusion DNA polymerase according to the manufacturer's protocol. With the primers pEHisTEV Gibson f 5'- aag ctt gcg gcc gca ctc gag-3' and pEHisTEV Gibson r 5'- gcc gcc ctg aaa ata cag gtt ttc ggt cg-3' the vector backbone was ampli-

fied from a pEHisTEV construct.³⁵ The vector backbone and the required gene coding for the 7-cyano-7-deazaguanine synthase were assembled using Gibson cloning.¹¹

After two separate cloning experiments the construct pEHisTEV:GkQueC with 6 point mutations in the coding DNA sequence (CDS) compared to accession NC_006510.1 (location 1000474–1001148, locus_tag “GK0975”) has been produced. Electro competent *E. coli* Top10F’ cells were used to amplify and maintain the construct. The *E. coli* BL21 (DE3) strain was used for protein expression.³⁵

3.5.4.5 Sequencing

Sequencing was performed by Microsynth AG. 1000ng of each DNA-fragment plus primers were sent for sequencing to the company in a reaction vessel. The resulting sequences were analysed with the software CLC-Main Workbench 7.

3.5.5 **Cultivation and protein expression**

3.5.5.1 Small scale cultivation

20mL LB^{Kan} medium was inoculated with a single colony of the strain of interest and grown at 37°C overnight (overnight culture). This overnight culture was used to inoculate the main culture, consisting of 150mL LB^{Kan} medium in 300mL baffled Erlenmeyer flasks. The cultures were grown at 37°C and 110rpm. At an OD₆₀₀ between 0.6 and 0.8, the cells were induced with 150µL 1M IPTG and 15µL 1M ZnSO₄ and incubated for 16 hours at 37°C. In order to harvest the cells, the main culture was centrifuged at 4,000 rpm for 10 minutes at 4°C. The resulting pellet was either treated with the BugBuster lysis kit for analytical purposes or frozen at -20°C until further use.

3.5.5.2 Large scale cultivation

20mL LB^{Kan} medium was inoculated with a single colony and grown at 37°C overnight. This overnight culture was used to inoculate the main culture, consisting of 500mL LB^{Kan} medium in 2-L baffled Erlenmeyer flasks. The cultures were grown at 37°C and 110rpm. At an OD₆₀₀ between 0.6 and 0.8, the cells were induced with 0.5mL of 1M IPTG, 50 µL 1M ZnSO₄ and incubated for 16 hours at 37°C. In order to harvest the cells the main culture was centrifuged at 4,000rpm for 10 minutes at 4°C. The pellet was resuspended in buffer A and disrupted by ultrasonication. The

cell fragments were separated from the soluble proteins by ultracentrifugation at 40,000 rpm for 45 min and 4 °C. Finally, the proteins were purified using Ni-affinity chromatography.

3.5.5.3 Protein purification

Proteins were purified by Ni-affinity chromatography using the ÄKTA Purifier 100 with the fraction collector Frac-950. The supernatant from cultivation and centrifugation procedure containing buffer-A was used for loading the His Trap™ FF column (5mL). Buffer-B was used for elution. The enzyme containing fractions were pooled and rebuffed in desalting buffer using the ÄKTA Pure System equipped with a HiPrep™ 26/10 Desalting (53 mL) column. During this procedure, all solutions and samples were stored on ice. After rebuffing, the protein solutions were concentrated to a concentration between 10 and 15mg/mL by centrifugation and stored at -20°C.

3.5.5.4 SDS-Page to control expression levels of the different 7-cyano-7-deazaguanine synthases

5µL sample, 2.5µL NuPAGE LDS Sample Buffer (4X), 1.5µL deionized water and 1µL 500 mM DTT as a reducing agent were combined to a total reaction volume of 10µL and heated for 10 minutes at 70 °C. Afterwards, the samples were loaded on NuPAGE® Bis-Tris gels. 7µL of Page Ruler Prestained Protein Ladder 10-170kDa was used as standard.

Run conditions:

- Voltage: 200 V constant
- Run Time: 40 minutes with MOPS Buffer

Protein bands were visualized by treating the gel for 1 hour with Simply Blue solution. Afterwards, the gel is washed 2 times and destained in H₂O.

3.5.5.5 BugBuster lysis

A cell amount with OD₆₀₀ of 5 was centrifuged 5 minutes at 13.2 krpm. The supernatant was discarded and the cell pellet resuspended in 400µL CellLytic B Cell Lysis solution. After incubation for 10 minutes at room temperature the sample was resuspended by vortexing for another 10 minutes on the Vortex Genie 2. The next centrifugation step (5 minutes and 13.2 krpm) lead to the first cell pellet

(sample 1) which was resuspended in 200 μ L 6M urea. The supernatant was centrifuged again for 30 minutes at 13.2 krpm. The supernatant was filled into a new vessel (sample 3) and the cell pellet was resuspended in 200 μ L 6M urea (sample 2). Thereafter, a SDS-PAGE was performed with these 3 samples.

3.6 Activity assays

All experiments were carried out in biological duplicates and technical triplicates.

3.6.1 *In vitro* activity assay for characterisation of 7-cyano-7-deazaguanine synthases

A reaction solution was prepared, by combining 7-cyano-7-deazaguanine synthase (15 μ L of a 10 mg/mL stock), CDG (1mM dissolved in 0.5 M KOH), 10 mM ATP and 5 mM (NH₄)₂SO₄, and filled up with buffer to a reaction volume of 100 μ L. Hepes buffer (100 mM), 200 mM NaCl, 20 mM MgCl₂ and 10 mM DTT were used as buffer system, adjusted to a pH of 7.5. Additionally, blanks for substrate (CDG) and product (preQ₀) were prepared, consisting of 1 mM substrate or product and buffer. Generally, the assay reaction was carried out at 30°C and 1,000 rpm on an Eppendorf Thermomixer. The reaction was stopped by adding MeOH (80% of the reaction volume), DMSO (20% of the reaction volume) and KOH (1M, 50% of the reaction volume). After centrifugation for 3 minutes at 13.4 krpm the supernatant was analyzed by HPLC.³⁵

3.6.2 Activity assay and calculation of the specific activity of 7-cyano-7-deazaguanine synthases

The *in vitro* activity assay was prepared as described above and performed for 1 hour at 30°C. Assuming linear increase of product concentration, the specific activity for the formation of preQ₀ was calculated as follows:

3.6.2.1 Calculation of enzyme activity

Depending on the protein amount (mg) in the samples, the specific enzyme activity was calculated and given in mU/mg.

$$\frac{5\text{mg}}{\text{mL}} * \frac{15\mu\text{L}}{100} \mu\text{L} = \frac{0.75\text{mg}}{\text{mL}} \text{enzyme in reaction}$$
$$\frac{0.16\mu\text{mol PreQ}_0}{60\text{min.}} = 2.67\mu\text{mol/min}$$

$$\frac{\frac{2.67\mu\text{mol}}{\text{min}}}{\frac{0.75\text{mg}}{\text{mL}}} = \frac{3.5\text{mU}}{\text{mg}} \text{ enzyme activity}$$

3.6.3 Activity assay for exploration of the reaction mechanism of 7-cyano-7-deazaguanine synthase

The preparations and measurements were done in cooperation with the Center of Medical Research in Graz, Austria and the group of Prof. Ruth Birner-Grünberger. The *in vitro* activity assay was performed with QueC from *G. kaustophilus* and was prepared as described above, for 20 minutes at 30°C and 600 rpm. The buffer system was once used with addition of DTT and once without. Samples of 20 µL were taken after 5, 10 and 20 minutes. The reaction in the samples was stopped with 80 µL ice-cold MeOH (quadruple amount of sample). After centrifugation for 10 minutes at 13 krpm, the supernatant was isolated from the pellet and dried with a speed vacuum system. Further, the samples were resolved in ACN for the measurement with capHPLC-FT.

3.6.3.1 Method for detection of ATP, ADP and AMP with capHPLC

The analysis of ATP, ADP and AMP were performed using a capHPLC Agilent 1100 with a HILIC PolyWAX LP 100-Å and a TSQ Quantum Ultra Mass Spectrometer (Thermo Fisher Scientific, USA). The detection was performed at a flow rate of 10 µL per minute for 35 minutes.

Solvent A: 10 mM ammonium acetate in ddH₂O

Solvent B: 10 mM ammonium acetate in 90% acetonitrile

A stepwise gradient was used starting with 100% solvent B for 12 minutes, decreased to 0% solvent B (100% solvent A) after 17 minutes, held from 17 to 30 minutes and equilibrated to 100% solvent B from 30 to 35 minutes.

3.6.4 HPLC based substrate and product detection

The carboxylic acid substrates and potential corresponding nitrile products in the samples were analyzed by HPLC using a Chromolith performance RP 18E 4.6x100 mm HPLC column or a Phenomenex Gemini® NX 3 C18 110 Å, LC column (150 x 2.0 mm) with a SecurityGuard™ Cartridge 4 x 2.0 mm column. For

each column and substrate a specific method was used, to ensure specific separation and analysis.

3.6.4.1 Method „KDO CDG“ for HPLC-UV and HPLC-MS

The analysis was carried out using a Chromolith Performance RP 18E 4.6x100 mm HPLC column. The column temperature was set at 30°C. The analysis was performed at a flow of 1.2 mL/min over 5.5 minutes. At the beginning of the analysis, the mobile phase consisted of 100% 0.1% formic acid in deionised H₂O. After 0.5 minutes, a stepwise gradient was used starting with an increase of acetonitrile (ACN) to 30% within 3.5 minutes, increased to 100% ACN after 4 minutes, held from 4 to 4.5 minutes and re-equilibrated from 4.51 to 5.5 minutes.

3.6.4.2 Method „Phenomenex PreQ₀“ for HPLC-MS

The analysis was carried out using a Phenomenex Gemini® NX 3 C18 110 Å, LC column (150 x 2.0 mm) with a SecurityGuard™ Cartridge 4 x 2.0 mm column. The mobile phase consisted of 20% ammonium acetate (20 mM) and 80% acetonitrile (ACN) at a flow rate of 0.2 mL/min and 20°C. A stepwise gradient was applied starting with 2% ACN for 6 minutes, increased to 40% ACN from 6.1 to 13 minutes, decreased to 2% ACN from 13.1 to 15 minutes and equilibrated from 15.1 to 20 minutes.

3.6.4.3 Method „Indole-method“ for HPLC-MS used for Indole-3-carboxylic acid, 2-methyl-4-oxo-4,5,6,7-tetrahydro-1H-indole-3-carboxylic acid and the corresponding nitriles

The analysis was carried out using a Chromolith Performance RP 18E 4.6x100 mm HPLC column. The column temperature was set at 30°C. The analysis was performed at a flow of 1.2mL/min over 7 minutes. The mobile phase consisted of 100% 0.1% formic acid in deionised H₂O. A stepwise gradient was used starting with an increase of acetonitrile (ACN) to 65% within 5 minutes, increased to 100% ACN after 5.5 minutes, held from 5.5 to 6 minutes and equilibrated from 6.01 to 7 minutes.

3.6.4.4 Method “Cinnamonnitrile” for HPLC-MS used for cinnamic acid and the corresponding nitrile

The analysis was carried out using a Phenomenex Gemini® NX 3 C18 110 Å, LC column (150 x 2.0 mm) with a SecurityGuard™ Cartridge 4 x 2.0 mm column. The mobile phase consisted of 98% ammonium acetate (20 mM) and 2% acetonitrile (ACN). The analysis was performed at a flow rate of 0.2 mL/min, a column temperature of 20°C and over 18 minutes. A stepwise gradient was used for separation starting with 10% ACN, increased to 70% ACN within 5 minutes, held from 5.01 to 10 minutes, further increased to 90% ACN from 10.01 to 12 minutes and decreased to 10% ACN from 12.01 to 18 minutes.

3.6.4.5 Method „Cinnamonnitrile“ for HPLC-UV and HPLC-MS

The analysis was carried out using a Chromolith Performance RP 18E 4.6x100 mm HPLC Column. The column temperature was set at 30°C. The detection was performed at a flow of 1.2mL/min over 5 minutes. The mobile phase consisted of 100% 0.1% formic acid in deionised H₂O. A stepwise gradient was used starting 50% acetonitrile (ACN). After one minute ACN was increased to 100% within 0.5 minutes, held from 1.5 to 3.5 minutes and equilibrated from 3.51 to 5 minutes to 50% ACN.

3.6.4.6 Method „PCA“ for HPLC-UV and HPLC-MS used for Pyrrole-2-carboxylic acid

The analysis was carried out using a Chromolith Performance RP 18E 4.6x100 mm HPLC Column. The column temperature was set at 30°C. The detection was performed at a flow of 1.2mL/min over 5.1 minutes. The mobile phase consisted of 100% 0.1% formic acid in deionised H₂O. A stepwise gradient was used starting with 30% acetonitrile (ACN) increased to 100% from 1 to 3 minutes, held from 3 to 5 minutes and equilibrated from 5 to 5.1 minutes.

3.6.5 Fluorescence-based Thermal Shift (FTS) assay

A number of carboxylic acids were chosen, mainly compounds for which the corresponding nitrile product references were available. To check if the chosen carboxylic acids were binding to the QueCs and were influencing the thermo stability of the four active QueCs, a FTS assay was done. With a real-time PCR machine, reaction solutions of the different QueCs were analysed consisting of 2mM sub-

strate (1 μ L of 50mM stock), 2 mM ATP, 2 mM (NH₄)₂SO₄, 2 μ L enzyme (10 ng/ μ L) and 4 μ L SYPRO orange dye (50x dilution) filled up with appropriate buffer (100 mM HEPES, 200 mM NaCl, 20 mM MgCl₂ and 10 mM DTT) to reaction volume of 25 μ L in each well of a 96-well plate. The microtiter plate was covered with optical-clear adhesive foil, shaken on the Titramax vibration shaker and centrifuged for one minute at 1,000rpm. A temperature gradient from 25°C up to 95°C, with a holding time of 1 minute at each degree, was used. The increase of the fluorescence signal was monitored online, when proteins were unfolded.³⁶

To check if the chosen carboxylic acids were potentially binding to the QueCs and were influencing the thermostability of the four active QueCs, the FTS assay was done under several conditions:

- Enzyme + buffer
- Enzyme + buffer + ATP
- Enzyme + buffer + ATP + substrate
- Enzyme + product
- Enzyme + buffer + ATP + product
- Enzyme + substrate
- Enzyme + buffer + ATP + unnatural substrate

Table 3 gives the names of the substrates and associated abbreviations which were applied for the exploration of the substrate scope of the different QueCs.

Table 3: Listing of all carboxylic acids, which were used for the exploration of the substrate scope of QueCs from different organism with FTS assay

Substrates	shortcuts	molecular weight [g/mol]
Pyrrole-2-carboxylic acid	T2	111.1
2-Pyridinecarboxylic acid	T3	123.11
Benzoic acid	T5	122.12
Indole-3-carboxylic acid	T6	161.16
Cinnamic acid	T8	148.16
Pyrazine carboxylic acid	T9	124.1
Pyrrole-3-carboxylic acid	T12	111.1
2-Methyl-4-oxo 4,5,6,7-tetrahydro- 1 <i>H</i> -indole-3-carboxylic acid	T13	193.2
3- Phenylpropionic acid	T14	150.17
Mandelic acid	T15	152.15

3.6.6 *In vitro* reconstruction of Queosine biosynthesis in *G. kaustophilus*: two step cascade from 7-carboxy-7deazaguanine to PreQ₁

The *in vitro* reconstruction of the last step of the preQ₀ biosynthetic pathway and the reduction to preQ₁ was performed in one reaction vessel.

3.6.6.1 Cultivation, protein expression and purification of nitrile reductase from *G. kaustophilus*

20 mL LB^{Kan} medium was inoculated with a single colony and grown at 37°C overnight. This overnight culture was used to inoculate the main culture, consisting of 500 mL LB^{Kan} medium in 2-L baffled Erlenmeyer flasks. The cultures were grown at 37°C and 110rpm. At an OD₆₀₀ between 0.6 and 0.8, the cells were induced with 0.5mL of 1M IPTG and incubated for 16 hours at 37°C. In order to harvest the cells, the main culture was centrifuged at 4,000rpm for 10 minutes at 4°C.

The pellet was resuspended in NRed buffer, disrupted by sonification and centrifuged by ultracentrifugation at 40krpm for 45 minutes and at 4°C. The thermostable proteins, including mainly the desired *GkNRed*, were separated from others by heat precipitation at 70°C for 10 minutes and separated by centrifugation at 4 krpm, 4°C for 10 minutes. The supernatant, containing sufficiently pure (70%) nitrile reductase was stored at -20°C.⁸

3.6.6.2 Activity assay for the two step cascade from 7-carboxy-7deazaguanine to preQ₁

The activity assay was prepared as described in table 4 and carried out at 55°C for one hour, followed by a temperature drop to 30°C for the rest of the reaction. After 10 minutes, 1 hour, 7 hours and 24 hours samples of 50µL each have been taken. In table 4, the reaction preparations of the different activity assay stages are summarised.

Table 4: Summary of ingredients for the *in vitro* reconstruction of queosine biosynthesis in *G. kaustophilus*: two step cascade from 7-carboxy-7-deazaguanine to preQ₁

Reaction	Reaction components	Addition of
reaction from CDG to preQ ₀ (10 minutes at 55°C)	NRed buffer 145µL, 1mM CDG in 0.5M KOH, 1.25mM ATP, 5mM (NH ₄) ₂ SO ₄ , 7-cyano-7-deazaguanine synthase (15µL of a 10mg/mL stock)	
continued start reaction for 100% conversion (1 hour at 55°C)	150µL reaction solution from start reaction	2mM ATP
second reaction (6 hours at 30°C)	120µL from continued start reaction	nitrile reductase (15µL of stock), NADPH (3µL of 100mM stock)
continued second reaction for 100% conversion (overnight at 30°C)	88µL from second reaction	NADPH (5µL of 100mM stock)

The reaction was stopped by adding MeOH (80% of the reaction volume), DMSO (20% of the reaction volume) and 1M KOH (20% of the reaction volume). After centrifugation for 3 minutes, the supernatant was analysed by HPLC-MS (Method „Phenomenex PreQ0“).

3.6.7 ³¹P NMR experiments for co-product identification in 7-cyano-7-deazaguanine synthase catalysed nitrile formation

The ³¹P spectra were measured at 202.354MHz. The measurement was done with broad-band proton decoupling at 30°C and a locked field on 10% D₂O. Under consideration of 85% H₃PO₄ all chemical shifts could be reproduced. The parameters summarized in table 5 were set during the measurement.³⁵

Table 5: Parameters for ^{31}P NMR-spectrometry measurement.³⁵

Parameter	adjustment
sweep width	20kHz
acquisition time	0.81s
pulse width	45°
line broadening	3Hz
relaxation delay	1.0s
scans	64

The scans were ranked with a delay of 60s. Under these conditions 30 spectra were measured.

Different solutions were prepared with AMP, ADP, ATP, K_2HPO_4 , and tetra-sodium pyrophosphate. For dilution of the substances above, glycine buffer (100mM) with 20mM MgCl_2 and 10% D_2O were used. The evaluation was carried out as described in the literature.³⁷

The reaction mix contained glycine buffer (100 mM, pH 9.5), 20mM MgCl_2 , 10% D_2O , 1mM ATP, 5mM $(\text{NH}_4)_2\text{SO}_4$, CDG (1mM dissolved in 0.5M KOH) and 0.2 mg QueC (of a 10mg/mL stock) from *G. kaustophilus* in a reaction volume of 500 μL .³⁵

3.6.8 Active site analysis

The experiment for analysis of the active site of QueC was carried out as described in our paper.³⁵

4 Results and discussion

4.1 Selection of 7-Cyano-7-deazaguanine synthases

QueC from *G. kaustophilus* und *E. coli* had been cloned into the pEHisTEV vectors and transformed into *E. coli* BL21 (DE3) strain in preliminary experiments. The gene coding for QueC (accession Nr. NC_006510.1 location 1000474..1001148, locus_tag „GK0975“) was fundament for a BLAST search to find other potential 7-cyano-7-deazaguanine synthases. From a long search report six 7-cyano-7-deazaguanine synthases were chosen from diverse sources (see table 6).

Table 6: 7-Cyano-7-deazaguanine synthases, which have been selected based on a BLAST search.

7-Cyano-7-deazaguanine synthases	accession codes, location	kingdom, phylum, class, order, family, genus
<i>Pectobacterium atrosepticum</i>	NZ_CP009125.1, (1291182..1291877)	Bacteria, Proteobacteria, Gamma Proteobacteria, Enterobacteriales, Enterobacteriaceae, <i>Pectobacterium</i>
<i>Archaeoglobus sulficallidus</i>	CP005290.1, (1578638..1579342)	Archaea, Euryarchaeota, Archaeoglobi, Archaeoglobales, Archaeoglobaceae, <i>Archaeoglobus</i>
<i>Bacillus subtilis</i>	NC_000964.3, (1439448..1440107)	Bacteria, Firmicutes, Bacilli, Bacillales, Bacillaceae, <i>Bacillus</i>
<i>Cucumis sativus</i>	NC_026655.1	Plantae, Angiosperms, Cucurbitales, Cucurbitaceae, <i>Cucumis</i>
<i>Streptomyces rimosus</i>	NZ_JMGX01000038.1 (5525..6199)	Bacteria, Actinobacteria, Actinobacteria, Actinomycetales, Streptomycetaceae, <i>Streptomyces</i>
<i>Anoxybacillus flavithermus</i>	NC_011567.1 (1947599..1948264)	Bacteria, Firmicutes, Bacilli, Bacillales, Bacillaceae, <i>Anoxybacillus</i>

As criteria for the selection, literature knowledge, expected stability, expected expressability and diversity have been applied. The sequence alignments of all chosen 7-cyano-7-deazaguanine synthases with QueC from *G. kaustophilus* is shown in the appendix.

4.2 Construction of *E. coli* BL21 strains expressing 7-cyano-7-deazaguanine synthases from different organisms

In order to characterise different QueCs it was essential to clone the specific QueC genes into the pEHisTEV vector to create proteins with fusion tags for a simple purification. Therefore, the pEHisTEV vector backbone was amplified by PCR and loaded onto a preparative agarose gel (figure 3) and afterwards purified.

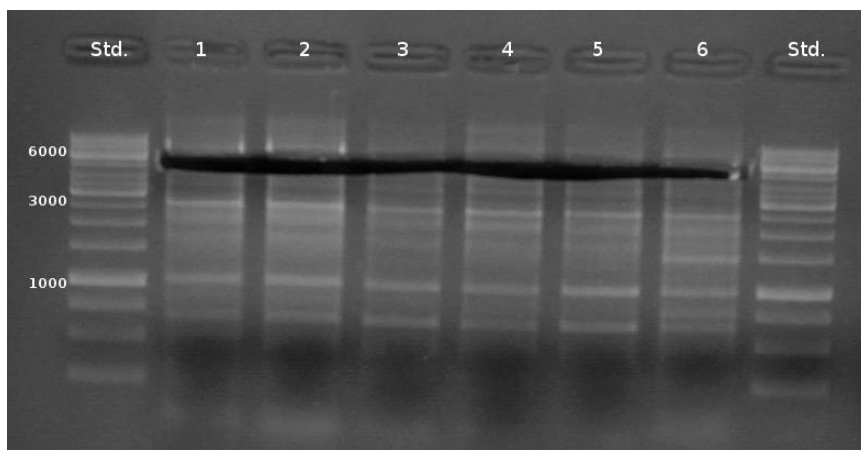


Figure 3: Preparative agarose gel of amplified pEHisTEV vector. Slot 1 to 6 show the application of amplified pEHisTEV vectors, without gel slices of pEHisTEV vectors with the size of interest (5343bp). GeneRuler™ DNA Ladder Mix was used as standard.

The QueC genes from *A. sulficallidus*, *B. subtilis*, *C. sativus*, *S. rimosus*, *A. flavithermus* and *P. atrosepticum* were ordered as codon optimised G-Blocks for *E. coli* and cloned into the pEHisTEV vector by Gibson cloning, desalted and transformed into *E. coli* Top 10F' cells. To check the cloning procedure, a control was performed by digesting plasmid constructs with the restriction enzymes XbaI and XhoI (figure 4). The cuts should generate 2 fragments with expected sizes of approximately 800bp and 5300bp. As shown in slot 1, restriction enzyme XhoI cut the plasmid of *S. rimosus* two times and created fragments of 177bp, 675bp and 5193bp.

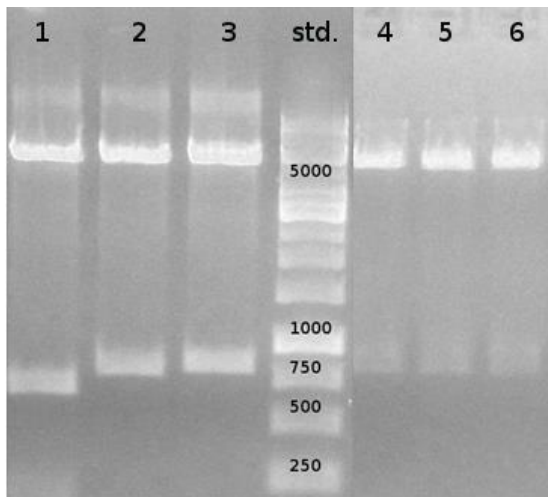


Figure 4: Control agarose gel of QueC fragments cloned into pEHisTEV vector by Gibson cloning. Digest was done with restriction enzymes XbaI and XhoI. Slot 1: Digest of QueC fragment of *S. rimosus* in pEHisTEV vector. Slot 2: Digest of QueC fragment of *A. flavithermus* in pEHisTEV vector. Slot 3: Digest of QueC fragment of *C. sativus* in pEHisTEV vector. Slot 4: Digest of QueC fragment of *P. atrosepticum* in pEHisTEV vector. Slot 5: Digest of QueC fragment of *A. sulficallidus* in pEHisTEV vector. Slot 6: Digest of QueC fragment of *B. subtilis* in pEHisTEV vector. GeneRuler™ DNA Ladder Mix was used as standard.

Subsequently, the samples were sent for sequencing and those with positive sequences were selected and transformed into *E. coli* BL21 cells.

A small scale cultivation of *E. coli* BL21 cells, including 7-cyano-7-deazaguanine synthase genes from *A. sulficallidus*, *B. subtilis*, *C. sativus*, *S. rimosus*, *A. flavithermus* and *P. atrosepticum*, was performed. The cells were induced with 1M IPTG and 0.1 mM ZnSO₄. After cultivation, the cells were harvested, treated with the BugBuster lysis kit and analysed with SDS-PAGE, in order to elucidate the amount of expressed proteins and potential inclusion bodies. The first cloning round brought no positive expression results. Except the positive control with the 7-cyano-7-deazaguanine synthase from *G. kaustophilus*, none of the cultivates showed an overexpression of the protein 7-cyano-7-deazaguanine synthase in any fraction. Only the common protein pattern of *E. coli* was visible in all SN bands.

We assumed that the pEHisTEV vector was nonfunctional, probably due to mutations in the promoter region, since the constructs gave positive results from sequencing the CDS region. These constructs were then double digested with HindIII and NdeI, and the resulting inserts were used for ligation with the backbone of a well expressing pEHisTEV vector from which the HNL-1 gene (E. Köhler, ACIB GmbH, Graz) had been removed with the same restriction enzymes (see figure 5).

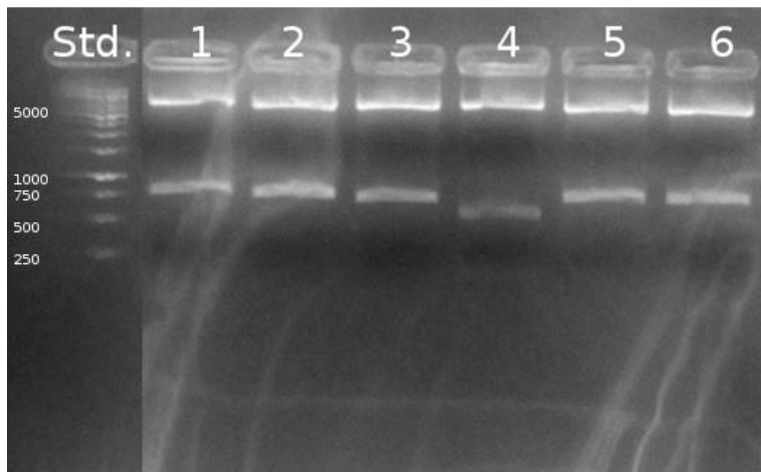


Figure 5: Control agarose gel of QueC fragments in nonfunctional pEHisteV vector. Digest was done with restriction enzymes HindIII and NdeI. Slot 1: Digest of QueC fragment of *C. sativus*. Slot 2: Digest of QueC fragment of *B. subtilis*. Slot 3: Digest of QueC fragment of *P. atrosepticum*. Slot 4: Digest of QueC fragment of *S. rimosus*. Slot 5: Digest of QueC fragment of *A. sulficallidus*. Slot 6: Digest of QueC fragment of *A. flavithermus*. GeneRuler™ DNA Ladder Mix was used as standard.

The pEHisteV:DtHNL-1 vector was digested with HindIII and NdeI. Vector backbone and each insert were ligated with T4-ligase and transformed into *E. coli* Top 10F' cells. Subsequently, the samples were sent for sequencing and those with positive sequences were selected and transformed into *E. coli* BL21 cells.

Furthermore, small scale cultivation was done with all *E. coli* BL21 cells which carried the six different QueC genes.

The cells were induced with 1mM IPTG and 0.1 mM ZnSO₄. After cultivation, the cells were harvested, treated with the BugBuster lysis kit and analysed with SDS-PAGE, in order to determine the amount of expressed protein and potential inclusion bodies. The results are given in figure 6.

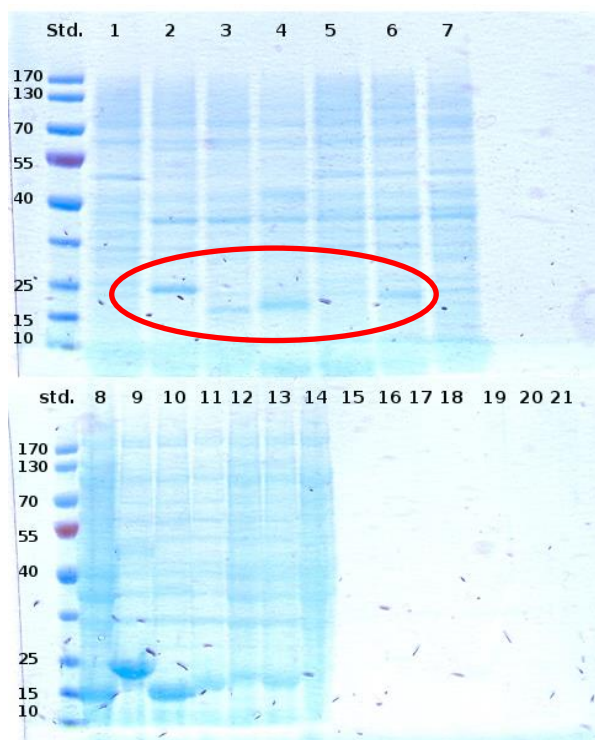


Figure 6: SDS-control gel of the different fractions of the BugBuster lysis. Page Ruler Prestained Protein Ladder (10-170kDa) was used as standard. The samples with different QueCs were arranged as follows: First *A. flavithermus*, second *A. sulficallidus*, third *B. subtilis*, fourth *P. atrospeticum*, fifth *C. sativus* and sixth *S. rimosus*. Slot 8,9,10, 11, 12, and 14 give pellet 1 (cell components). Slot 15 to 21 show pellet 2 (inclusion body fraction). Slot 1 to 7 show the supernatant to show the expression levels of soluble 7-cyano-7-deazaguanine synthases from different organisms. The results of the negative control are shown in slot 7, 14 and 21. QueC of *A. sulficallidus* (26.4kDa), *B. subtilis* (24.5kDa), *S. rimosus* (25.3kDa) and *P. atrospeticum* (25.4kDa) show a slight overexpression marked with a red ellipse.

In figure 6, the expression levels of 6 different QueCs were compared to select those which showed the highest expression results. With two of the enzymes no overexpression could be achieved under the chosen expression conditions (1mM IPTG, 0.1mM ZnSO₄ and 25°C). For QueC of *A. sulficallidus*, *B. subtilis*, *S. rimosus* and *P. atrospeticum* a slight overexpression was found (shown in slot 2, 3, 6 and 4, marked with a red ellipse). QueC of *A. sulficallidus*, *B. subtilis* and *P. atrospeticum* were used for the further experiments. Five from the 8 generated enzymes could be utilized for this work.

The first centrifugation (pellet 1) separated aggregated protein of all 6 different QueCs (slot 8 to 13).

The 7-cyano-7-deazaguanine synthases were expressed with an *N*-terminal His-tag under the control of the T7-promotor. The T7 promoter is considered to be a very strong promoter.³⁸ At the chosen expression conditions, maybe the stress in the cell increased and had an impact on the incomplete folding of the proteins. The

faster the expression is driven, the less time remains for the proper folding of the proteins. To circumvent this effect, the induction temperature was reduced to 25°C. The results are given in figure 7.

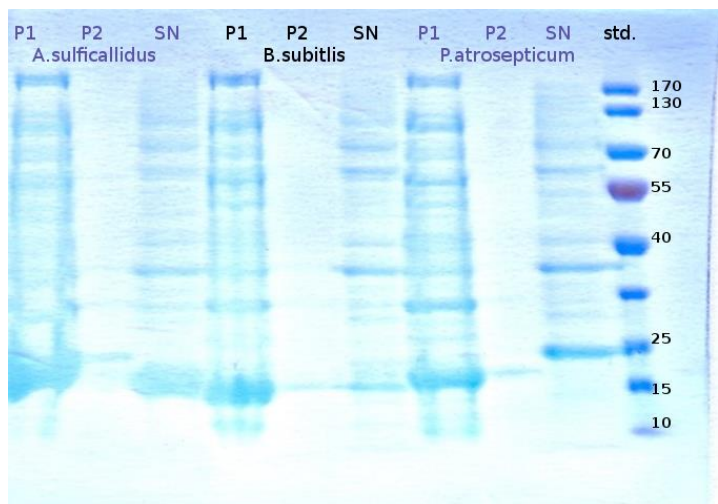


Figure 7: SDS-control gel of the different fractions of the BugBuster lysis. Page Ruler Prestained Protein Ladder (10-170kDa) from Fermentas has been used as standard. P1 pictures cell components which were separated in the first centrifugation step of the BugBuster lysis. P2 visualizes inclusion bodies. SN pictures the expression levels of the 7-cyano-7-deazaguanine synthases from different organisms by induction with 1mM IPTG and 0.1 mM ZnSO₄ at 25°C.

Unfortunately, reduction of the temperature in the expression phase did not improve the level of soluble QueCs. For continuing troubleshooting, a possibility would be the production of the protein by auto-induction, or the use of weaker promoters. The aim of this work was the production of sufficient amount enzyme to perform a characterisation, which succeeded without further expression.

The proteins from *A. sulficallidus*, *B. subtilis*, and *P. atrosepticum* were produced in shake flasks and purified by Ni-affinity chromatography. Figure 8 shows the purified enzyme fractions.

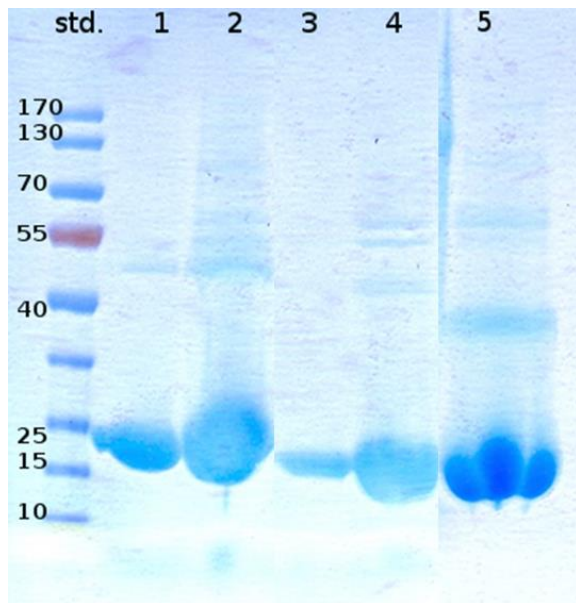


Figure 8: SDS-control gel of the different fractions of the protein purification with Ni-affinity chromatography. In slot 1 the purified enzyme and in slot 2 the purified enzyme-concentrate from *A. sulficallidus* is given. In slot 3 the purified enzyme and in slot 4 the purified enzyme-concentrate from *P. atrosepticum* is given. In slot 5 the purified enzyme-concentrate from *B. subtilis* is given. Page Ruler Prestained Protein Ladder (10-170kDa) is used as standard.

All three enzymes could be produced in high purity. (slot 2,4 and 5). The protein preparation from *B. subtilis* seems to consist of 3 proteins (slot 5). This could have an influence on the functionality of the protein. Activity tests will show if the enzyme is active after the process of purification.

4.3 Optimization of culture conditions to obtain possibly high expression levels

To improve QueC expression levels, 7-cyano-7-deazaguanine synthases of *G. kaustophilus* and *E. coli* were cultivated on small scale, using different induction conditions:

- 1mM IPTG
- 1mM IPTG and 0.1 mM ZnSO₄
- 0.1mM IPTG and 0.1 mM ZnSO₄

The cultivated cell pellet were treated with BugBuster lysis kit and proteins visualized by SDS-PAGE (figure 9). Band 1 to 6 shows the formation of potential inclusion bodies. Band 7 and 10 show the expression levels with induction us-

ing 1mM IPTG. Band 8 and 11 shows the expression levels upon induction with 1mM IPTG and 0.1 mM ZnSO₄. Band 9 and 12 showed the expression levels upon induction with 0.1mM IPTG and 0.1 mM ZnSO₄.

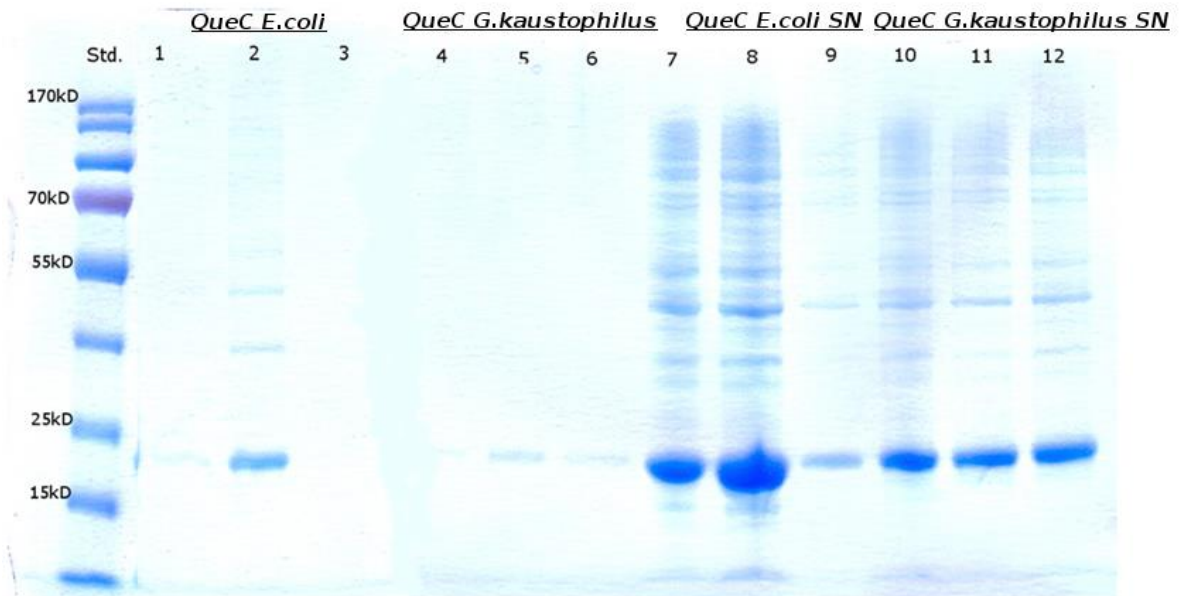


Figure 9: SDS-control gel of the different fractions of the BugBuster lysis. Slot 1 to slot 6 shows the monitoring of the inclusion bodies formed during the cultivation. Slot 7 and 10 shows the expression of soluble QueCs using 1mM IPTG. Slot 8 and 11 shows the expression of soluble QueC using 1mM IPTG and 0.1 mM ZnSO₄. Slot 9 and 12 shows the monitoring of the expression level of QueC using 0.1mM IPTG and 0.1 mM ZnSO₄.

The induction with 1mM IPTG and 0.1 mM ZnSO₄ showed the best expression levels for QueCs of *G. kaustophilus* and *E. coli*.

The proteins from *G. kaustophilus* and *E. coli* were produced in shake flask cultivation and purified by Ni-affinity chromatography (figure 10).

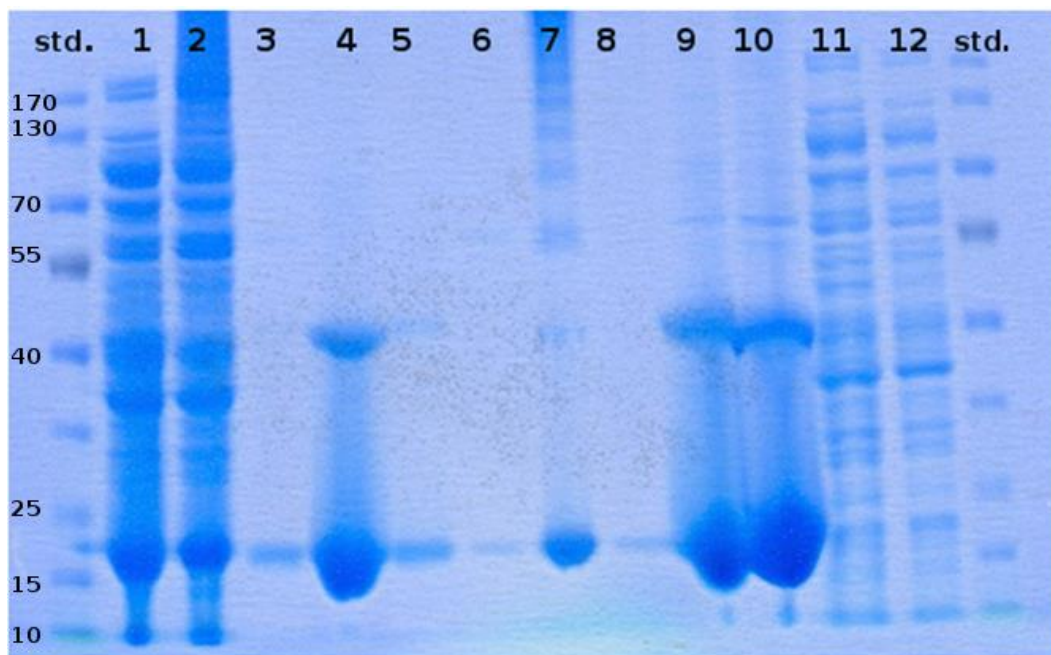


Figure 10: SDS-control gel of the different fractions of the protein purification with Ni-affinity chromatography. Slot 1 and 2 show the crude lysate from QueC of *E. coli* and *G. kaustophilus*. Slot 3 to 5 show selected fractions, which were taken during purification of QueC of *E. coli*. Slot 6 to 8 show selected fractions, which were taken during purification of QueC of *G. kaustophilus*. Slot 9 and 10 show purified enzyme stock of QueC from *E. coli* and *G. kaustophilus*, respectively. Page Ruler Prestained Protein Ladder (10-170kDa) was used as standard.

For both proteins, stocks could be produced with approximately 80% of the desired proteins (see slot 9 and 10). However, in both samples additional bands were visible at about 55kDa. The size of the additional bands corresponds with the double weight of the individual proteins. Therefore, it can be suggested that dimers of the QueC proteins are present.

4.4 Assay development

An activity assay had to be established for the characterisation of the 7-cyano-7-deazaguanine synthase. First, 20mM HEPES-buffer containing 100mM NaCl, 10mM MgCl₂, 10 mM DTT and 5 mM ammonium sulfate, adjusted to a pH of 7.5 was used as buffer system. The reaction solution contained the same components as described in the experimental section, but an ATP stock solution was used with a concentration of 500mM. At this concentration, the solution was extremely viscous and the error during pipetting increased.

To avoid this error, an ATP stock solution was chosen with a lower concentration (25 mM). Furthermore, 20mM HEPES buffer had a too low buffer capacity for our

reaction system, because the substrate CDG was only soluble in strong base. Therefore, the buffer capacity was increased from 20mM to 40mM and further increased to 100mM HEPES in order to obtain a stable measurement result and increase the reproducibility. At the beginning, a heat shock (80°C, 10 minutes) procedure was used for termination of the reaction. Thereby, not the total amount of protein precipitated and clogging of the column during detection with HPLC was a risk. The stopping strategy was changed from a heat shock procedure to adding MeOH (100% of the reaction volume) to the reaction system.

A further problem arose in the measurement of product and substrate. Initially, no or too little substrate (CDG) could be detected via HPLC measurements. The solution was to change the stopping conditions. To stay in solution CDG needs a highly alkaline environment. Furthermore the reproducibility of detection of product preQ₀ was low and needed to be improved to accomplish the measurement of the time dependent reaction progress of this protein. To circumvent these issues, the stopping strategy was changed from adding only MeOH (100% of the reaction volume) to adding MeOH (80% of the reaction volume), DMSO (20% of the reaction volume) and 1M KOH (50% of the reaction volume). With the improved activity assay (experimental section) run for one hour with 30°C, a specific activity of 3.5mUmg⁻¹ of protein from *G. kaustophilus* was determined.

4.5 Exploration of the reaction mechanism of 7-cyano-7-deazaguanine synthases

7-Cyano-7-deazaguanine synthase catalyzes the conversion of CDG to preQ₀ at the expense of ATP (see scheme 1).¹ At the time of the thesis, it had not be determined if ADP or AMP is formed from ATP during the reaction.

To shed light on the reaction mechanism, bioconversions from CDG to preQ₀ were performed with QueC from *G. kaustophilus* and analysed by different methods to determine the nature of the co-products.

4.5.1 Exploration experiments by capHPLC analysis

First, an activity assay was employed, where DTT was present in the buffer system. The analysis was performed by capHPLC. The preparations and measure-

ments were done in cooperation with the Center of Medical Research in Graz, Austria and the group of Prof. Ruth Birner-Grünberger.

By monitoring the amount of ATP, ADP and AMP during the reaction, we aimed to get information about the reaction mechanism. In figure 11 the HPLC-results monitoring the blank, consisting of all reaction components except enzyme, is given. In figure 12 the HPLC-results monitoring the sample, consisting of all reaction components and enzyme, is given.

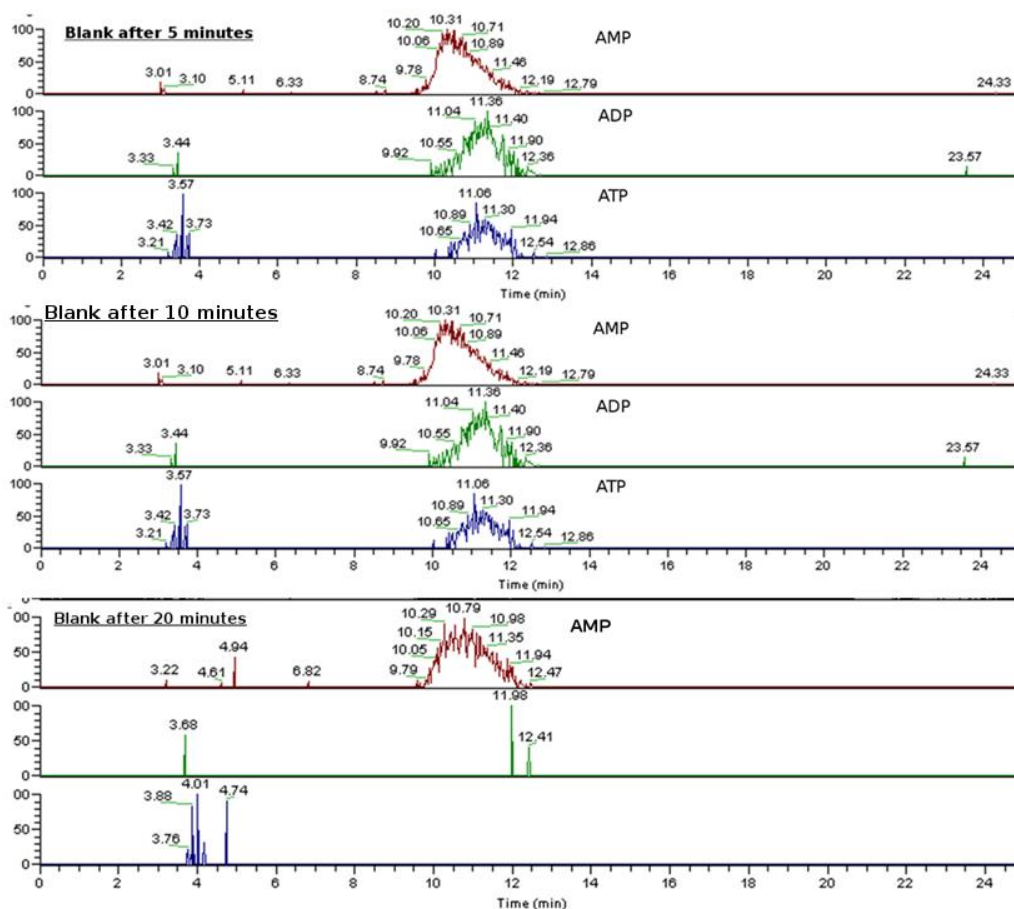


Figure 11: HPLC analysis, showing ATP and the formation of AMP and ADP over time from the blank, where no 7-cyano-7-deazaguanine synthase from *G. kaustophilus* was present. After 5, 10 and 20 minutes samples were taken, the reaction terminated and analysed with HPLC.

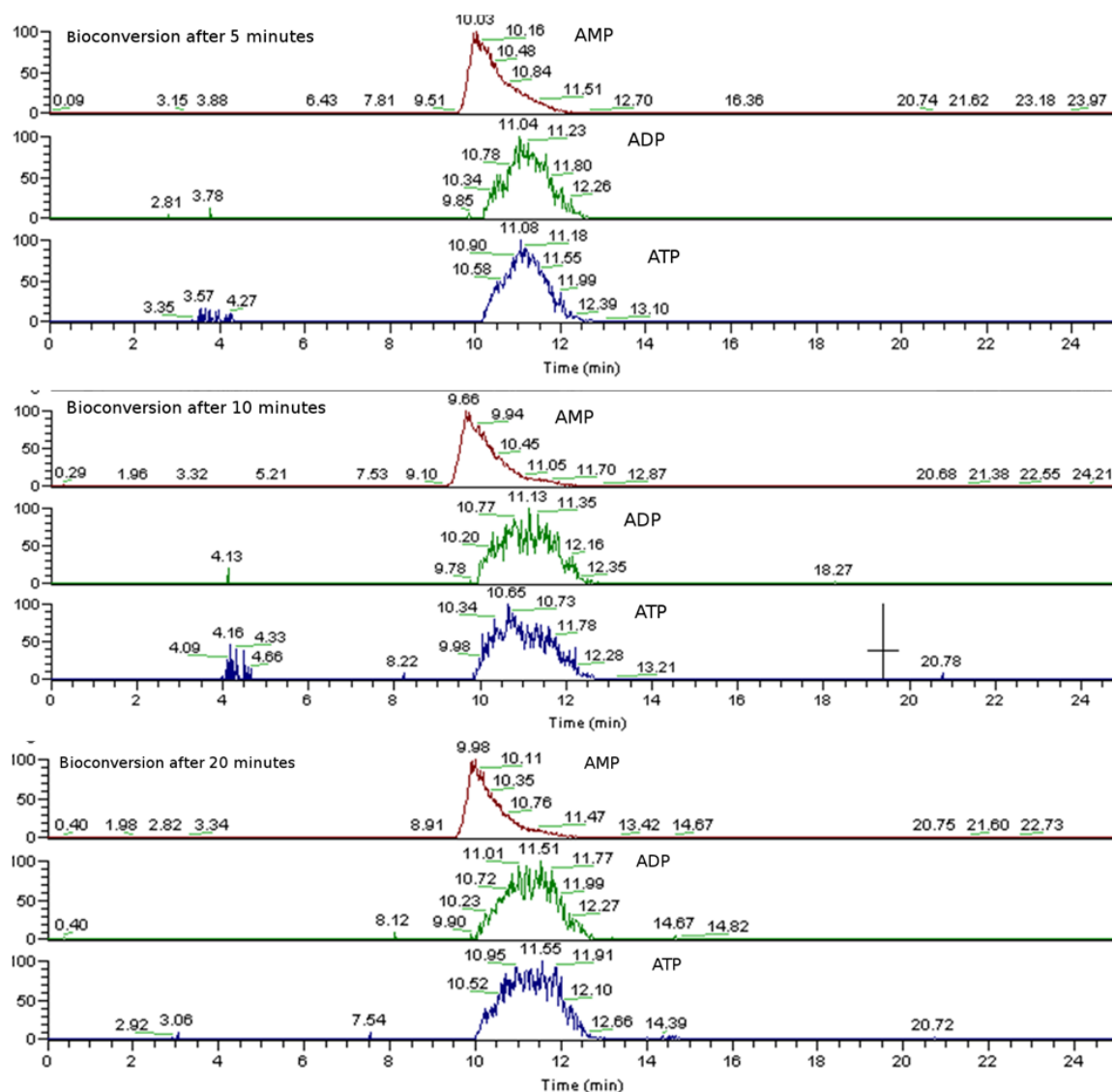


Figure 12: HPLC analysis, showing ATP and the formation of AMP and ADP over time from the bioconversion, where 7-cyano-7-deazaguanine synthase from *G. kaustophilus* converted CDG to preQ₀ under consumption of ATP. After 5, 10 and 20 minutes samples were taken, the reaction terminated and analysed with HPLC.

Over time, the ATP levels in the sample were decreasing and AMP levels were increasing in small amounts (see figure 12). However, also in the blanks, consisting of the reaction solution except enzyme, ATP was hydrolysed after 5 minutes incubation time (see figure 11). To conclude, maybe the reducing agent DTT in the buffer system was hydrolysing the ATP in the reaction solution.

Since the experiment-setting delivered no meaningful results to understand the nature of the co-products, exploration of the reaction mechanism was continued with different reaction conditions.

The second setting omitted the addition of reducing agent DTT in the buffer system, to prevent ATP-hydrolysis. Moreover, fresh ATP stocks were used.

In order to determine the actual amount of ATP, ADP and AMP at different time points during the bioconversion, calibration curves of ATP, ADP and AMP were created (see figure 13) and their linear fit equations were used for calculation.

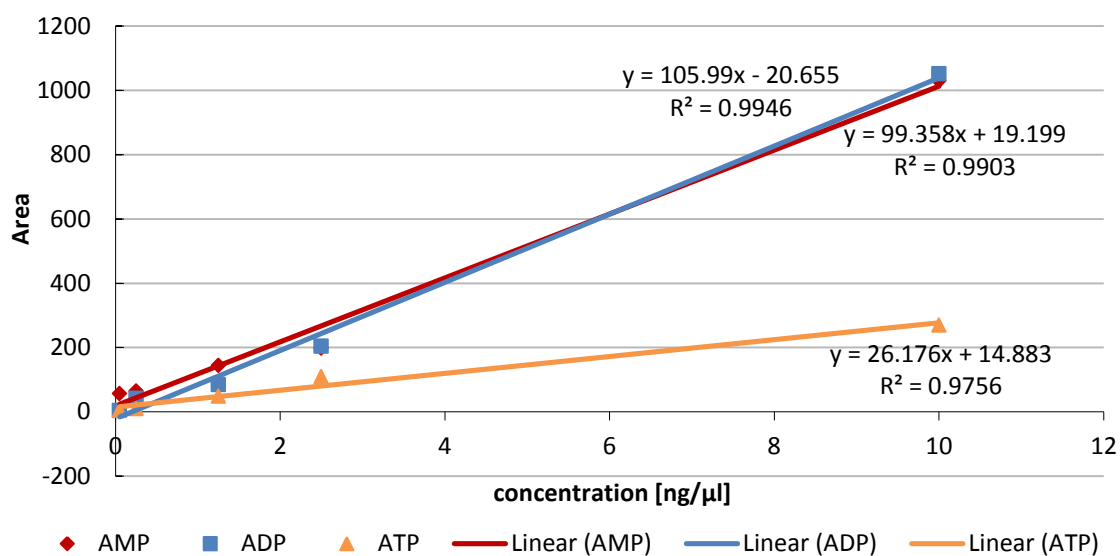


Figure 13: Application of the calibration curves for the determination of ATP, ADP and AMP concentrations (ng/μL) which are related to the detection areas from the HPLC measurements.

In figure 14, monitoring of amounts of ADP and AMP during the reaction and corresponding blanks for ADP and AMP, containing all reaction components except enzyme, are given.

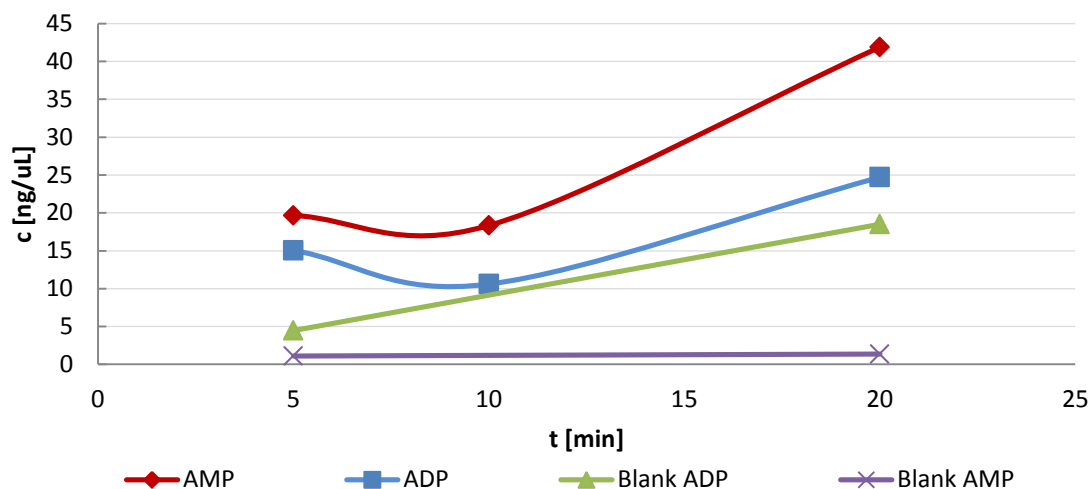


Figure 14: Monitoring of the ADP and AMP formation during the activity assay with QueC from *G. kaustophilus* at 5, 10 and 20 minutes.

In figure 15 monitoring of ATP consumption during the reaction and corresponding blank is given.

It seems that the increase of ADP in the sample was similar to the ADP increase in the blank (see figure 14). The reason for this increase may be the natural hydrolysis of ATP at 30°C. Furthermore, it came to a formation of AMP over time, during the reaction, but the AMP amount in the blank stayed constant, indicating AMP as the coproduct of the nitrile-forming reaction.

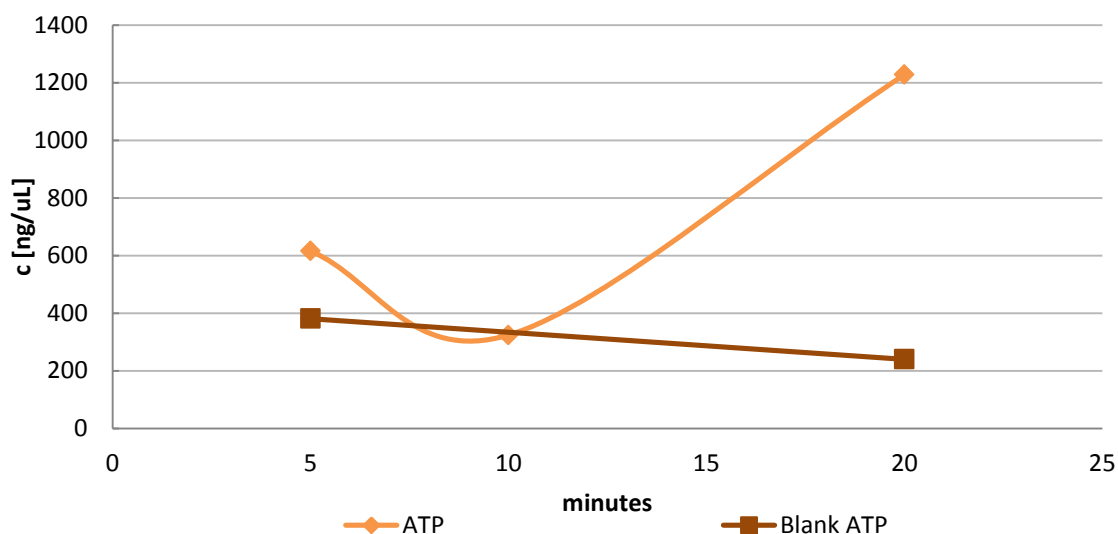


Figure 15: Monitoring of the ATP consumption during the activity assay with QueC from *G. kaustophilus* at 5, 10 and 20 minutes.

Unfortunately, the ATP concentration seemed to increase over time too (see figure 15). For this phenomenon, no explanation could be found. These measurements (figure 14 and 15) appeared to be inconsistent under the tested conditions. So no multiple measurements were done and no error limits were given.

Since the analysis did not work well in this experiment, NMR-spectrometry was chosen to explore the reaction catalyzed 7-cyano-7-deazaguanine synthase.

4.5.2 Exploration of the net reaction products by NMR spectrometry

To analyze and identify the fate of ATP in enzymatic nitrile formation, ^{31}P NMR spectra of ATP, ADP, AMP, phosphate and pyrophosphate were measured by NMR-spectrometry as a reference and a standard biotransformation with QueC from *G. kaustophilus* was carried out in the NMR tube and measured. This work was done in cooperation with Hansjörg Weber from the Institute of Organic Chemistry (University of Technology, Graz). Figure 16 shows spectra of the phosphorous species present in the reaction in the course of time.³⁵

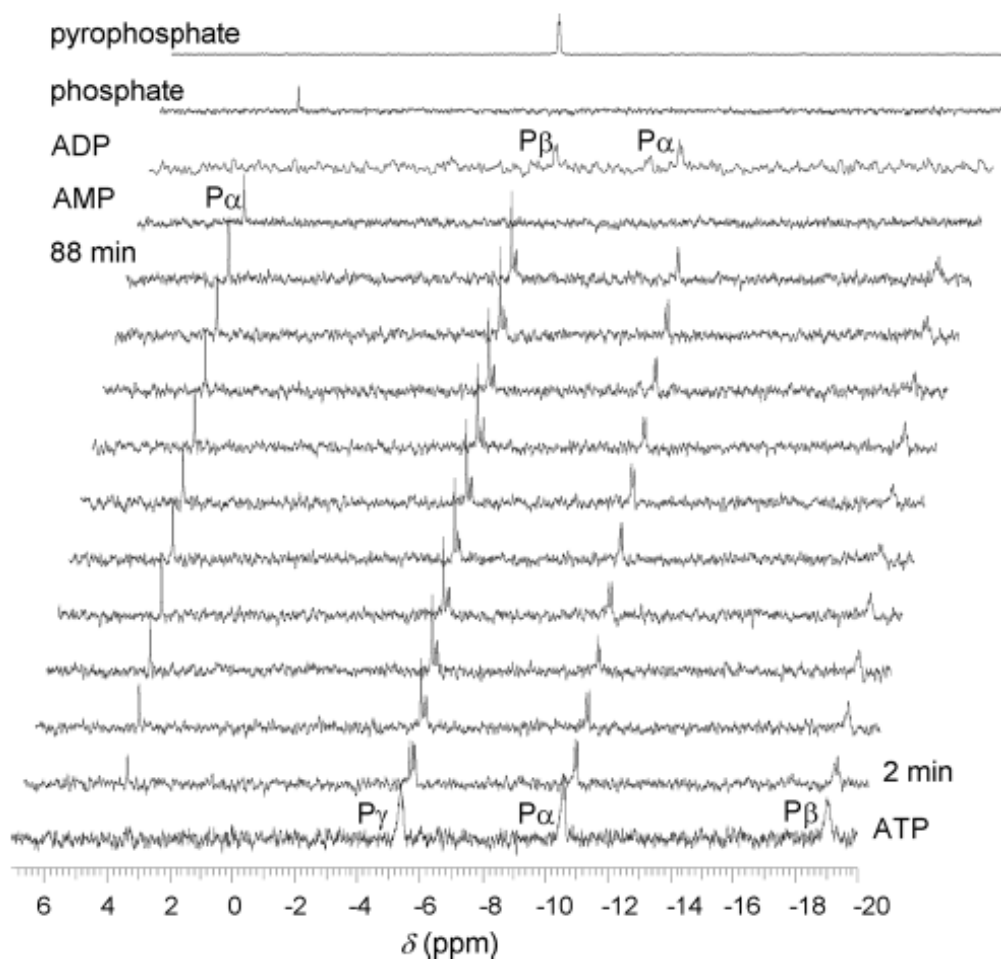
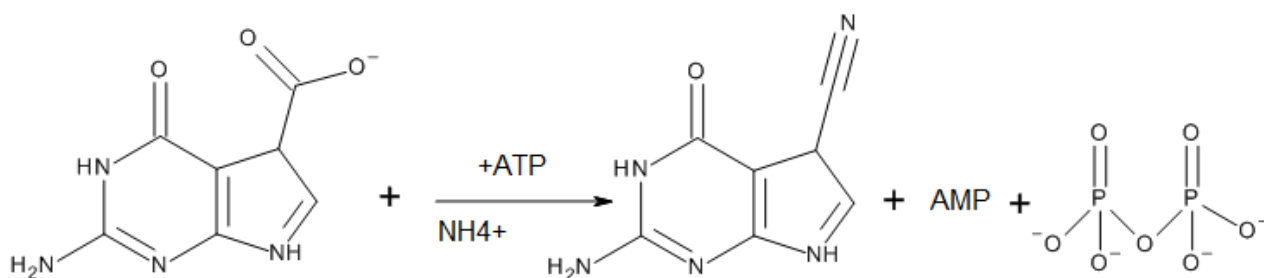


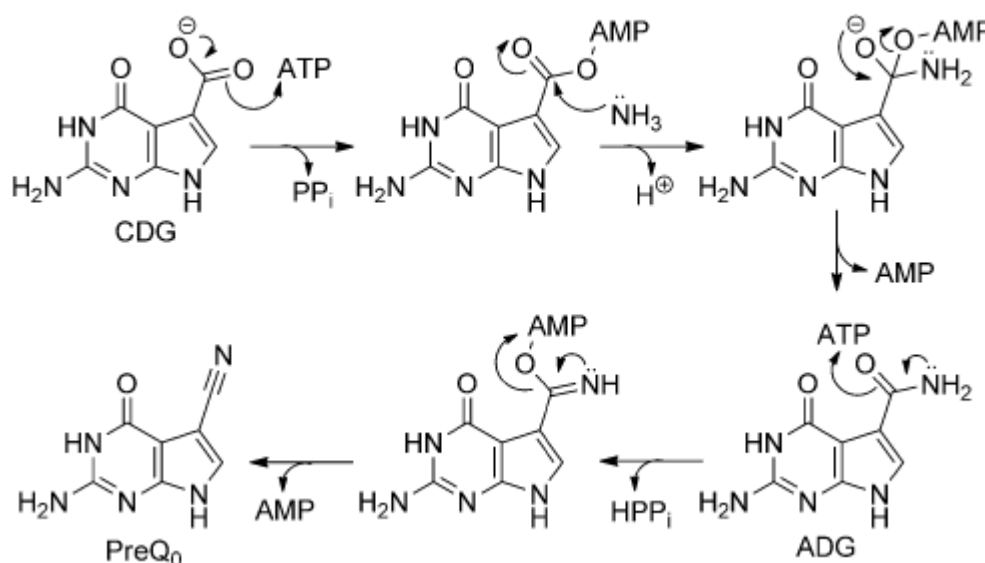
Figure 16: Monitoring of phosphorous containing species during preQ₀ formation compared with the reference measurements with ATP, ADP, AMP, phosphate and pyrophosphate. The bottom spectrum shows the biotransformation mixture without addition of CDG. In the top four spectra, the reference measurements are displayed. 30 spectra were recorded during 1.28h. Every third spectrum is shown here over time course.³⁵

On the bottom, the spectrum of reaction mixture of the activity assays is recorded without the addition of CDG. Here it can be seen, that only the 3 signals from the ATP reference are visible. After addition of the substrate CDG, peaks appear, which indicate AMP and pyrophosphate formation due to their chemical shifts that are identical with the shifts of the reference measurements. Based on these measurements, the reaction outcome of QueC catalyzed nitrile formation is proposed in scheme 4. During the whole measurement, no ADP formation could be detected.



Scheme 4: Net-reaction scheme of ATP dependent nitrile formation

QueC converts 7-carboxy-7-deazaguanine (CDG) to 2-amino-5-cyanopyrrolo[2,3-d]pyrimidin-4-one (preQ₀). In this reaction, ATP is consumed and AMP and pyrophosphate are formed as by-products. Vahe Bandarian and his group from the University of Arizona confirmed these results and worked at the elucidation of the reaction mechanism in 2015 (see scheme 5).³⁹



Scheme 5: Proposed mechanism of ToyM from *Streptomyces rimosus*.³⁹

During the described reaction CDG gets adenylated by consumption of one ATP. Thereby, CDG is activated and 7-amido-7-deazaguanine (ADG) is formed. After a dehydration step, the nitrile preQ₀ is formed by consumption of a second ATP.³⁹

In a pyrophosphate dependent assay, Vahe Bandarian tested if CDG and ADG substrates are activated similarly and demonstrated that the enzyme ToyM cataly-

ses the adenylation reaction on CDG and ADG in a similar way to form the nitrile preQ₀, AMP and pyrophosphate. The ³¹P NMR experiments in this work detected AMP and pyrophosphate formation after addition of QueC enzyme to the reaction. So, this net reaction proposal can be confirmed by the pyrophosphate dependent assay from Vahe Bandarian.³⁹

4.5.3 Exploration of the active site residues from 7-cyano-7-deazaguanine synthases

In the literature, the crystal structure of QueC of *B. subtilis* was already described. There, a conserved P-loop region was identified. Furthermore, a zinc ion was identified, in close proximity to a cysteine-rich motif. Furthermore, a magnesium- and a phosphate ion were modelled into the structure.⁵ In cooperation with Tea Pavkov-Keller from the Institute of Molecular Biosciences (University of Graz), the active site of QueC of *G. kaustophilus* was analysed, using a model based on the crystal structure of QueC from *B. subtilis* (figure 17).

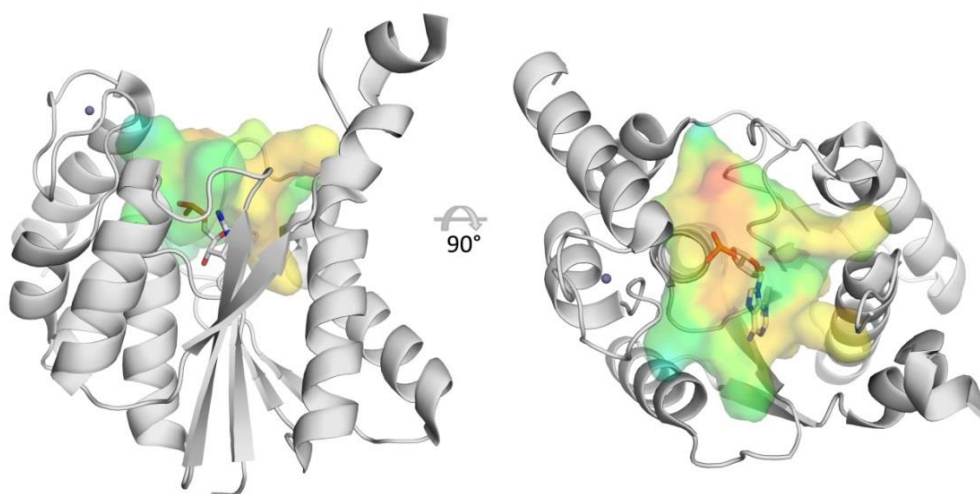


Figure 17: View of the crystal structure of QueC from *G. kaustophilus* designed under use of the crystal structure of QueC from *B. subtilis*, where AMP is modelled to the active site cavity. All proposed residues are conserved in GkQueC and BsQueC. The hydrophilic regions are plotted in blue and hydrophobic residues are plotted in red.³⁵

In the analysis a QueC-AMP complex was generated. It was found that Q39, T119, R97 and N98 are most probably involved in the ATP-binding during the reaction. Although some residues have a distance in the crystal structure to the substance, it is suspected that in the dynamic situation they are flexible and involved in the enzymatic reaction.

Figure 18 indicates that substrate binding probably is accomplished by a tyrosine and aspartate. Tyrosine could be Y129 or Y187. Aspartate D125 or D131 maybe help in binding of the primary and secondary amines of the substrates pyrimidines's part.³⁵ All deterministic residues are conserved among QueC of *B. subtilis* and at QueC of *G. kaustophilus* in the sequence (see Appendix).

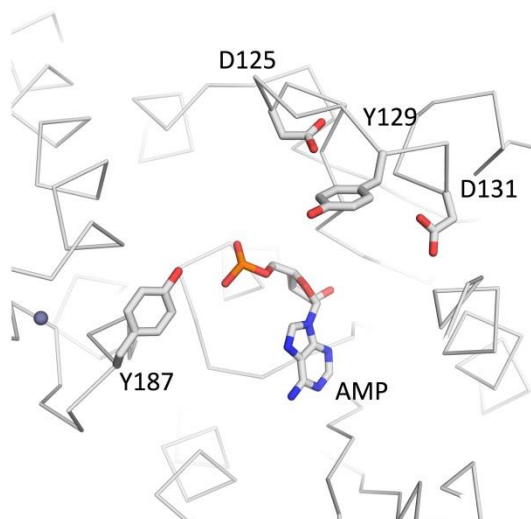


Figure 18: Active site view of structure of QueC from *G. kaustophilus* designed under use of the crystal structure of QueC from *B. subtilis* where residues are shown, which might be involved in the AMP and CDG binding. The zinc ion is shown as a grey sphere.³⁵

D131 is part of a flexible loop of QueC of *G. kaustophilus* and together with the metal ions zinc and magnesium it could participate in the deprotonation of ammonium. Thereafter, the flexible loop may feed the ammonium ion to the active site and stabilize the transition state.⁴⁰

The reaction of QueC seems to be a highly endergonic process. During this reaction two dehydration processes take place. The substrate is activated by a nucleophilic reaction with ATP. Here three modes of activation are possible: either as acylphosphate, acyladenylates or acylpyrophosphate. Our ³¹P experiments rule out the formation of an acylphosphate, because not phosphate and ADP were observed. QueC seems to be very similar to NAD⁺ synthetases, because also these enzymes activate deamido-NAD⁺ with ATP and an ammonium ion is involved in the reaction.^{41,40}

In literature, ToyM from *S. rimosus* was described to convert CDG to preQ₀, by forming an amide intermediate (ADG) like NAD⁺ synthetases do. At the expense of a second molecule of ATP, ADG is finally converted in a second dehydration step to preQ₀. Also asparagine synthetases use ATP for the adenylation of the substrate molecule and make them ready for the condensation with the amine nitrogen.^{42,39}

4.6 Characterisation of different QueCs

To define the physiochemical properties of the QueCs from different origin, an *in vitro* activity assay was used, changing the one parameter at a time. The formation of the natural product preQ₀ during the reaction from the natural substrate CDG was determined and product concentrations were calculated using the equation of the calibration curve plotted in figure 19.

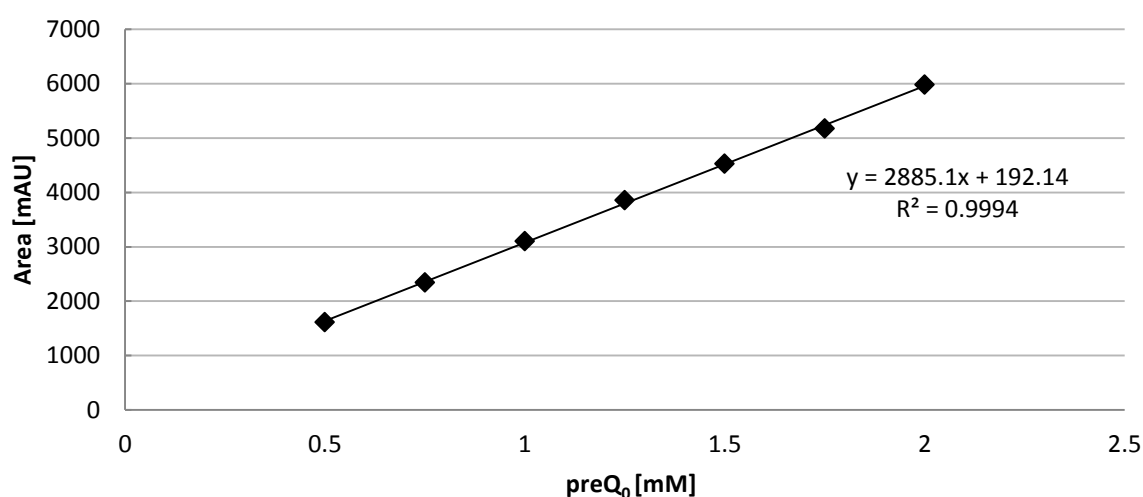


Figure 19: Calibration curve for the determination of the preQ₀ concentration (mM) by read-out of the Area in mAU (milli Absorbance units) of preQ₀ from the HPLC measurements (UV trace, 254nm).

4.6.1 Functionality and specific activity of 7-cyano-7-deazaguanine synthases

To determine if all cloned and expressed enzymes are active *in vitro*, the above describe activity assay for characterisation of 7-cyano-7-deazaguanine synthase was done overnight at 30°C.

Four of the five purified enzymes showed activity for the conversion of CDG to preQ₀. Surprisingly, the protein from *B. subtilis*, showed no activity. Although it has been described in literature and its crystal structure determine, no activity assay was described.⁵ Maybe the protein forms aggregates, as a result from a high cysteine content that is less represented in the QueCs from the other origins described herein.

To define the specific activity related to the amount of enzyme, with each different QueC enzyme an *in vitro* activity assay was performed for 1 hour at 30°C. The results are summarized in figure 20. The specific activities were calculated using the calibration curve, plotted in figure 19.

QueC from *G. kaustophilus* and *E. coli* showed the highest specific activity with 3.5mU/mg. QueC from *A. sulficallidus* and *P. atrosepticum* showed a specific activity of 3.3mU/mg.

The relative activities normalized to the activity of QueC of *G. kaustophilus* is shown in figure 20.

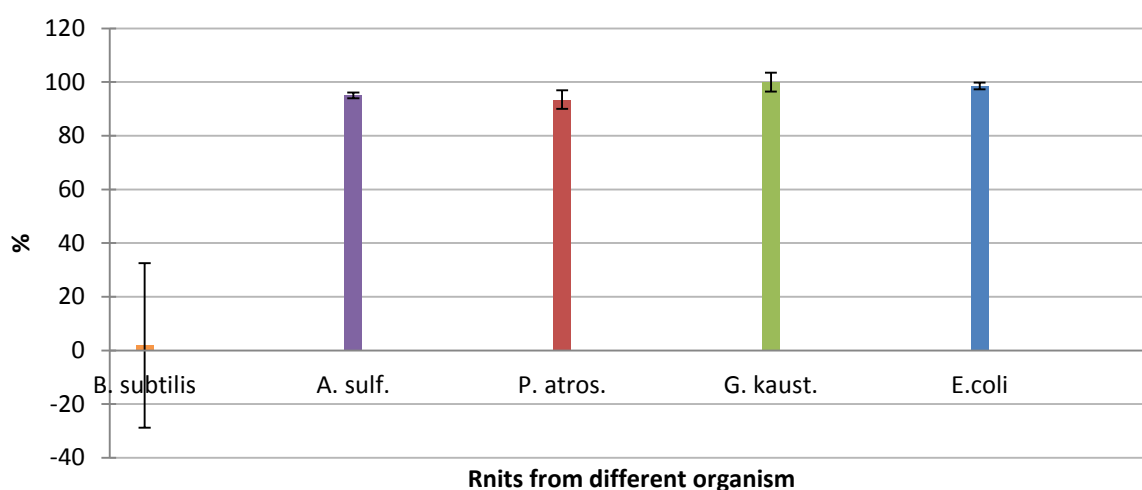


Figure 20: Relative activities of five QueCs from different organism referring to the activity of QueC from *G. kaustophilus*.

The measurements of the 7-cyano-7-deazaguanine synthase from *B. subtilis* showed a high standard deviation. To conclude, the reproducibility of replicate reactions is significantly lower compared to the activities from the other QueCs plotted in figure 20.

A. sulficallidus is a thermophilic organism, which was isolated from black rust formed on a steel surface of a borehole observatory in the Pacific Ocean.⁴³

G. kaustophilus is also a thermophilic organism which was isolated from deep-sea sediment from the Mariana Trench.⁴⁴ By comparing the *G. kaustophilus* enzyme with the *A. sulficallidus* enzyme, first-mentioned could better deal with the prevailing assay conditions.

4.6.2 Determination of temperature and pH optimum of 7-cyano-7-deazaguanine synthases of *G. kaustophilus* and *E. coli*

For the determination of the temperature optimum of QueC from *G. kaustophilus* *in vitro* activity assays were performed over 2 hours at temperatures between 25°C and 80°C (figure 21). The temperature optimum was defined by determination of product preQ₀ amount formed during the reaction.

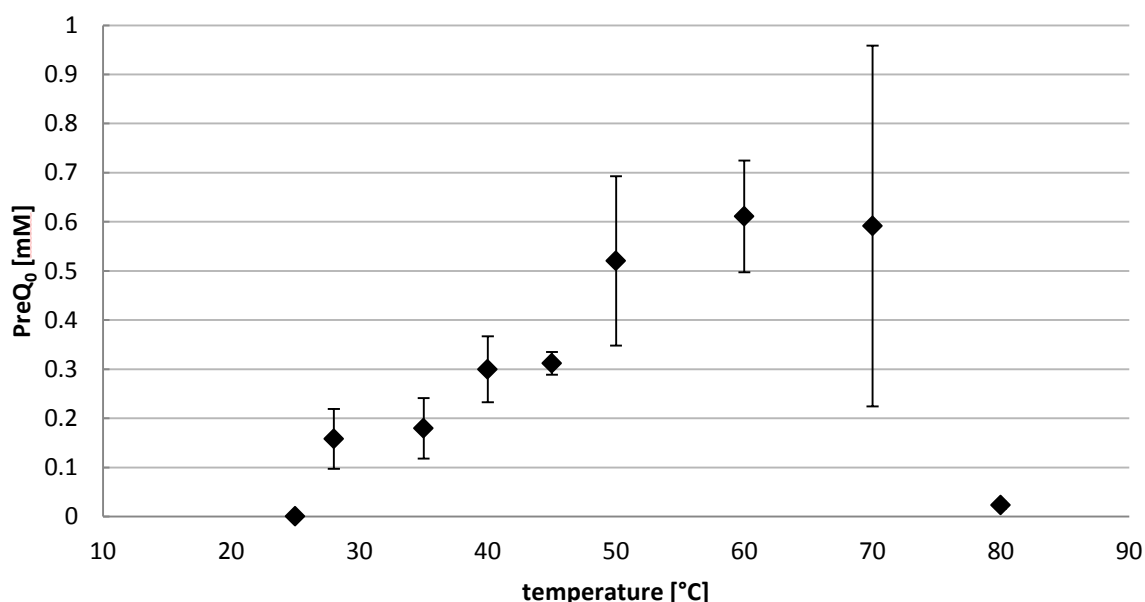


Figure 21: Effect of temperature on the activity of QueC from *G. kaustophilus*: The optimum temperature for the enzyme was determined by plotting different temperatures against the amount of generated product preQ₀ in mM.

It seems that QueC from *G. kaustophilus* had a temperature optimum at 60°C (see figure 21). But with increase in temperature also the standard deviation of the measurements increased. At 70°C, an extremely high standard deviation of the different measurements was visible. A reason for this could be the partial enzyme denaturation with increasing temperature. With increased temperature also the solubility of CDG and preQ₀ increase, which would explain the partially high product implementations. At high temperature also decomposition of co-factor ATP could lead to a decreased reproducibility at reaction repetitions.

Due to the partly conflicting results at the determination of the temperature optimum, the melting temperature of the QueC from *G. kaustophilus* in the used buffer system (HEPES buffer with pH 7.5) was determined by a fluorescence -based thermal shift assay in cooperation with Tea Pavkov-Keller from the Institute of Molecular Biosciences (University of Graz) (see figure 22). In figure 22 the plot of temperature against relative fluorescence units is plotted. This measurement was performed without the addition of substrate or co-factor ATP.

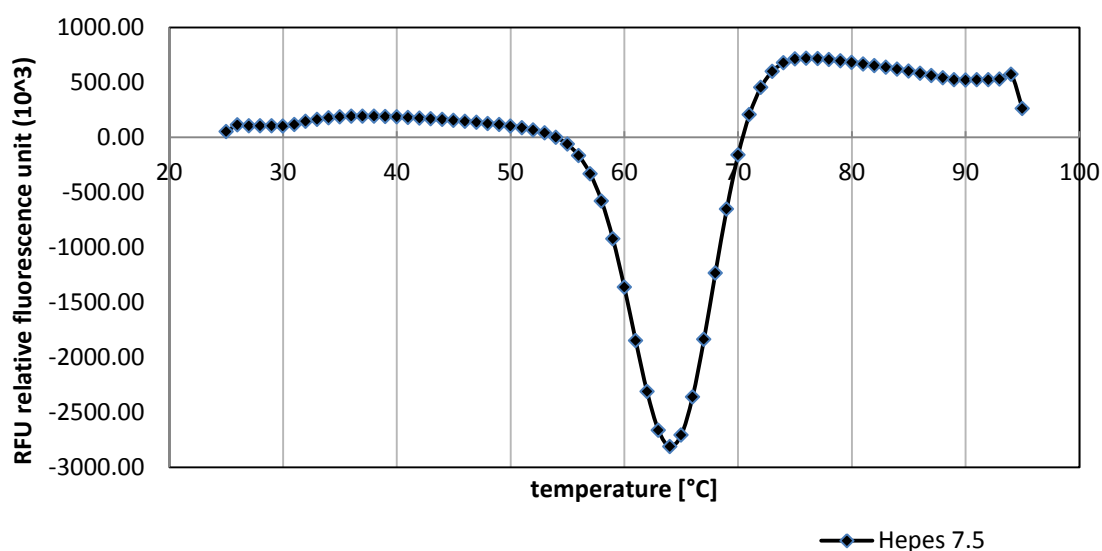


Figure 22: Fluorescence-based thermal shift assay for determination of the melting temperature of QueC from *G. kaustophilus* in HEPES buffer with pH 7.5. Temperature was plotted against relative fluorescence units (10³) of the TAMRA reporter signal after detection.

The highest relative fluorescence signal of the TAMRA reporter signal during online monitoring of the melting curve marks the melting temperature of the investigated protein. At this temperature the unfolding of the protein is completed.²⁶ The melting temperature of the QueC enzyme in HEPES buffer at pH 7.5 was 64°C.

To estimate the influence of substrate and co-factor on the melting temperature another fluorescence -based thermal shift assay was performed with addition of CDG and ATP using various buffers. The results are plotted in figure 23.

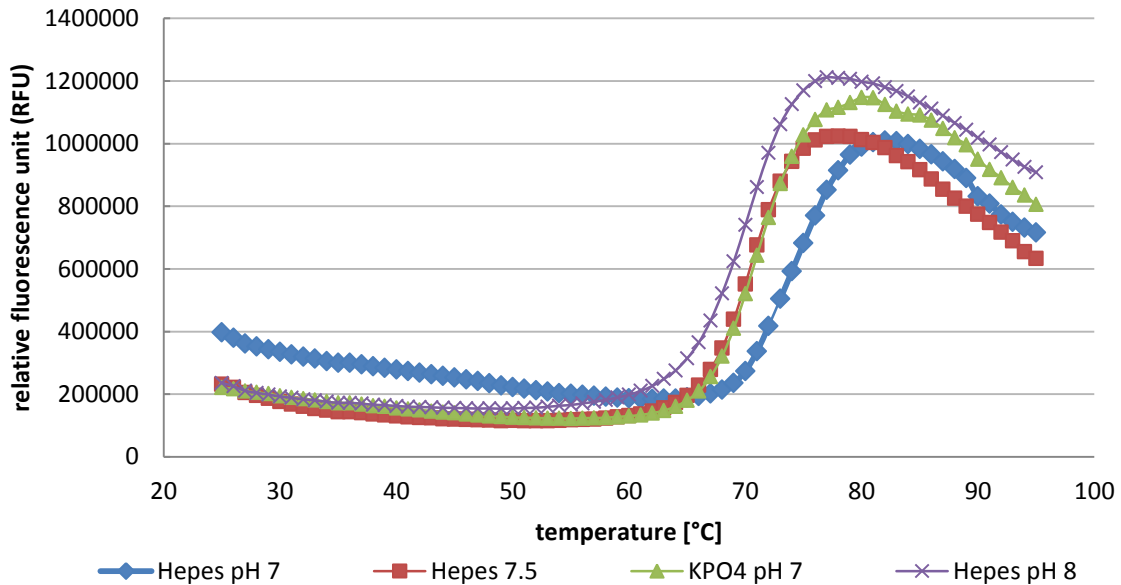


Figure 23: Fluorescence-based thermal shift assay for determination of the melting temperature of QueC from *G. kaustophilus* in buffers with different pH values. Temperature was plotted against relative fluorescence units (10^3) of the TAMRA reporter signal.

With natural substrate and co-factor ATP the melting temperature of QueC from *G. kaustophilus* increased to 82°C in HEPES buffer at pH 7.5. To conclude, CDG and ATP stabilized the structure of the protein and thus made the unfolding more endothermic, which, in turn, lead to an increase of the melting temperature.

Without substrate and co-factor the unfolding of the protein started at 54°C. With substrate and co-factor, the starting point of unfolding increased to 59°C. By comparing the melting temperatures in different buffers with each other, no big difference between the different pH values and buffers were obvious. The melting temperature was in all systems nearly the same.

For the determination of the pH optimum of QueC from *G. kaustophilus in vitro* activity assays were performed over 1 hour at 60°C using different buffer systems as summarized in table 7.

Table 7: Summary of all buffer systems with corresponding pH values, used for the determination of the pH optimum of QueC from *G. kaustophilus*.

buffer system	pH
HEPES buffer	7 to 8
Tris-HCl buffer	8 to 9
Glycine buffer	9 to 10
Carbonate buffer	10 to 10.5

The pH optimum was defined on basis of the amount of product preQ₀ formed during the reaction (figure 24).

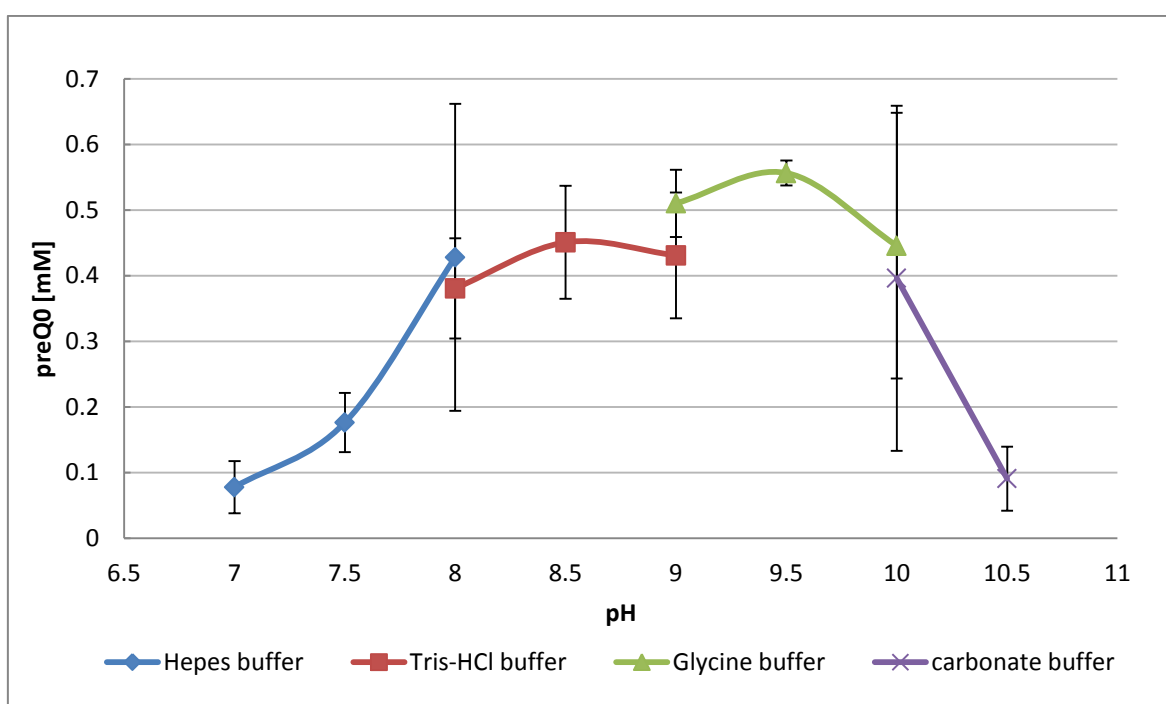


Figure 24: Effect of buffer system and pH on the activity of QueC from *G. kaustophilus*: The optimum buffer system and pH for the enzyme was determined by plotting different buffer systems and pH values against the amount of generated product preQ₀.

Apparently, QueC from *G. kaustophilus* exhibits optimal activity at pH 9.5 in glycine buffer. In HEPES buffer at pH 7.5 compared to glycine buffer at pH 9.5, QueC from *G. kaustophilus* showed only one-third activity. Between pH 7.5 in HEPES buffer and pH 10 in carbonate buffer an enzyme activity could be measured and bioconversion from CDG to preQ₀ was possible.

For the determination of the temperature optimum of QueC from *E. coli in vitro* activity assays were performed over 1.5 hours at temperatures between 25°C and

75°C. The temperature optimum was defined by determination of product preQ_0 amount formed during the reaction (figure 25).

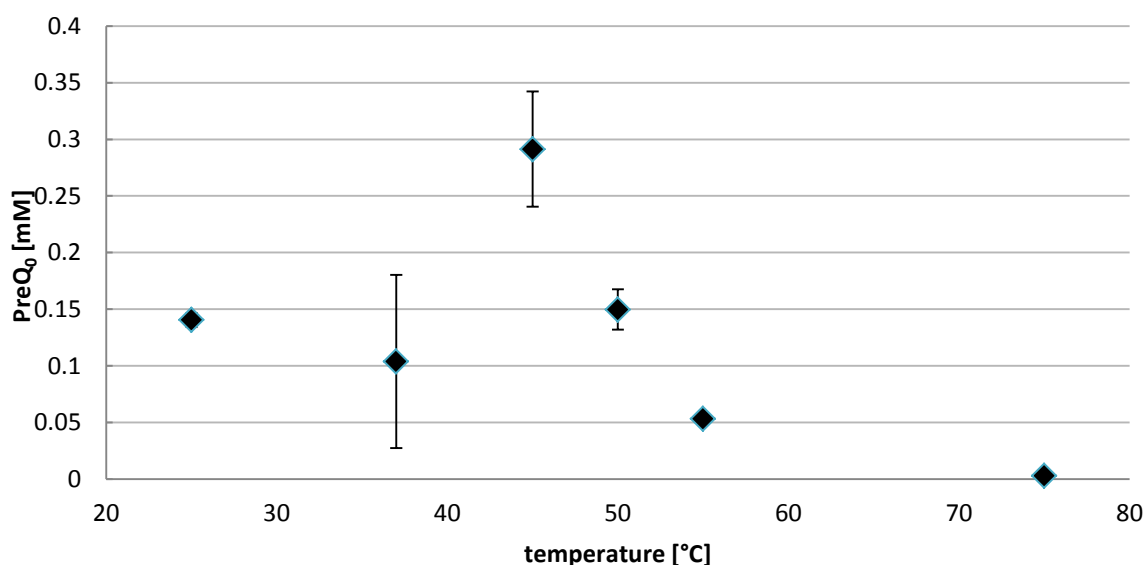


Figure 25: Effect of temperature on the activity of QueC from *E. coli*: The optimum temperature for the enzyme was determined by plotting different temperatures against the amount of generated product preQ_0 .

It seems that QueC from *E. coli* had a temperature optimum at 45°C. But this result is clouded by the high standard deviation of the results between 37 and 45°C, which impairs the reproducibility of the results.

Due to the low reproducibility of the results at the determination of the temperature optimum, the melting temperature of the QueC from *E. coli* in the used buffer system (HEPES buffer with pH 7.5) was determined by a fluorescence -based thermal shift assay (see figure 26). This measurement was performed without the addition of substrate or the co-factor ATP. To estimate the influence of substrate and co-factor on the melting temperature, another fluorescence-based thermal shift assay was performed with addition of CDG and ATP using various buffers and pH's. These results are also figured in figure 26.

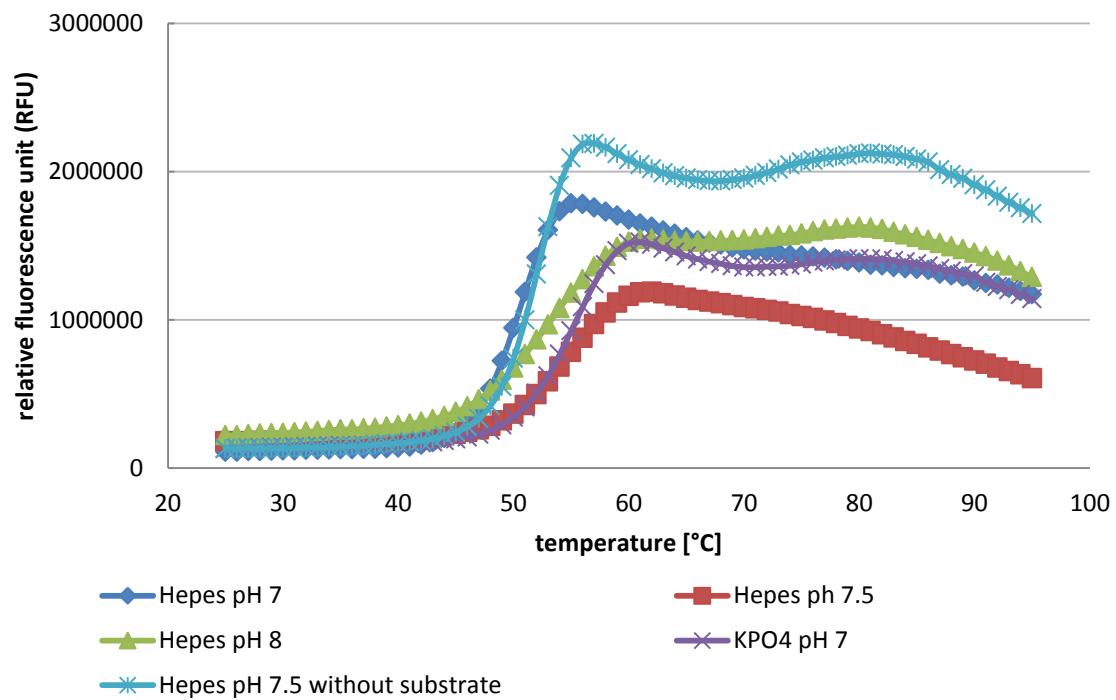


Figure 26: Fluorescence-based thermal shift assay for determination of the melting temperature of QueC from *E. coli* in buffers with different pH values. Temperature was plotted against relative fluorescence units (10^3) of the TAMRA reporter signal.

The melting temperature of the QueC from *E. coli* in HEPES buffer with pH 7.5 and without addition of CDG and ATP was 56°C.

With natural substrate and co-factor ATP the melting temperature of QueC from *E. coli* increased to 62°C in HEPES buffer at pH 7.5. In both cases unfolding of the protein started at 40°C. This explains the low reproducibility of replicate reactions at 45 °C in the determination of the temperature optimum (see figure 25).

By comparing the melting temperatures in different buffers with each other, HEPES buffer at pH 7, at pH 8 and KPO_4 -buffer caused a decrease of the melting temperature. In all other buffer systems the melting temperature of QueC from *E. coli* was nearly the same.

For the determination of the pH optimum of QueC from *E. coli* an in vitro activity assays were performed over 1.5 hour at 28°C using different buffer systems, summarized in table 8.

Table 8 Summary of all buffer systems with corresponding pH values, used for the determination of the pH optimum of QueC from *E. coli*.

buffer system	pH
sodium citrate buffer	4.5 to 6
potassium phosphate buffer	6 to 7
HEPES buffer	6.5 to 8
Tris-HCl buffer	7.5 to 9
Glycine buffer	8.5 to 10
Carbonate buffer	10 to 10.5

The pH optimum was defined by determination of product preQ₀ amount formed during the reaction (figure 27).

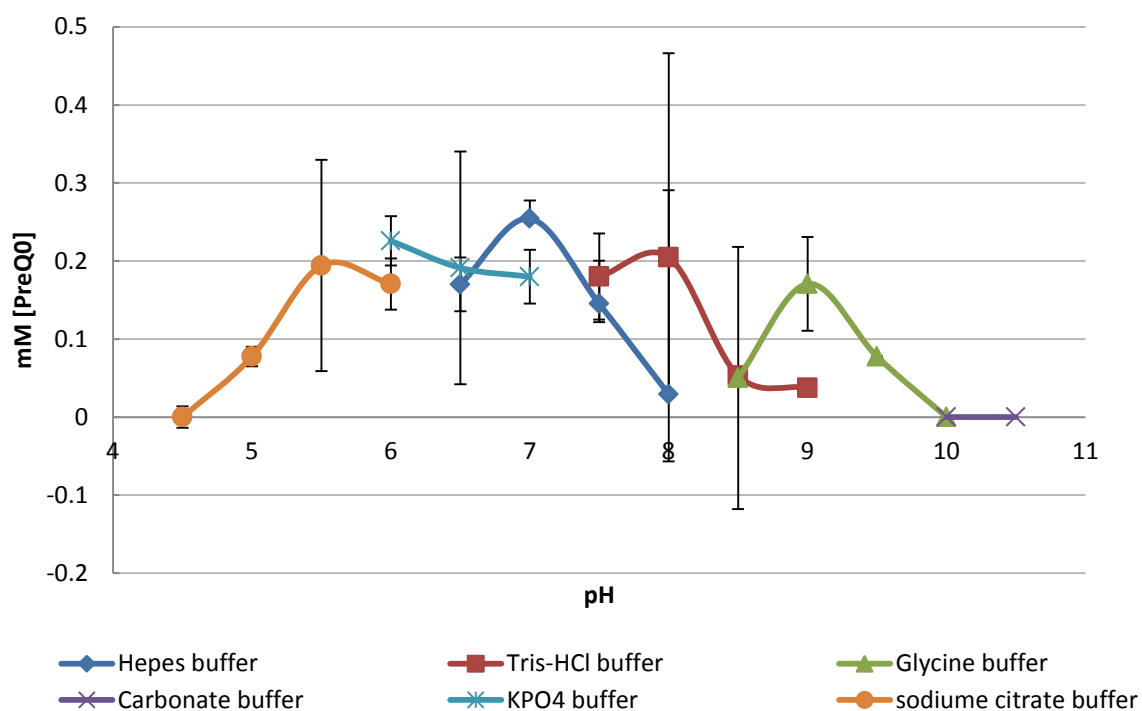


Figure 27: Effect of buffer system and pH on the activity of QueC from *E. coli*: To find the best buffer system and pH optimum for the enzyme, different buffer systems and pH values were plotted against the amount of generated product preQ₀.

The enzyme showed activity over a wide pH range from pH 5 in sodium citrate buffer to pH 9.5 in glycine buffer. However, a clear optimum can not be concluded from this data because of high standard deviations, by repeating the assay in biological duplicates and technical triplicates.

4.6.3 Stability of 7-cyano-7-deazaguanine synthases from *G. kaustophilus* and *E. coli* on ice

To shed light on the storage stability of the QueC enzymes from *G. kaustophilus* and *E. coli*, they were stored on ice over 96 hours. During this time period, 6 samples were taken and an *in vitro* activity assay for characterisation of 7-cyano-7-deazaguanine synthase was performed, for QueC from *G. kaustophilus* for 30 minutes at 60°C and for QueC from *E. coli* for 1.25 hours at 37°C.

In the first 6 hours of storage up and downs could be detected concerning the enzyme activity. These fluctuations were due to equilibration effects. Between 6 and 28 hours, both enzymes lost some activity. However, between 28 and 96 hours, a stable enzyme activity for both enzymes could be detected. Consequently, after complete equilibration of the enzymes to the new environment the storage on ice is no problem.

4.6.4 Exploration of the substrate scope of the different QueCs

4.6.4.1 Measurements with HTP Fluorescence-based Thermal Shift (FTS) assay

The main question of enzyme characterisation, however, was the substrate specificity of this enzyme class. A number of carboxylic acids were chosen, mainly compounds for which the corresponding nitrile product references were available. To check if the chosen carboxylic acids were binding to the QueCs and continuous were influencing the thermostability of the four active QueCs, a HTP Fluorescence-based Thermal Shift (FTS) assay was done in cooperation with Tea Pavkov-Keller from the Institute of Molecular Biosciences (University of Graz). With this assay an increase of the protein melting temperature can be monitored, using fluorescence based detection with the SYPRO Orange protein gel stain dye. When the protein is melting, the dye binds to the hydrophobic surface of the protein and starts to emit light.²⁶

Figure 28 and 29 show the results of the measurements with QueC from *G. kaustophilus* and QueC from *P. atrosepticum*.

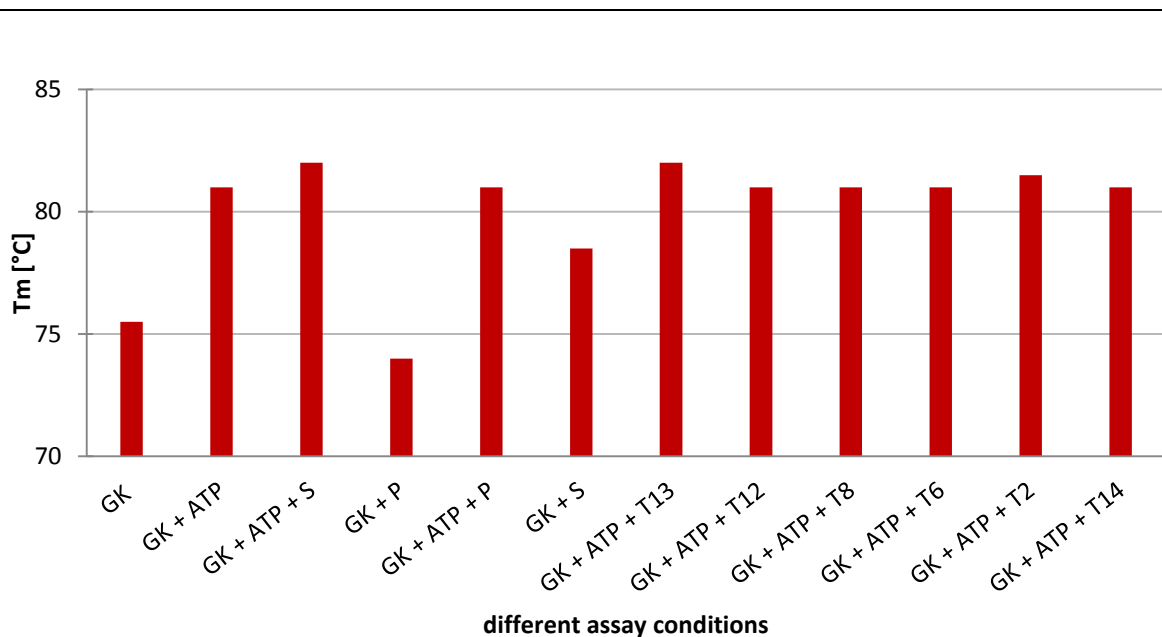


Figure 28: Melting temperatures detected by fluorescence-based thermal shift assay for exploration of the substrate scope of **QueC from *G. kaustophilus*** in HEPES buffer at pH 7.5. Different assay conditions are plotted against the melting temperature (°C). The used shortcuts are described in “Experimental procedure”.

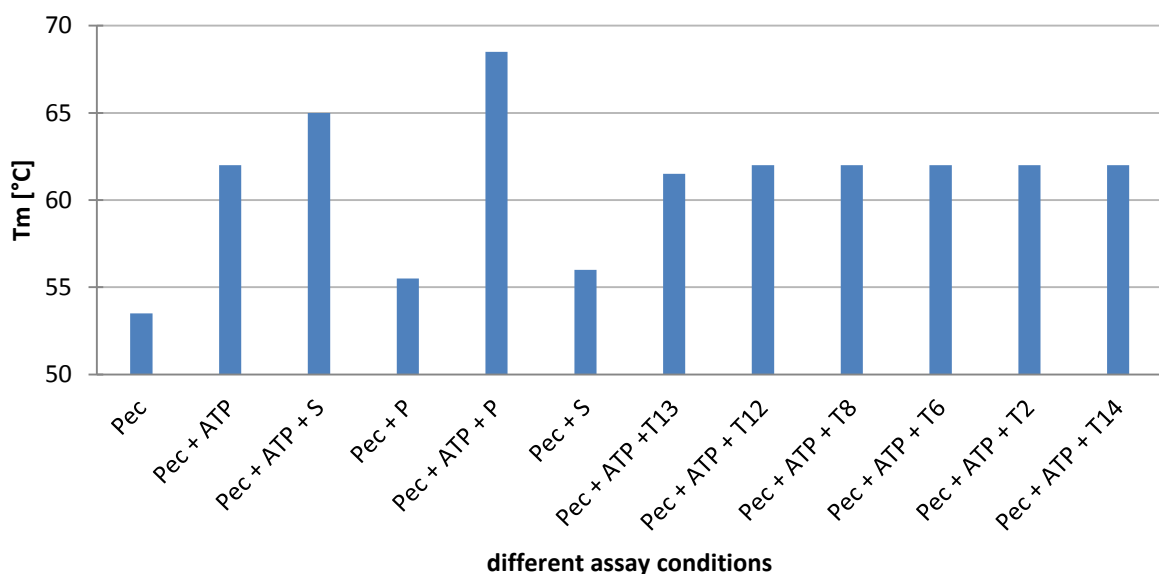


Figure 29: Melting temperatures detected by fluorescence-based thermal shift assay for exploration of the substrate scope of **QueC from *P. atrosepticum*** in HEPES buffer at pH 7.5. Different assay conditions are plotted against the melting temperature (°C). The used shortcuts are described in “Experimental procedure”.

In the reactions where ATP was added, the melting temperature was every time significantly higher than in those without ATP. This indicates that ATP binds to the enzyme and exhibits a stabilizing effect. The QueC enzymes with a size of around 25kDa are, compared to ATP, relatively small. ATP is a co-substrate. Therefore,

ATP can stabilise the enzyme and consequently more energy is needed for unfolding and melting the enzyme. Those samples, which included unnatural substrates showed no significant change in the melting temperature, which indicates that no interactions took place.

In those samples where product (preQ₀) was added, the melting temperature was lower than in those with the natural substrate (CDG). To conclude, product inhibition is not likely during the reaction. A repetition of the HTP Fluorescence-based Thermal Shift (FTS) assay was done with QueC enzymes from *G. kaustophilus*, *E. coli* and *P. atrosepticum*.

As written above, ATP stabilizes QueCs and increases the T_m significantly. Addition of the natural substrate increases the T_m of only one additional degree. The stabilizing effect of a substrate in the presence of ATP is expected to be difficult to determine. Therefore, the reactions were performed with natural and unnatural substrates and without ATP.

The results of QueC from *A. sulficallidus* is absent in this summary because with this enzyme no useful measurements could be achieved with the HTP Fluorescence-based Thermal Shift (FTS) assay. In the monitoring no proper melting curve was seen and thus no exact melting temperatures could be determined.

Figure 30 shows the measurement with QueC form *G. kaustophilus*.

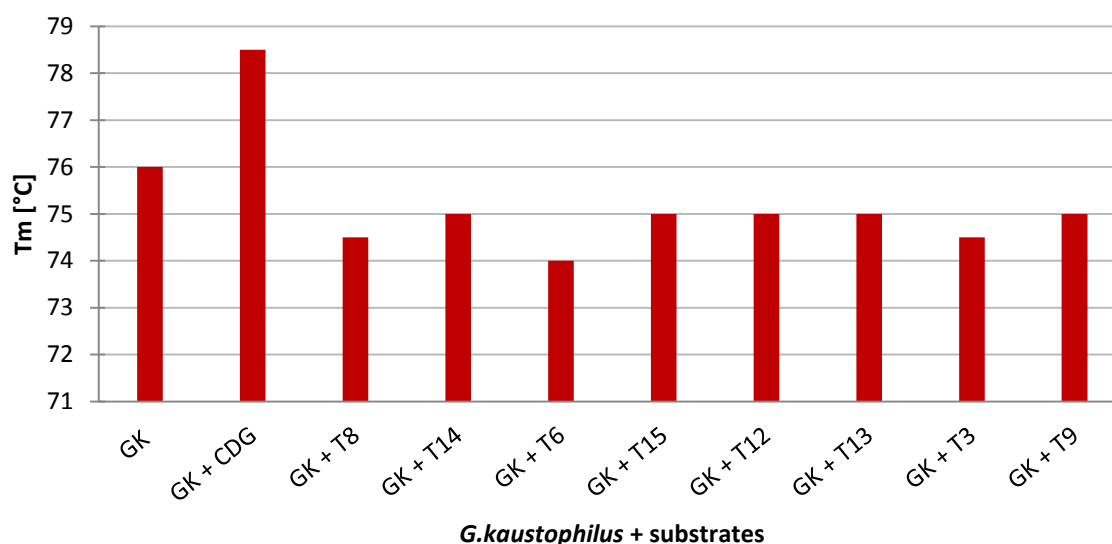


Figure 30: Melting temperatures detected by fluorescence-based thermal shift assay for exploration of the substrate scope of **QueC from *G. kaustophilus*** in HEPES buffer at pH 7.5, **without ATP**. Different assay conditions are plotted against the melting temperature (°C). The used shortcuts are described in “Experimental procedure”.

The addition of the natural substrate CDG to the enzyme reaction brought an increase of 2.5°C compared to the melting temperature of enzyme without substrate. The addition of unnatural substrates T8, T14, T6, T15, T12, T13, T3 and T9 to QueC from *G. kaustophilus* brought no significantly increase of the melting temperature. On the contrary, the melting temperatures decreased.

In figure 31, the measurement with QueC form *E. coli* is plotted.

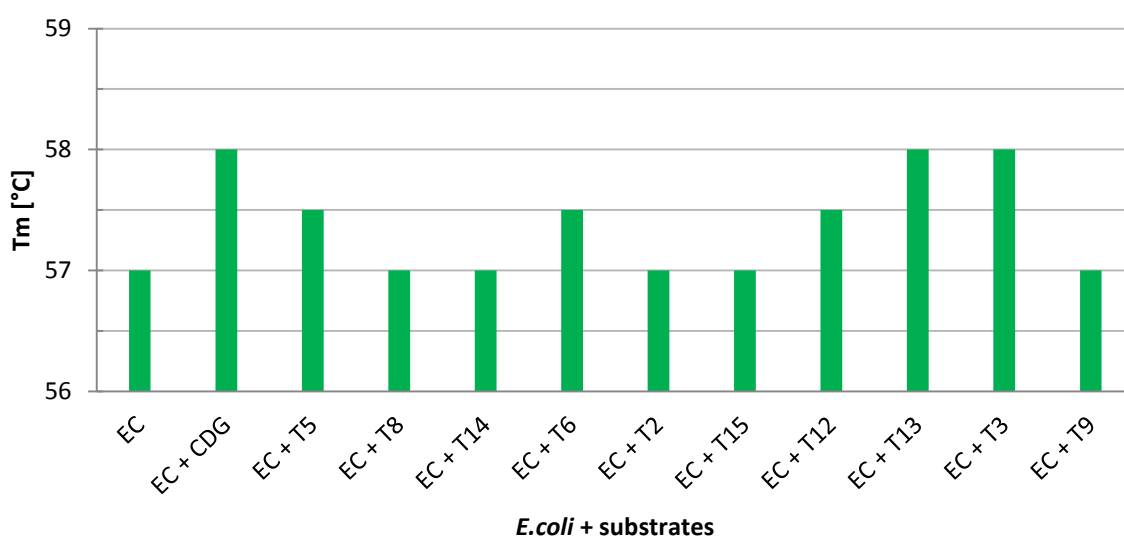


Figure 31: Melting temperatures detected by fluorescence-based thermal shift assay for exploration of the substrate scope of **QueC from *E. coli*** in HEPES buffer at pH 7.5, **without ATP**. Different assay conditions are plotted against the melting temperature (°C). The used shortcuts are described in “Experimental procedure”.

The addition of the natural substrate CDG to the enzyme reaction brought an increase of 1°C compared to the melting temperature of enzyme without substrate. The addition of unnatural substrates T13 and T3 to QueC of *E. coli* increased the melting temperature also to 58°C. The addition of the other unnatural substrate T8, T14, T6, T2, T15, T12 and T9 to QueC from *E. coli* brought no significantly increase of the melting temperature. To conclude, T13 and T3 had maybe a positive influence on the stability of the enzyme. This may mean that they could be substrates or inhibitors.

Figure 32 shows the measurement with QueC form *P. atrosepticum*.

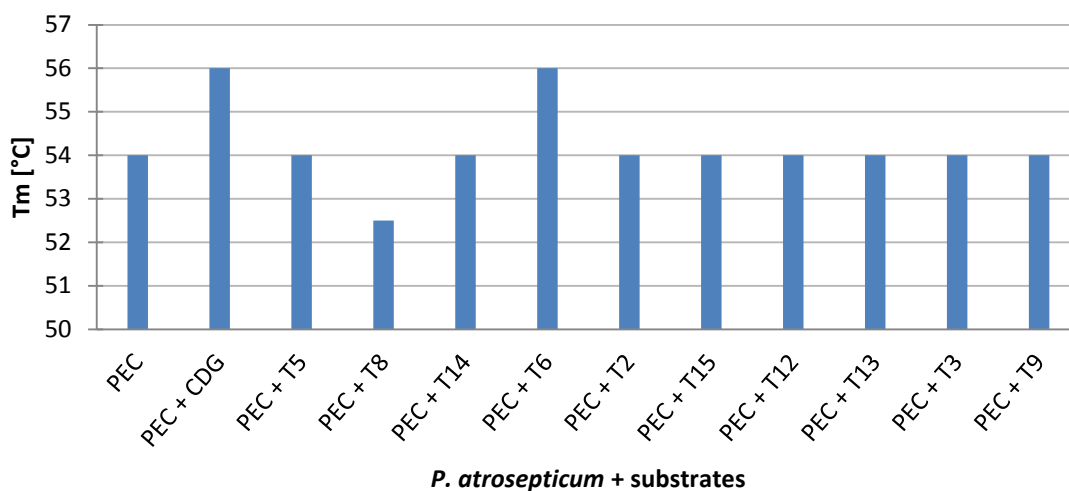


Figure 32: Melting temperatures detected by fluorescence-based thermal shift assay for exploration of the substrate scope of **QueC from *P. atrosepticum*** in HEPES buffer at pH 7.5, **without ATP**. Different assay conditions are plotted against the melting temperature (°C). The used shortcuts are described in “Experimental procedure”.

The addition of the natural substrate CDG to the enzyme brought an increase of 2°C compared to the melting temperature of enzyme without substrate. The addition of unnatural substrate T6 to QueC from *P. atrosepticum* increased the melting temperature also to 56°C. The addition of the other unnatural substrate T8, T14, T2, T15, T12, T13, T3 and T9 to QueC from *P. atrosepticum* did not yield an increase of the melting temperature. To conclude, T6 was somehow stabilising the enzyme and contributed an increase of the melting temperature.

To conclude, T3, T6 and T13 are perhaps potential substrates for QueC. In order to check if the 4 active QueCs are able to convert these 3 potential substrates overnight assays were performed and carboxylic acids and nitriles were analysed by HPLC-MS.

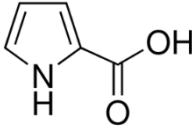
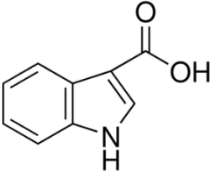
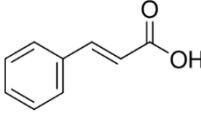
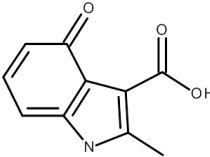
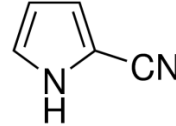
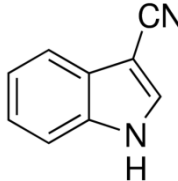
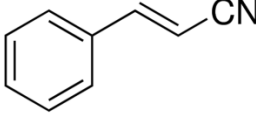
4.6.4.2 Measurements with HPLC-UV and HPLC-MS

For a few carboxylic acids HPLC-methods were developed, mainly for carboxylic acids, where corresponding nitrile product references were available. The exploration of the substrate scope of QueC from *G. kaustophilus*, *E. coli*, *P. atrosepticum* and *A. sulficallidus* was done with an *in vitro* activity assay for characterisation of 7-cyano-7-deazaguanine synthase, performed overnight at 30°C. As positive control, additional reactions with the natural substrate CDG were performed, to proof

the functionality of each enzyme. The chosen carboxylic acids are summarized in table 9. The corresponding nitrile from 2-methyl-4-oxo4,5,6,7-tetrahydro-1H-indole-3-carboxylic acid is missing, because it was not possible to order it.

The detection of carboxylic acids and corresponding nitriles was done with HPLC-MS. The results of QueC from *A. sulficallidus* are missing, because HPLC-measurements delivered no useful results.

Table 9: Carboxylic acids, which have been used for exploration of the substrate scope with HPLC.

Carboxylic acids and corresponding nitriles	short cut	structure
Pyrrole-2-carboxylic acid	S2	
Indole-3-carboxylic acid	S6	
(E)-Cinnamic acid	S8	
2-methyl-4-oxo4,5,6,7-tetrahydro-1H-indole-3-carboxylic acid	S13	
Pyrrole-2-carbonitrile	S2	
Indole-3-carbonitrile	P6	
Cinnamonitrile	P8	

The results of the HPLC-measurements are plotted in figure 33.

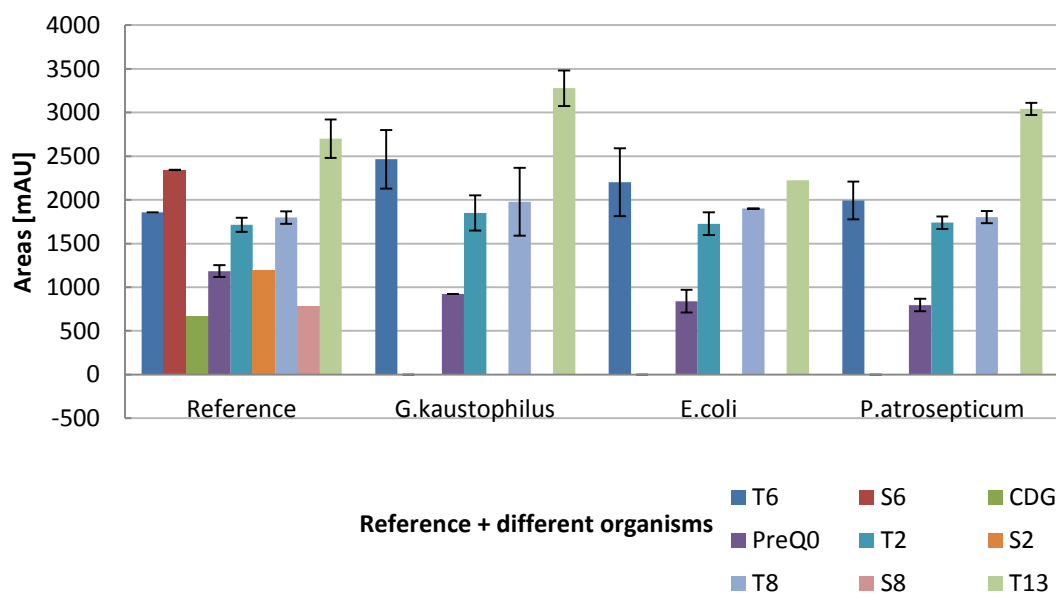


Figure 33: Summary of all HPLC measurements for exploration of the substrate scope of QueC from *G. kaustophilus*, *E. coli* and *P. atrosepticum* in HEPES buffer at pH 7.5. In the blank, 1mM of each carboxylic acid and nitrile was used.

The bioconversion from CDG to preQ₀ was successful with all three QueCs. However, as shown in figure 33 no conversion of an unnatural substrate could be detected. Since HPLC method developing is very time consuming, no further methods were established to screen more carboxylic acids as potential substrates. QueC from *G. kaustophilus*, *E. coli*, and *P. atrosepticum* seem to have a strict substrate affinity to the natural substrate CDG. Previous work with the successor of 7-cyano-7-deazaguanine synthase in the bio catalytic pathway, the nitrile reductase, showed a restriction of the wild type enzyme to the natural substrate preQ₀ as well⁸

To date, the 7-cyano-7-deazaguanine synthase is the only enzyme known that can convert a carboxylic acid to a nitrile.^{39,1} To make this enzyme usable for industrial applications, an investigation of the active site was done for QueC from *G. kaustophilus*.³⁵ This could lead to a deeper understanding of the essential resi-

dues and open the perspective to target the substrate binding site by site specific mutagenesis in a rational manner to extend the scope substrate of the enzyme in the future. Since such an approach was unfortunately unsuccessful for nitrile reductases (QueF), it can be assumed that it may be as challenging for QueC enzymes.

4.7 In Vitro reconstruction of Queosine biosynthesis in *G. kaustophilus*: two step cascade from 7-carboxy-7-deazaguanine to preQ₁

The *in vitro* reconstruction of the last step of the preQ₀ biosynthetic pathway and the reduction to preQ₁ was performed in one reaction vessel. The reaction was carried out at 55°C for the first hour and then the temperature was reduced to 30°C for the rest of the reaction.

The conversion was monitored by HPLC. Results of the HPLC measurement are shown in figure 34.

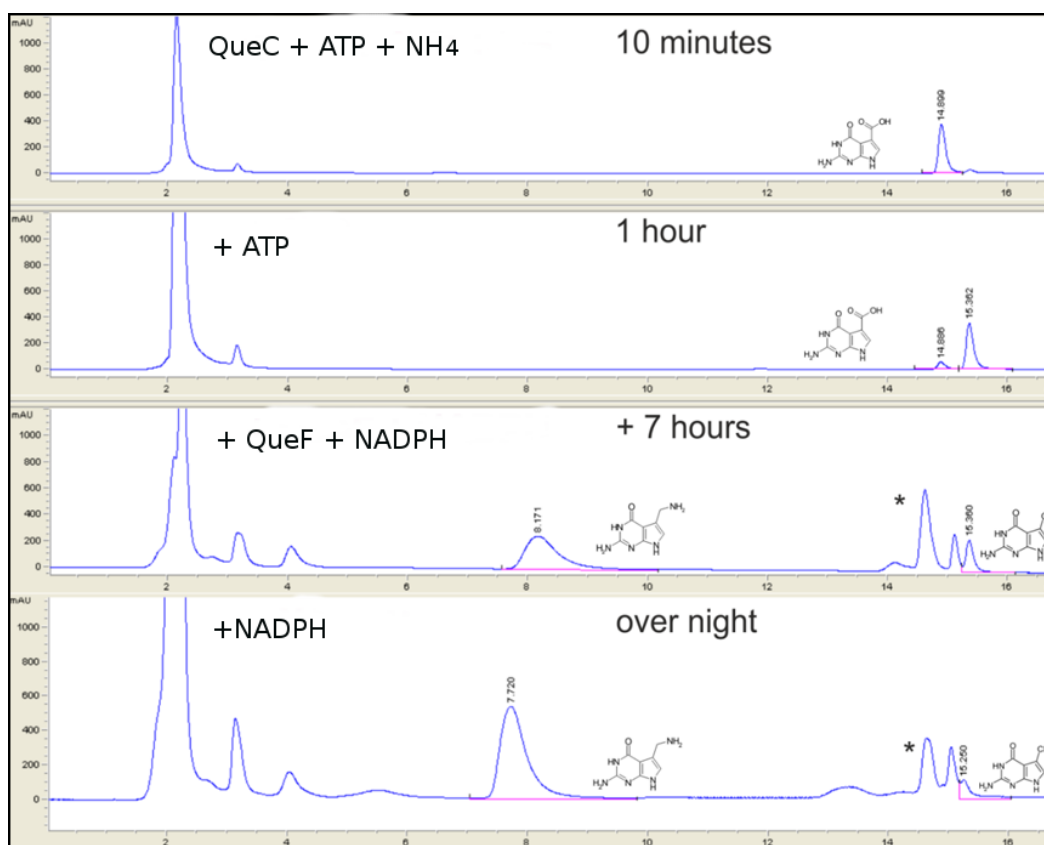


Figure 34: HPLC chromatograms, showing conversion of the natural substrate CDG to preQ₀ and further to preQ₁ with 7-cyano-7-deazaguanine synthase and 7-cyano-7-deazaguanine reductase from *Geobacillus kaustophilus*. The simulation was performed in a reaction buffer containing 100mM Tris, 50 mM KCl and 1mM TCEP (pH7.5). The conversion was stopped with a stopping-solution, containing 80% MeOH and 20% DMSO. (*) Impurities from the QueF preparation (low-molecular weight components).

First, QueC from *G. kaustophilus* converted CDG to preQ₀ under consumption of ATP and NH₄. After ten minutes, predominantly CDG was detected and a small amount of preQ₀. After one hour and further addition of ATP, to ensure complete conversion, preQ₀ was formed. PreQ₀ served as the substrate for GkNRedWT, which reduced the nitrile to the primary amine preQ₁ in an NADPH-dependent reaction. After 7 hours, the preQ₀ peak decreased and preQ₁ was formed. For full conversion, NADPH was again added to the reaction vessel, and the reaction was run over night. After addition of GkNRedWT, a peak adjacent to CDG appeared. GkNRedWT was purified by heat precipitation. Perhaps, these impurities arise from the heat purification protocol and are low-molecular components. To investigate this hypothesis, GkNRedWT was alternatively purified by Ni-affinity chromatography and the *in vitro* reconstruction was performed again. However, this repetition with better purified enzyme gave the same result and these unidentified peaks were again present, indicating that the additional peaks may be the result of cofactor degradation. However, further experiments were not performed.

To conclude, the reconstruction of two steps of the queuosine biosynthesis in *G. kaustophilus* was successful. CDG, preQ₀ and preQ₁ could be detected by HPLC.

5 Conclusion

The cloning of six putative 7-cyano-7-deazaguanine synthases into the pEHisTEV-vector from different organisms was successfully performed. With QueC from *G. kaustophilus*, *E. coli*, *P. atrosepticum*, *A. sulficallidus* and *B. subtilis* relatively high expression levels by induction with 1mM IPTG and 0.1mM ZnSO₄ could be achieved. Exploration of the biophysical properties of QueC enzymes were performed with these 5 enzymes.

For the characterisation of the enzymes a specific activity assay was developed. Several problems had to be solved during the establishing process. For this reason, several stages of assay development were necessary. Substrate CDG and product preQ₀ were not soluble in the reaction buffer system, consisting of 100mM HEPES buffer plus 100mM NaCl, 10mM MgCl₂, 10 mM DTT and 5 mM ammonium sulfate, adjusted to a pH of 7.5. Hence, analysis with HPLC was nearly impossible, due to the low reproducibility and mass balance. With a highly alkaline environment and a higher pH value, the reproducibility of analysis was improved. The stopping reaction was adjusted from inactivation by heat shock, to adding only MeOH (100% of the reaction volume) and finally to adding MeOH (80% of the reaction volume), DMSO (20% of the reaction volume) and 1 M KOH (50% of the reaction volume) to the reaction solution.

At the laboratory start of work, the reaction mechanism of QueC was not described in detail in literature. For this reason, exploration experiments were done. By monitoring the amount of ATP, ADP and AMP during the reaction, we wanted to get information if ADP or AMP is formed from ATP during the reaction process.

The capHPLC based analysis did not lead no significant result. Further on, NMR spectrometry was done. By monitoring ³¹P NMR spectra of ATP, ADP, AMP, phosphate and pyrophosphate, AMP and pyrophosphate formation was detected during the reaction of QueC.

In conclusion, 7-cyano-7-deazaguanine synthase converts 7-carboxy-7-deazaguanine (CDG) to 2-amino-5-cyanopyrrolo[2,3-d]pyrimidin-4-one (preQ₀). In this reaction ATP is consumed and AMP and pyrophosphate are formed as by-products.

The active site residues from 7-cyano-7-deazaguanine synthases were explored by molecular modelling experiments. In the analysis, a QueC-AMP complex was generated. It was found that Q39, T119, R97 and N98 are probably involved in the ATP-binding during the reaction. Substrate binding of CDG and probably involves a tyrosine and an aspartate.

Characterisation of the enzymes has been started by proofing the activity of all five enzymes, which could be successfully expressed, with an *in vitro* activity assay. QueC from *G. kaustophilus*, *E. coli*, *P. atrosepticum* and *A. sulficallidus* showed activity for the conversion of CDG to preQ₀. QueC from *B. subtilis* showed no activity under the same conditions.

For characterisation of QueC from *G. kaustophilus* and *E. coli* the temperature and pH optima were determined with *in vitro* activity assays. QueC from *G. kaustophilus* had its temperature optimum at 60°C and pH 9.5 in glycine buffer. QueC from *E. coli* showed highest apparent activity at 45°C and pH 7 in HEPES buffer.

Further on, exploration of the substrate scope was done with QueC from *G. kaustophilus*, *E. coli*, *P. atrosepticum* and *A. sulficallidus* by using an *in vitro* activity assay and HPLC detection and an FTS assay. QueC from *G. kaustophilus*, *E. coli*, *P. atrosepticum* and *A. sulficallidus* seem to have a strict substrate specificity to the natural substrate CDG.

To summarize, several QueCs from different organisms can be expressed in *E.coli*. Four QueCs showed activity in the developed activity assay. Furthermore, the net reaction products of 7-cyano-7-deazaguanine synthase are explored and confirmed very recent literature from Vahe Bandarian et al.³⁹

6 References

6.1 Literature

1. McCarty, R. M., Somogyi, A., Lin, G., Jacobsen, N. E. & Bandarian, V. The deazapurine biosynthetic pathway revealed: in vitro enzymatic synthesis of PreQ(0) from guanosine 5'-triphosphate in four steps. *Biochemistry* **48**, 3847–52 (2009).
2. Phillips, G. *et al.* Diversity of archaeosine synthesis in crenarchaeota. *ACS Chem. Biol.* **7**, 300–5 (2012).
3. Battaglia, U., Long, J. E., Searle, M. S. & Moody, C. J. 7-Deazapurine biosynthesis: NMR study of toyocamycin biosynthesis in *Streptomyces rimosus* using 2-¹³C-7-¹⁵N-adenine. *Org. Biomol. Chem.* **9**, 2227–32 (2011).
4. Reader, J. S., Metzgar, D., Schimmel, P. & de Crécy-Lagard, V. Identification of four genes necessary for biosynthesis of the modified nucleoside queuosine. *J. Biol. Chem.* **279**, 6280–5 (2004).
5. Cicmil, N. & Huang, R. H. Crystal structure of QueC from *Bacillus subtilis*: an enzyme involved in preQ1 biosynthesis. *Proteins* **72**, 1084–8 (2008).
6. Gaur, R. & Varshney, U. Genetic Analysis Identifies a Function for the queC (ybaX) Gene Product at an Initial Step in the Queuosine Biosynthetic Pathway in *Escherichia coli*. *J. Bacteriol.* **1**, 6893–6901 (2015).
7. Buchholz, K. & Kasche, V. Biocatalysts and Enzyme Technology. *Wiley-Blackwell*, 626 pages (2012).
8. Wilding, B. *et al.* Nitrile Reductase from *Geobacillus kaustophilus*: A Potential Catalyst for a New Nitrile Biotransformation Reaction. *Adv. Synth. Catal.* **354**, 2191–2198 (2012).
9. Van Lanen, S. G. *et al.* From cyclohydrolase to oxidoreductase: discovery of nitrile reductase activity in a common fold. *Proc. Natl. Acad. Sci. U. S. A.* **102**, 4264–9 (2005).
10. Daniel G Gibson, Lei Young, Ray-Yuan Chuang, J. C. V. Enzymatic assembly of DNA molecules up to several hundred kilobases. *Nat. Methods* **6**, 343 – 345 (2009).
11. Gibson. Enzymatic Assembly of Overlapping DNA Fragments. *Methods Enzymol.* **498**, 349–61. (2011).
12. Blattner, F. R. *et al.* The Complete Genome Sequence of *Escherichia coli* K-12. *Sci. Mag.* **277**, 1453–1462 (1997).

-
13. E. L. Tatum and Joshua Lederberg. Gene recombination in the bacterium *Escherichia coli*. *J. Bacteriol.* **53** (6), 673–684 (1941).
 14. Huang, C.-J., Lin, H. & Yang, X. Industrial production of recombinant therapeutics in *Escherichia coli* and its recent advancements. *J. Ind. Microbiol. Biotechnol.* **39**, 383–99 (2012).
 15. Lederberg, J. A view of genetics. *Sci. Mag.* **131**, 269–76 (1960).
 16. Berlyn, M. K. B. Linkage Map of *Escherichia coli* K-12, Edition 10: The Traditional Map. *Microbiol. Mol. Biol. Rev.* 814–984 (1998).
 17. Ramos, C. R. R. A high-copy T7 *Escherichia coli* expression vector for the production of recombinant proteins with a minimal N-terminal His-tagged fusion peptide. *Brazilian J. Med. Biol. Res.* **37**, 1103–1109 (2004).
 18. Doyle, S. A. High throughput protein expression and purification. *Springer Protocols*, 314 pages (2009).
 19. Liu, H. & Naismith, J. H. A simple and efficient expression and purification system using two newly constructed vectors. *Protein Expr. Purif.* **63**, 102–111 (2009).
 20. T. Dawn Parks, K. K. L. Release of Proteins and Peptides from Fusion Proteins using a Recombinant Plant Virus Proteinase. *Anal. Biochem.* **216**, 413–417 (1993).
 21. Skoog, Douglas, Holler, James, Leary, J. Principles of Instrumental Analysis 4th Edition. *Springer Verlag* **2**, (2006).
 22. Gottwald, W. RP-HPLC für Anwender. *VCH Verlagsgesellschaft* 65 (1993).
 23. Pous-Torres, S., Torres-Lapasió, J. R. & García-Álvarez-Coque, M. C. Comparison of the performance of Chromolith Performance RP-18e, 1.8- μm Zorbax Eclipse XDB-C18 and XTerra MS C18, based on modelling approaches. *Anal. Bioanal. Chem.* **405**, 2219–31 (2013).
 24. Phenomenex, I. Phenomenex manual. *Phenomenex Key Prod. Buyer's Guide*. 37 (2008).
 25. Reusch, W. Nuclear Magnetic Resonance Spectroscopy. (2013). at <<https://www2.chemistry.msu.edu/faculty/reusch/VirtTxtJml/Spectrpy/nmr/nmr1.htm>>
 26. Lavinder, J. J., Hari, S. B., Sullivan, B. J. & Magliery, T. J. High-Throughput Thermal Scanning: A General, Rapid Dye-Binding Thermal Shift Screen for Protein Engineering. *J. Am. Chem. Soc.* **131**, 3794–3795 (2009).
 27. H. Beyer. Organische Chemie, 22. Auflage, *Hirzel Verlag* (1991).

-
28. Peter Pollak, Gérard Romeder, Ferdinand Hagedorn, H.-P. G. Ullmann's Encyclopedia of Industrial Chemistry, *Wiley-VCH*(2002).
 29. Schwetlick, K. Organikum, 22. Edition (German), *Wiley-VCH*(2004).
 30. Dewan, S. K., Singh, R. & Kumar, A. One pot synthesis of nitriles from aldehydes and hydroxylamine hydrochloride using sodium sulphate (anhyd) and sodium bicarbonate in dry media under microwave irradiation. *Ark. Free J. Org. Chem.* 1424–6376 (2006).
 31. Elisa Lanfranchi, Kerstin Steiner, Anton Glieder, Ivan Hajnal, Roger A. Sheldon, S. van P. and M. W. Mini-Review: Recent Developments in Hydroxynitrile Lyases for Industrial Biotechnology. *Recent Pat Biotechnol.* **7**, 197–206 (2013).
 32. Asano, Y. Overview of screening for new microbial catalysts and their uses in organic synthesis — selection and optimization of biocatalysts. *J. Biotechnol.* **94**, 65–72 (2002).
 33. Wiedner, R., Gruber-Khadjawi, M., Schwab, H. & Steiner, K. Discovery of a novel (R)-selective bacterial hydroxynitrile lyase from *Acidobacterium capsulatum*. *Comput. Struct. Biotechnol. J.* **10**, 58–62 (2014).
 34. M. Winkler, A. Glieder, and K. S. *Comprehensive Chirality: C-X Bond Formation: Hydroxynitrile Lyases: From Nature to Application. Compr. Chirality*, vol. 7 350–371 (Elsevier Inc., 2012).
 35. Winkler, M., Dokulil, K., Weber, H., Pavkov-keller, T. & Wilding, B. The Nitrile Forming Enzyme 7-Cyano-7-Deazaguanine Synthase from *Geobacillus kaustophilus* : A Reverse Nitrilase ? *ChemBioChem*, **16**, 2373–8 (2015).
 36. Mitrovic, A. *et al.* Thermostability improvement of endoglucanase Cel7B from *Hypocrea pseudokoningii*. *J. Mol. Catal. B Enzym.* **103**, 16–23 (2014).
 37. Inclán, M. *et al.* Molecular Recognition of Nucleotides in Water by Scorpion-Type Receptors Based on Nucleobase Discrimination. *Chem. - A Eur. J.* **20**, 3730–3741 (2014).
 38. Siebenlist, U. & Gilbert, W. Contacts between *Escherichia coli* RNA polymerase and an early promoter of phage T7. *Proc. Natl. Acad. Sci. U. S. A.* **77**, 122–126 (1980).
 39. Nelp, M. T. & Bandarian, V. A Single Enzyme Transforms a Carboxylic Acid into a Nitrile through an Amide Intermediate. *Angew. Chem. Int. Ed. Engl.* **54**, 10627–9 (2015).
 40. Rizzi, M., Bolognesi, M. & Coda, A. A novel deamido-NAD⁺-binding site revealed by the trapped NAD-adenylate intermediate in the NAD⁺ synthetase structure. *Structure* **6**, 1129–1140 (1998).

-
41. Kang, G. B. *et al.* Crystal structure of NH₃-dependent NAD⁺ synthetase from *Helicobacter pylori*. *Proteins* **58**, 985–8 (2005).
 42. Fresquet, V., Thoden, J. B., Holden, H. M. & Raushel, F. M. Kinetic mechanism of asparagine synthetase from *Vibrio cholerae*. *Bioorg. Chem.* **32**, 63–75 (2004).
 43. Steinsbu, B. O. *et al.* *Archaeoglobus sulfaticallidus* sp. nov., a thermophilic and facultatively lithoautotrophic sulfate-reducer isolated from black rust exposed to hot ridge flank crustal fluids. *Int. J. Syst. Evol. Microbiol.* **60**, 2745–52 (2010).
 44. Takami, H. *et al.* Thermoadaptation trait revealed by the genome sequence of thermophilic *Geobacillus kaustophilus*. *Nucleic Acids Res.* **32**, 6292–303 (2004).

6.2 Lab-book

Lab book (469, KDO, 1) and Lab book (618, KDO, 2) from Katharina Dokulil

Appendix

Strain information

The strains that were generated in this work, were deposited in the strain collection data base from ACIB.

Table 10: Strain designation and culture collection number of collected strains with QueC from different organisms.

Culture collection number	Strain designation
ST934/7266	<i>E. coli</i> _BL21_pEHISTEV_QueC_Gkaustophilus
ST933/7265	<i>E. coli</i> BL21 pEHISTEV_QueC_Ecoli
ST932/7264	<i>E. coli</i> BL21 pEHISTEV_QueC_Patrosepticum
ST931/7263	<i>E. coli</i> BL21 pEHISTEV_QueC_Bsubtilis
ST930/7262	<i>E. coli</i> BL21 pEHISTEV_QueC_Asulficallidus

DNA sequences

QueC *G. kaustophilus*

ATGATGAAGATGAATGAAGAAAAGGCGGTCGTCGTCTTTAGCGGCGGC-
 CAAGACAGCACGACGTGTTTGTGTTTTGGGCGAAAAACAGTTTGGTGAAGTGGAAAG-
 CGGTGACGTTTGACTACGGCCAGCGCCATCGCCGGGAAATTGACGTCGCTCAAG-
 CGATCGCTGACGAGCTTGGCGTCCGCCATACAGTGCTT-
 GATTTGTGCTTCTCGGGCAGTTGGCGCCGAACGCCTT-
 GACGCGGCGCGACATTGCCATTGAACAAAAGAAAGGCGAG-
 CTGCCGACGACGTTTGTGGACGGACGCAATTTgTTGTTTTTAT-
 CATTGCGcGCgGTGTTtGCCAAACAGCGGGGCGCGCCATATTGTGACtG-
 GAGTGTGCGAAACAGATTTTACGCGGCTATCCGGACTGCCGCGATGTGTTTAT-
 CAAATCATTGAACGTCACGCTGAATTTAGCGATGGATTACGAATTTGTCATTCA-
 TACGCCGCTCATGTGGCTGACGAAAGCGGAGACGTGGAAGCTCGCTGATGAG-
 CTCGGGGCGCTCGAGTTCATTCGCACGAAGACGCTGACGTGCTATAACGGCAT-
 CATCGCCGACGGCTGCGGCGAATGCCAGCATGTGCGCTGCGCAAG-
 CGCGGGTTGGATGAcTATTTGCGGGAAAAAGCGGAGGTGGAGTCGCGATAA

QueC *E. coli*

ATGAAACGTGCTGTCGTTGTGTTTCAGTGGAGGCCAGGATTCCACCAC-
 CTGTCTGGTGCAGGCATTACAACAATATGATGAAGTCCATTGCGTGACGTTTCGAT-

TACGGTCAGCGACATCGCGCAGAAATCGACGTGGCACGCGAACTGGCGCT-
GAAACTGGGAGCACGCGCGCATAAGGTTCTTGATGTAACGCTGCTCAACGAG-
CTGGCGGTGAGCAGCCTGACACGTGACAGCATTCCGGTGCCTGATTATGAACCT-
GAAGCCGATGGCATCCCGAATACGTTTGTCCAGGGCGTAATATTTTGTTCCT-
GACGCTGGCGGCAATATATGCGTATCAGGTAAAAGCAGAAGCCGTAATTAC-
CGGCGTCTGTGAAACGGATTTCTCCGGCTACCCGGATTGCCGCGATGAGTTTGT-
GAAAGCACTAAACCATGCCGTCAGTTTGGGCATGGCGAAAGATATTCGTTTT-
GAAACGCCGCTGATGTGGATTGATAAAGCGGAAACCTGGGCGCTGGCAGATTAT-
TACGGCAAACCTGGATTTAGTCCGTAACGAAACGTTGACCTGCTATAACGGCAT-
TAAAGGCGACGGTTGCAGTCATTGTGCGGCATGTAATTTACGCGCCAACGGTTT-
GAATCATTATCTGGCCGATAAACCGACGGTGATGGCAGCGATGAAGCA-
GAAAACCGGGTTGAGGTAA

QueC *A. flavithermus*

ATGAAAAAGGAGAAAGCTGTAGTGGTTTTTAGTGGTGGCCAGGATAGCACTA-
CATGTCTGTTTTGGGCGAAGAAACATTTTGCCGAAGTAGAAGCCGTTACTTTTGAC-
TATAATCAACGACATCGCCTGGAGATCGATGTCGCCGCGTCGATCGCCAAAGAG-
CTGAATGTATCACACACAGTATTAGACATGTCGTTGTTGCATCAACTTGCCC-
CAAACGCTTTAACCCGTAGCGACATTGCAATTGAGCAGAAAGAAGGT-
CAGTTGCCCTCTACATTTGTG-
GATGGCCGTAATCTTCTGTTTCTGTCTTTTGC GGCGGTTCTGGCTAAGCA-
GAAGGGTGCTCGCCATTTGGTTACAGGTGTTTGTGAAACTGACTTTTCGGGTTA-
TCCCGATTGTGAGATGTGTTTATCAAATCTCTAAACGTTACCCTTAATTTAGCTATG-
GACTATCAATTCGTAATACATACACCACTGATGTGGCTTAACAAAGCAGAGACCTG-
GAAACTGGCCGATGAATTAGGCGCCCTGGAGTTTGTACGTAACAAAACACT-
CACGTGTTACAATGGTATAATTGCAGATGGTTGCGGAGA-
ATGCCCGGCCTGCGTGCTCCGCAAACGCGGCCTGGATCAGTACAT-
GAACGAAAAAAAAAGGCGCTAACGTCAGATA

QueC *A. sulfaticallidus*

ATGCACGCGGTTCTTATCTTCAGCGGCGGGGTTGATAGTACGACGCTGTTATAT-
TACTTAATTTCTAAAGGCTATGAAGTCCATGCCCTCACCTTTATTTACGGT-
CAAAAACATGCAAGGGAGGTGGACGCATCTAAAAGATCGCAAAACTGCTGGGAAT-
TAAACACAAAGTTGTTGATATCACTTCGATTACGAGCTGATTTCCCGGGGTTCCCT-
GACAGGTGGTGAGGAAGTACCAAAGATTTCTACACCGAAGAGACACAGAACT-

GACAATAGTTCCGAACCGGAATATGATCCTGTTAGCAATCGCCGGCGGC-
TATGCTGTCAAAGAAAATATAAGAGAGGTATACTACGCCGCCACAAGTCGGATTA-
TTCTATTTACCCTGATTGTCGCAAGGAATTTGTGAAGGTCATG-
GATGCGGCCCTGTATCTGGCGAACTTATGGACACCCGTGGAATTAAG-
CGCCGTTTGTAGACATCGAAAATCCGAGATTGTGGCCTGGGCT-
TAAACTGGGTGTTCCGTATGAACTGACGTGGAGCTGTTACGAGGG-
GAAAGAACGTCCCTGTTTAAGCTGCGGGACATGCCTGGAACGGACCGAAG-
CATTTCTGATGAATAATGCTAGAGATCCACTGCTTACGGAAAAGGAATG-
GAACGAGGCAGTGAAAATTTATGAGGAAAAGAAAATGAAGTTTA

QueC *C. sativus*

ATGAAAAGAGCAGTGGTAGTTTTTAGCGGCGGTCAGGACAGTACAACGTGTCT-
GATTCAGGCTCTTCATCAGTATGACGAAGTACATTGCGTAACATTTGATTATG-
GACAACGTCATCGTGCAGAAATTGATGTGGCACGTGAGCTTGCTCT-
GAAACTCGGTGCTCGGGCCATAAAGTATTAGACGTTACATTGCTGAACGAG-
CTCGCTGTCTCATCGCTTACTAGAGACTCCATCCCGGTTCCCGATTATGAGCCG-
GACGCGAGCGGTATCCCAAATACCTTCGTTCCAGGTAGAAATATTCTTTTTCT-
GACCCTTACGGCCATTTATGCGTAT-
CAGGTAAAGGCCGAGGCAGTAATAACTGGTGTGTGTGAGACTGATTTTT-
CAGGGTACCCGGACTGCCGTGACGAGTTTGTTAAGGCGTTGAAT-
CATGCAGTCGATCTTGGGATGGCGAAAGAGACTCGCTTCGAAACGCCTCTTA-
TGTGGCTGGATAAAGCCGAGACTTGGGCGTTAGCGGATTACTGGGGAAAATTA-
GACATTGTACGAAACGAGACGCTGACCTGTTATAATGGTATTAAGGAGA-
TGGCTGCGGGCAGTGCGCCGCGTGCAACCTGCGTGCAAACGGACTGAATCACTAC-
CTCGCCGATAAGGCTGGTGTGATGGCGGCTATGCAGAAGAAAACAGGTCT-
GAAATAA

QueC *P. atrosepticum*

ATGAAACGCGCAGTTGTTGTCTTTAGTGGCGGGCAGGATAGCACCACGTGTTT-
GATCCAAGCTCTGCAAGACTATGATGATGTTCACTGTATTACATTGATTACGGC-
CAGCGACACCGAGCAGAGATCGAAGTGCGCAGGAATTGAGC-
CAAAAACCTTGGTGCAGCAGCTCATAAGGTAAGTGGATGTAGGATTGCTGAAT-
GAACTGGCTACTTCCTCTTTGACTCGCGACTCCATTCCAGTGCCAGATTATGATGC-
CAATGCCCAAGGTATCCCAACACTTTTGTTCTGGGCGCAATATTCTGTTTCT-

GACCTTAGCCAGTATTTATGCGTATCAGGTGGGTGCCGAGGCTGTGATTAC-
CGGTGTCTGCGAAACCGACTTTTCCGGCTATCCCGACTGCCGGGATGAATTTGT-
TAAAGCGTTAAATCAAGCTATTGTGCTTGGTATTGCACGCGA-
TATTCGTTTCGAAACCCCACTTATGTGGTTAAATAAAGCG-
GAAACTTGGGCTCTTGCAGATTACTACCAGCAGTTAGACACCGTTCGTTATCATA-
CTTGACATGTTATAACGGGATCAAAGGCGATGGTTGTGGTCAGTGTGCGGCCTGC-
CATCTTCGTGCAAACGGGCTGGCGCAATATCAGAAAGATGCCGCGACCGT-
GATGGCATCCCTAAAACAGAAGGTTGGGTTGAGATAA

ToyM *S. rimosus*

ATGCCCGAGTCCCCTGTGGAGGCAGACCCGTTTTTCAGCCGTTGTTGTCCTGTCTG-
GAGGTATGGATTCCACTACTTTATTAGCGCATTACGCAATGTTACGCTACCGCC-
TAACTGCGGTGACCGTAGATTATGGTCAACGGCATCGTCGGGAAATT-
GACGCTGCGCGAACGATAGCTGGTCATTATGGTGCCGAACATCATGTTCGTAGATCT-
TAGTGGTATTGGTGTCTGTTGGGAGGATCGGCTCTGACCGATTCTGAAGTA-
GATGTACCATCGGGGCATTATGCCGAGGAATCCATGAGAGCCACGGTTGTCC-
CAAATCGAAATGCTATATTGGCTAATGTTGCCGTGGGTGCTGCCGTTGCTAG-
GCAGGCCGGTATCGTTGCCTTGGGAATGCATGCCGGGGATCACTTTGTGTATCCG-
GACTGCCGACCTGCGTTCGTGCAAGCCTTGGACG-
GACTGGTGCGTGTGCAAACGAGGGGTTCCGCACTCCTAGGGTTGAAGCGCCGTT-
TATCCACTGGTCGAAAACGGATATCGCGCGCTACGG-
GAGTCGGCTCGAGGCGCCCCTGGATAAAAGCTGGTCGTGTTATAGGGGCGGG-
GAACTGCATTGTGGTACGTGTGGCACCTGTTACGAGCGCAGGGAGGCTTTTCGT-
GATGCCGATGTTCCCGATCCAACGGAGTACCTGGATGCTGCAACCGAATTTGCAG-
CCCCATAA

QueC *B. subtilis*

ATGAAAAAAGAAAAAGCGATCGTTGTGTTTTTCAGGCGGCCAGGATT-
CAACGACCTGTCTGCTGTGGGCATTAAGAGTTTCGAGGAGGTGGAAACAGT-
GACCTTTCATTATAATCAGAGACATTCGCAAGAAGTAGAGGTCGCCAAATC-
TATCGCAGAAAAGCTAGGCGTGAAAAACCATTTACTTGATATGTCCCTGTAAAC-
CAGCTGGCACCCAATGCCTTAACACGGAATGATATCGAGATTGAAGT-
TAAAGATGGTGAGCTGCCGTCAACGTTTGTACCGGGACGTAACCTTAGTGTCTTCTGT-
CATTTGCTTCAATACTCGCGTATCAGATTGGCGCACGCCACATCATTAC-
CGGCGTTTGCAGACTGATTTTAGTGGTTACCCAGATTGTCGCGATGAATTTGT-

CAAATCATGCAATGTAACCGTAAATCTGGCTATGGAAAAACCGTTTGTACATACA-
 TACGCCACTGATGTGGCTAAATAAAGCTGAAACATGGAAGCTTGCAGACGAG-
 CTGGGTGCTCTGGATTTTGTAAAAATAATACCCTTACCTGTTACAATGGCAT-
 CATTGCAGACGGATGCGGGGAGTGTCCGGCATGTCACCTCAGGAGTAAGGGT-
 TACGAAGAATATATGGTATGAAAGGTGAACGTGCCTAA

Protein sequences

QueC *G. kaustophilus* (NC_006510.1 (1000474..1001148))

MMKMNEEKAVVVFSGGQDSTTCLFWAKKQFGEVEAVTFDYGQRHRREIDVAQAIA-
 DELGVRHTVLDLSLLGQLAPNALTRRDIAIEQKKGELPTTFVDGRNLLFLSFAAVFAKQR-
 GARHIVTGCETDFSGYPDCRDVFIKSLNVTNLAMDYEFVIHTPLMWLTKAETWKLA-
 DEGALEFIRTKTLTCYNGIADGCGECPACALRKRGLDDYLREKAEVESR

QueC *E. coli* (NC_000913.3 (464852..465547))

MKRAVVVFSGGQDSTTCLVQALQQYDEVHCVTFDYGQRHRAEIDVARELALKLGA-
 RAHKVLDVTLNELAVSSLTRDSIPVPDYEPADGIPNTFVPGRNILFLTLAAIYAYQV-
 KAEAVITGCETDFSGYPDCRDEFVKALNHAVSLGMAKDIRFETPLMWIDKAETWALA-
 DYYGKLDLVRNETLTCYNGIKGDGCSHCAACNLRANGLNHY-
 LADKPTVMAAMKQKTGLR

QueC *A. flavithermus* (NC_011567.1(1947599..1948264))

MKKEKAVVVFSGGQDSTTCLFWAKKHFAEVEAVTFDYNQRHRLEIDVAASIAKEL-
 NVSHTVLDMSLLHQLAPNALTRSDIAIEQKEGQLPSTFVDGRNLLFLSFAA-
 VLAKQKGARHLVTGCETDFSGYPDCRDVFIKSLNVTNLAMDYQFVIHTPLMWLN-
 KAETWKLADDELGALEFVRNKTLTCYNGIADGCGECPACVLRKRGLDQYMNEKKGANVR

QueC *A. sulfaticallidus* (CP005290.1, (1578638..1579342))

MHAVLIFSGGV DSTTLLYYLISKGYEVHALTFIYGQKHAREVDASKKIAKLLGIKHKVVDI-
 TSIHELISRGS LTGGEEVPKDFYTEETQKLTIVPNRNMILLAIAGGYAVKENI-
 REVYYAAHKS DYSIYPDCRKEFVKVMDAALYLANLWTPVELKAPFVDIEKSEIVGLGL-

KLGVVPYELTWSCYEGKERPCLSCGTCLERTEAFLMNNARDPLLTEKEWNEAVKIYEEK-
KNEV

QueC *C. sativus* (NC_026655.1)

MKRAVVVFSGGQDSTTCLIQALHQYDEVHCVTFDYGQRHRAEIDVARELALKLGA-
RAHKVLDVTLNELLAVSSLTRDSIPVPDYEPDASGIPNTFVPGRNIFLTLTAIYAYQV-
KAEAVITGVCETDFSGYPDCRDEFVKALNHAVDLGMAKETRFETPLMWLDKAETWALA-
DYWGKLDIVRNETLTCYNGIKGDGCGQCAACNLRANGLNHY-
LADKAGVMAAMQKKTGLK

QueC *P. atrosepticum* (NZ_CP009125.1, (1291182..1291877))

MKRAVVVFSGGQDSTTCLIQALQDYDDVHCITFDYGQRHRAEIEVAQELSQKL-
GAAAHKVLVDVGLLNELATSSLTRDSIPVPDYDANAQGIPNTFVPGRNIFLT-
LASIYAYQVGAEAVITGVCETDFSGYPDCRDEFVKALNQAVLGIARDIRFET-
PLMWLNKAETWALADYYQQLDVTYRYHTLTCYN-
GIKGDGCGQCAACHLRANGLAQYQKDAATVMASLKQKVGLR

ToyM *S. rimosus* (NZ_JMGX01000038.1 (5525..6199))

MPESPVEADPFSAVVVLSGGMDSTLLAHYAMLRYRLTAVTVDYGQRHRREIDAARTI-
AGHYGAEHHVVDLSGIGVLLGGSALTDSEVDVPSGHYAEESMRATVVPNRNAILAN-
VAVGAAVARQAGIVALGMHAGDHFVYPDCRPAFVEALDGLVRVANEGFATPRVEAP-
FIHWSKTDIARYGSRLEAPLDSKSWSCYRGGELHCGTCGTCYERREAF-
RDADVDPTEYLDAATEFAAP

QueC *B. subtilis* (NC_000964.3, (1439448..1440107))

MKKEKAIVVVFSGGQDSTTCLLWALKEFEVETVTFHYNQRHSQEVEVAK-
SIAEKLGVKNHLLDMSLLNQLAPNALTRNDIEIEVKDGELPSTFVPGRNLVFLSFASI-
LAYQIGARHIITGVCETDFSGYPDCRDEFVKSCNVTVNLAMEKPFVIHT-
PLMWLNKAETWKLADDELGALDFVKNNTLTCYNGI-
IADGCGECPACHLRSKGYEYEMVMKGERA

Alignment of protein sequences

Protein sequences of all six chosen QueCs are shown aligned with QueC from *G. kaustophilus*. The triangles mark the conserved regions in the sequence. The alignment was done with the Multiple sequence alignment tool clustalw2 (<http://www.ebi.ac.uk/Tools/msa/clustalw2/>).

```

100
Rnit Geobacillus kaustophilus  MMKMNEE - - - - KAVVVFSGG QDSTTCLFWA KKQFGEVAV TFDYGORHRR EIDVAQA IAD ELGVR-HTVL DLSLLGQL-A PNALTRRDIA IEQKGE - - - 91
Rnit Anoxybacillus flavithermus  MKK - - - - E - - - - KAVVVFSGG QDSTTCLFWA KKHFVAVAV TFDYNQRHL EIDVAASI AK ELNVS-HTVL DMSLLHOL-A PNALTRSDIA IEQKEGQ - - - 88
Rnit Bacillus subtilis  MKK - - - - E - - - - KAIIVFSGG QDSTTCLLWA LKEFEEVETV TFHYNQRHSQ EVEVAKSIAE KLGVK-NHLL DMSLLNQL-A PNALTRNDIE IEVKDGE - - - 88
Rnit Cucumis sativus  MKR - - - - - - - - - AVVVFSGG QDSTTCLIQA LHQYDEVHCV TFDYGORHRA EIDVARELAL KLGARAHKVL DVTLLNEL-A VSSLTRDS IP VPDYEPDASG 90
Rnit Pectobacterium atrosepticum  MKR - - - - - - - - - AVVVFSGG QDSTTCLIQA LQDYDDVHCI TFDYGORHRA EIEVAQELSQ KLGAAAHKVL DVGLLNEL-A TSSLTRDS IP VPDYDANIAQG 90
Toym Streptomyces rimosus  MPESPVEADP FSAVVVLSGG MDSTTLLAHY AMLRYRLTAV TVDYGORHRR EIDAARTIAG HYGAE-HHVV DLSGIGVLLG GSALTDSEYD VPSGHYAEES 99
Archaeoglobus sulfatocalidus  M - - - - - - - - - HAVLIFSGG VDSSTLLYYL ISKGYEVHAL TFIYGOKHAR EVDASKKI AK LLGIK-HKVV DIITSIHELIS RGSALTGGE-E VPKDFYTEET 88
Rnit Geobacillus kaustophilus  LPTTFVDGRN LFLSFAAVF AKQRGARHIV TGVCETDFSG YPDCRDYFIK SLNVTNLA - - - MDYEFVFIH TPLMMLTKAE TWKLADELGA LEFIRTKTLT 188
Rnit Anoxybacillus flavithermus  LPSTFVDGRN LFLSFAAVL AKQGARHLV TGVCETDFSG YPDCRDYFIK SLNVTNLA - - - MDYQFVFIH TPLMMLNKAE TWKLADELGA LEFVRNKTLT 185
Rnit Bacillus subtilis  LPSTFVPGRN LVFLSFAVIL AYQIGARHII TGVCETDFSG YPDCRDEFVK SCNVTVNLA - - - MEKPFVFIH TPLMMLNKAE TWKLADELGA LDFVKNNTLT 185
Rnit Cucumis sativus  IPNTFVPGRN IFLTLTAIY AYQVKAEEAVI TGVCETDFSG YPDCRDEFVK ALNHAVDLO - - - MAKETRFE TPLMMLDKAE TWALADYWGK LDIVRNETLT 187
Rnit Pectobacterium atrosepticum  IPNTFVPGRN IFLTLASIY AYQVGAEEAVI TGVCETDFSG YPDCRDEFVK ALNQAIVLG - - - IARDIRFE TPLMMLNKAE TWALADYQQQ LDTVRYHTLT 187
Toym Streptomyces rimosus  MRATVVPNRN AILANVAVGA AVARQAGIVA LGMHAGDHFV YPDCRPAFVE ALDGLVRVAN EGFATP-RVE APFIHWSKTD - - - IARYGSR LEAPLDKSWS 195
Archaeoglobus sulfatocalidus  QKLTIVPNRN MILLAIAGGY AVKENIREVY YAAHKSDDYSI YPDCRKEFVK VMDAALYLAN - - - LWTPVELK APFVDIEKSE - - - IVVGLGLK LGVPYELTWS 183
Rnit Geobacillus kaustophilus  CYNGLIADGC GEPACALRK RGLDEY - - - - - LREKAE VES - - - - - - - - - - - R 224
Rnit Anoxybacillus flavithermus  CYNGLIADGC GEPACVLRK RGLDQY - - - - - MNEKKG ANV - - - - - - - - - - - R 221
Rnit Bacillus subtilis  CYNGLIADGC GEPACHLRS KGYEEY - - - - - MVMKGG - - - - - - - - - - - A 219
Rnit Cucumis sativus  CYNGLIKGDGC GQCAA CNLRA NGLNHY - - - - - LADKAG VMAAMOKKTG LK 231
Rnit Pectobacterium atrosepticum  CYNGLIKGDGC GQCAA CHLRA NGLAAY - - - - - QKDAAT VMASLKQKVG LR 231
Toym Streptomyces rimosus  CYRGGELH-C GTGGTCYERR EAFRDADVDP PT - - - - - EYLD AATEFAAP - - - - - 238
Archaeoglobus sulfatocalidus  CYEGKERP-C LSCGTCCLERT EAFLMNNARD PLLTEKEWNE AVKIYEEKKN EV 234

```